DEVELOPMENT OF IMPACT RESISTANT
BORON/ALUMINUM COMPOSITES
FOR TURBOJET ENGINE FAN BLADES

by

P. MELNYK
I.J. TOTH

TRW
EQUIPMENT

prepared for

NATIONAL AERONAUTICS AND SPACE ADMINISTRATION

NASA Lewis Research Center

Contract NAS 3-17763

D.L. McDANELS, Project Manager

1. Report No NASA CR 134770	2. Government Accession No.	3 Recipient's Catalog No *N75-24747*
4 Title and Subtitle Development of Impact Resistant Boron/Aluminum Composites for Turbojet Engine Fan Blades.		5. Report Date May 1975
		6. Performing Organization Code
7. Author(s) P. Melnyk and I. J. Toth		8 Performing Organization Report No ER-7806
		10. Work Unit No.
9 Performing Organization Name and Address TRW INC. TRW Equipment 23555 Euclid Avenue Cleveland, Ohio 44117		11. Contract or Grant No. NAS 3-17763
		13 Type of Report and Period Covered Contractor Report
12. Sponsoring Agency Name and Address National Aeronautics and Space Administration Washington, D. C. 20546		
		14 Sponsoring Agency Code

15 Supplementary Notes

Project Manager, D. McDanels
NASA Lewis Research Center
Cleveland, Ohio 44135

16. Abstract

The objective of this program was to develop background technology for the fabrication of foreign object damage (FOD) or impact tolerant boron-aluminum composite fan blades for turbojet engines.

Composite fabrication was performed by vacuum press diffusion bonding by both the foil-filament array and preconsolidated monotape methods. The effect of matrix material, fiber diameter, matrix enhancement, fiber volume reinforcement, test temperature, angle-plying, notch, impact orientation, processing variables and fabrication methods on tensile strength and Charpy impact resistance were evaluated. Root attachment concepts were evaluated by room and elevated temperature tensile testing, as well as by pendulum-Izod and ballistic impact testing. Composite resistance to foreign object damage was also evaluated by ballistic impacting of panels using projectiles of gelatin, RTV rubber and steel at various velocities, sizes and impingement angles.

The program resulted in a significant improvement in the pendulum impact resistance of B-Al composites. This was accomplished primarily by the use of larger diameter boron fibers and a more ductile aluminum matrix material. However, it was also found that impact resistance can be strongly affected by changes in processing conditions by changing the nature of the fiber-matrix interface.

PRICES SUBJECT TO CHANGE

17. Key Words (Suggested by Author(s)) Composite materials Boron Aluminum Charpy Impact Tests, Impact Fan Blades	18. Distribution Statement Unclassified ~ Unlimited.		
19. Security Classif. (of this report) Unclassified	20 Security Classif. (of this page) Unclassified	21. No of Pages 93	22. Price* $3.00

SUMMARY

The objective of this program was to develop background technology
for the fabrication of foreign object damage (FOD) or impact tolerant boron-
aluminum composite fan blades for turbojet engines.

Composite fabrication was performed by vacuum press diffusion bond-
ing by both the foil-filament array and preconsolidated monotape methods.
The effect of matrix material, fiber diameter, matrix enhancement, fiber
volume reinforcement, test temperature, angle-plying, notch, impact
orientation, processing variables and fabrication methods on tensile strength
and Charpy impact resistance were evaluated. Root attachment concepts were
evaluated by room and elevated temperature tensile testing, as well as by
pendulum-Izod and ballistic impact testing. Composite resistance to foreign
object damage was also evaluated by ballistic impacting of panels using pro-
jectiles of gelatin, RTV rubber and steel at various velocities, sizes and
impingement angles.

The program resulted in a significant improvement in pendulum impact
resistance in B-Al composites. This was accomplished primarily by the use
of larger diameter boron fibers and a more ductile aluminum matrix material.
Of the two matrices studies, 1100Al and 5052Al, Charpy impact resistance was
significantly greater with 1100Al than 5052Al, but tensile strength was mod-
erately higher with 5052Al. Matrix enhancement by titanium foil improved
tensile strength and elastic modulus but reduced Charpy impact resistance.
Of the three types of angle-ply layups (namely $0°\pm22°$; $0\pm15°$ and $\pm15°$) which
were investigated, the $\pm15°$ construction produced the highest longitudinal
tensile strengths and Charpy values.

In root attachments (bladelike shapes) highest room temperature tensile
strength was obtained in specimens of $\pm15°$, 0.02 cm (8.0 mil) boron with a
single 6061Al inner wedge. Nearly equivalent strength level was also obtained
with the smaller, 0.014 cm (5.6 mil) fiber with the same angle-ply layup.
Tensile strength of root attachments was reduced by about 40% at the test
temperature of 233°C (450°F), where failure occurred by shearing process at
the outer root wedge-aluminum matrix interface.

In pendulum-Izod, highest impact energy was found in root attachment
specimens of $\pm15°$, 0.02 cm (8.0 mil) boron with a single 6061Al inner wedge.
The effect of angle-ply orientation on pendulum-Izod impact resistance was
consistent with the results obtained in Charpy specimens of the same fiber
size and angle-ply construction.

In ballistic testing, the 0.014 cm (5.6 mil) B-1100Al panels were
slightly better in soft projectile impact resistance than 0.02 cm (8.0 mil)
B-1100Al. Hard projectiles completely penetrated the test panels at very
low energy levels while the soft projectiles produced a more distributed
form of damage. Unreinforced Ti (6,4) was undamaged at ballistic impact
levels which produced severe damage in boron-aluminum.

FOREWORD

This technical report describes work performed for NASA-Lewis Research Center under Contract NAS.3-17763 during the period of 15 June 1973 through October 31, 1974. It was submitted by the authors in November 1974.

The contract with the Materials Technology Laboratory of TRW Inc., 23555 Euclid.Avenue, Cleveland, Ohio.44117,.was performed under the technical direction of Mr. D..L. McDanels of the NASA-Lewis Research Center, Cleveland, Ohio.

TRW personnel contributing to this program are: Dr. I. J. Toth, Program Manager; Mr. P. Melnyk, Engineer-Composite Fabrication and Evaluation; Dr. G. S. Doble, Principal Engineer-Ballistic Testing and Evaluation; Mr. C. A. Tyndall, mechanical testing; Mr. D. J. Engeman, metallography; Mr. W. F. Curtis, fractography; Messrs..A. L. Schumate and D. Cvelbar, fabrication.

TABLE OF CONTENTS

iv

LIST OF TABLES

-v-

LIST OF ILLUSTRATIONS

1.0   INTRODUCTION

1.1   Background

Previous studies have shown that the high strength and modulus obtained with boron-aluminum composites make them attractive candidate materials for aerospace applications. Most of the technology base and material application have been directed toward structural applications. However, in view of the attractive specific properties of these composites, they also have been considered for fan and compressor blade applications in turbojet engines.

More recently, development and testing of boron-aluminum fan blades have been carried out by the engine primes. These blades passed bench testing well; however, when actual blades were tested in engines, two problems became apparent. First, the blades should have additional impact resistance to become competitive with the conventional titanium blades currently used. Secondly, the root attachment techniques used for the blades caused fiber breakage during fabrication and stress concentrations at the root during testing and use.

1.2   Program Objective

The overall objective of this program was to develop background technology to fabricate improved fan blades using boron-aluminum. In compressor and fan applications, the major problem normally encountered is foreign object damage (FOD). Thus, the prime purpose of this program was to investigate methods of improving the impact resistance of boron-aluminum composites to the level where they would be acceptable as blading materials.

Three methods were investigated to improve the impact resistance of boron-aluminum composites. The first method investigated the effect of larger boron filament diameter on tensile strength, impact resistance and ease of fabrication. Limited data obtained for aluminum matrix composites made with 0.014 cm (5.6 mil) diameter boron filaments indicated that increased impact strength with the larger diameter fibers can be achieved. In addition, the use of the larger diameter fibers should provide easier composite fabrication using conventional fabrication techniques. The second area investigated was the matrix material. The trend for most applications has been to use the highest strength matrix possible, compatible with normal aluminum diffusion bonding fabrication techniques. This has led to composites exhibiting lower impact resistance than desired. For FOD-limited applications, such as fans and compressor blades, however, the toughness and ductility of the matrix should be of greater significance than high strength. For this reason, matrices of 1100 aluminum (high ductility, low strength, moderate impact resistance)

1

and 5052 aluminum alloy (moderate ductility, moderate strength, high impact resistance) were studied and properties compared. The third area investigated the·use of matrix enhancement material as a means to improve transverse strength and the effect of such matrix enhancement on the impact strength of the composites. Root attachment, which is another major area of concern with the development of boron-aluminum fan and compressor blades, was also investigated as part of the overall composite FOD problem.

1.3 Program Approach

The program was carried out in four tasks. A general flow diagram of the program is presented in Figure 1. Task I consisted of fabrication and characterization of composite panels made using uniaxial reinforcement. Two aluminum alloys were used for the matrix, and two diameters of boron filaments were used for the reinforcement. In addition, methods of matrix enhancement were also studied. These composites were evaluated by tensile tests, both longitudinal and transverse to the direction of reinforcement, and by impact tests. Task II consisted of the fabrication of similar composites, but using three selected angle-ply layups. The characterization was conducted in a similar manner to that of Task I. Task III consisted of the study of root attachment methods. The roots were bonded to bladelike shapes and the attachments were evaluated in tension and impact. In Task IV, the optimum materials and processes from the previous three tasks were utilized to produce additional root attachment (bladelike) shapes and flat composite panels. The root attachments were tested in tension at both room and elevated temperatures; the flat panels were used for the ballistic impact testing.

2

TASK I
- Uniaxial Process Dev.
- Uniaxial Characterization

TASK II
- Select 2 Crossply Orientations
- ⊗ Crossply Process Dev.
- Crossply Selection and Panel Fabrication
- Crossply Characterization
- ⊗ Select Best Combinations of Materials and Crossply Angles

TASK III
- Select 2 Root Attachment Designs
- ⊗ Fabricate Root Attachment Test Panels
- Characterize Root Attachments
- Select Best Root Attachment Design and Process ⊗

TASK IV
- Select Suitable Airfoil Design
- ⊗ Fabricate Bench Test Panels
- ⊗ Fabricate Demonstration Blades ⊗
- Bench Test Characterization
- Deliver Demonstration Blades to NASA-Lewis

TASK V
- Monthly Letter Reports
- Monthly Financial Report
- Quarterly Summary Report
- Final Report

⊗ Approval of NASA-Lewis Project Manager Required

Figure 1. Program Flow Diagram

2.0 MATERIALS

The prime purpose of this program was to investigate methods of improving the impact resistance of boron-aluminum composites to the level where they would be acceptable as blading material for applications in turbojet engines. In essence, this goal was to be accomplished through the use of new materials and optimization of processing variables. The trend for most applications has been to use the highest matrix strength possible, compatible with normal aluminum diffusion bonding fabrication techniques. Unfortunately, this has led to composites exhibiting lower impact resistance than desired. For FOD-limited applications, such as fans and compressor blades, however, the toughness and ductility of the matrix should be of greater significance than high strength. For this reason, matrices of 1100 aluminum (high ductility, low strength, moderate strength, high impact resistance) were selected for evaluation and comparison of properties. The matrix materials in the form of fully annealed foil were procured in three thickness sizes to accommodate two filament diameters and two levels of volume reinforcement requirements. 0.005 cm(2 mil) Beta III titanium foil in the fully annealed condition was used as matrix enhancement material. The selection of Beta III titanium was based on strength and ductility considerations.

Most of the data obtained in the past was generated on composites reinforced with 0.01 cm (4.0 mil) diameter filaments. Composites made with 0.01 cm (4.0 mil) diameter boron have demonstrated excellent specific strength and modulus properties. The pendulum and ballistic impact strength of these composites were found to be significantly less than conventional blade materials such as Ti(6Al,4V) and when blades from such composites were engine tested they did not meet the FOD requirements even with small birds.

Increasing the filament diameter is one of the methods that could be used to improve the impact strength of boron-aluminum composites. The larger diameter decreases the relative surface-to-volume ratio of the filament, thus allowing additional impact energy to be absorbed by debonding of the filament-matrix interface. The larger matrix pockets associated with the larger filaments are also less constrained making more of the inherent ductility of the matrix available for dissipation of additional impact energy. Based on the above considerations and the experimental evidence indicating improved impact resistance with increasing filament diameter, both 0.014 cm (5.6 mil) and 0.02 cm (8.0 mil) diameter boron filaments were selected for this program to evaluate the effect of such larger diameter filaments on the strength, impact resistance and ease of fabrication. The boron filament material was produced by the Avco Systems Division and supplied to the program by NASA.

3.0   TASK I - FABRICATION AND CHARACTERIZATION
OF UNIAXIAL COMPOSITE PANELS

The purpose of this task was to fabricate and characterize boron-aluminum composite panels with reinforcement of uniaxial orientation. The experimental effort in Task I was carried out in two stages: 1) preliminary study and 2) Task I reiteration. In the preliminary study, processing parameters of time, temperature, and pressure were optimized using one 0.02 cm (8.0 mil) diameter boron filament, two matrix materials (1100Al and 5052Al), and one volume fraction (50%). The objective was to obtain full composite consolidation at the lowest possible bonding temperature in order to achieve maximum tensile strain and impact resistance. The optimized processing parameters selected in the preliminary study were used for the fabrication of uniaxial tensile and Charpy panels in Task I reiteration.

3.1   TASK I - Preliminary Study

The optimization of processing variables was carried out using one 0.02 cm (8.0 mil) diameter filament, two matrix materials (1100Al and 5052Al), and one volume reinforcement (50%). Fabrication temperatures of 400°C (750°F), 428°C (800°F), 455°C (850°F), and 482°C (900°F) were used at the constant bonding pressure of 48.3 MN/M^2 (7.0 ksi) and constant time of 30 minutes.

3.1.1   Experimental Procedures

All test panels in Task I Preliminary Study were fabricated by the monotape method. The method consists of two fabrication steps: fabrication of fully dense monolayer sheets and bonding of cleaned monolayer sheets into multi-ply panels.

Preparation of Filament Mats

Filament mats used in the fabrication of monotapes were obtained by winding filaments on a 40.7 cm (16 in). diameter drum mounted on a filament winding machine. The distance between filaments was accurately maintained by drawing the filaments through a glass nozzle. A coating of polystyrene binder was provided to the filaments before being fed onto the drum. After drying the filament mat was removed from the drum and cut into plies.

Preparation of Aluminum Foil

The as-received aluminum foil was cleaned with methyl-ethyl-ketone (MEK) and etched in a 3% hydrofluoric, 30% nitric acid solution in water to remove the oxide layer. After etching the foils were thoroughly rinsed in water and wiped dry.

Assembly and Encapsulation

In the preparation of the monotape, the collimated filament mats were cut to size and sandwiched between two aluminum foils to make "green" mono- tape units. These units were next stacked into a pack using graphite coated stainless steel sheet material as separators. Normally such packs consisted of about twenty monotapes. The assembled pack was placed into a vacuum retort made of either stainless steel sheet or stainless seam welded pipe.

Pressing of Monotapes

Fabrication was accomplished in a hydraulic press. A set of existing flat dies machined from cast IN-100 nickel-base alloy was used for pressing. Heating was provided by HT Firerods built into the die assembly. Temperature was monitored and controlled by chromel-alumel thermocouples in the pressing package.

The monotapes were fabricated by the hot insertion, vacuum hot-pressure bonding technique. A small clamping load was maintained on the pack during polystyrene evacuation and heating to the bonding temperature. The holding time at clamping load for evacuation of polystyrene varied between 30 and 60 min. depending on pack size and bonding temperature. After tempera- ture equalization, pressing load was applied at a predetermined rate and main- tained constant for the duration of the bonding cycle. After bonding the pack was removed from the press and cooled under cynamic vacuum.

The monotapes were fabricated at 400°C (750°F), 428°C (800°F), 455°C (850°F), and 482°C (900°F) using constant bonding pressure of 48.7 MN/m^2 (7.0 ksi) and constant bonding time of 30 minutes. Identical bonding conditions were employed in the conversion of monotapes into test panels.

Pressing of Panels

The fully consolidated monotapes were converted into tensile and Charpy panels in a secondary bonding operation. The monotapes were cleaned and monotape thickness was adjusted by acid etching to provide the desired volume reinforcement. The cleaned monotapes were stacked into panels and vacuum encapsulated. Tensile panels with uniaxial reinforcement consisted of five plies. Panel size was 15.24 cm (6.0 in) x 10.16 cm (4.0 in) x 0.13 cm (0.052 in) to provide material for duplicate longitudinal and transverse speci- mens. The panels were diffusion bonded in open dies. Charpy panels were about 5.85 cm (2.3 in) x 8.9 cm (3.6 in) x 1.02 cm (0.4 in) to provide duplicate standard size test specimens in LT and TT orientations. The panels were bonded in a channel type die to provide the required lateral constraint. Temperature was measured and controlled by chromel-alumel thermocouples welded to the die. The test panels were fabricated at 455°C (850°F), 468°C (875°F) and 482°C (900°F) at constant pressure of 57.0 MN/m2 (8.0 ksi) and constant time of 30 minutes. Bonding temperatures of 400°C (750°F) and 428°C (800°F) were eliminated earlier because of lack of satisfactory bond in the monotapes.

Specimen Preparation

Straight-side specimens were used for tensile testing. Specimen size was 10.16 cm (4.0 in) x 0.64 cm (0.25 in) x as-pressed thick. In the preparation of the test specimens, longitudinal and transverse strips were removed from the panel by abrasive wheel slitting which were then abrasively ground to proper width. Priot to testing, aluminum tabs 3.71 cm (1-1/2 in) x 2.54 cm (1 in) x 0.127 cm (0.050 in) were cemented to test specimen ends with Armstrong A-12 adhesive. The use of such tabs was considered necessary to avoid a potential damage to the composite by the serrations in the test grips.

The configuration of the Charpy V-notch specimens is shown in Figure 2. The specimens were prepared by a combination of abrasive and EDM machining techniques. Rectangular specimen shapes were obtained from the panels by abrasive slitting and grinding as before. The notches were placed by the EDM technique to minimize filament damage and to ensure the required notch radius. The notches in both LT and TT specimens were placed in the panel pressing, as distinguished from the panel slit surface.

Mechanical Testing

Tensile specimens were tested in an Instron Universal testing machine at a cross-head speed of 0.051 cm (0.020 in) per minute. A 1.27 cm (0.5 in) clip-on extensometer was used during testing to measure elastic modulus and strain to failure.

Pendulum impact testing of Charpy specimens was performed on the Sontag Universal Impact testing machine. Upon impact the absorbed energy was automatically registered on the scale. Duplicate specimens were tested in each orientation.

Analytical Tests

Analytical tests included visual examination, optical microscopy and SEM fractography. Visual examination provided an overall view of the fracture; in the case of Charpy specimens it also helped to determine the existence and the extent of specimen deformation by shear. Optical microscopy was used to determine filament distribution, soundness of bond, as well as composite damage adjacent to the crack. SEM fractography was used to fully characterize the cracks with special emphasis on matrix-fiber bond, debonding and fiber pullout.

2.165

45°

1.085

.080

.010R

NOTCH MUST BE SQ
WITH THESE FACES
WITHIN .002 FIR

.394

0.315

.394
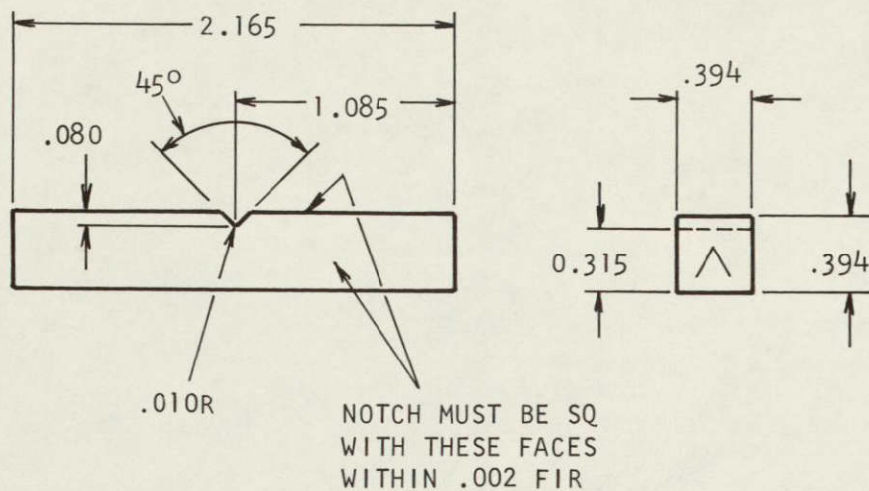
a. CHARPY "V-NOTCH" SPECIMEN

LT

TT

LT(S)
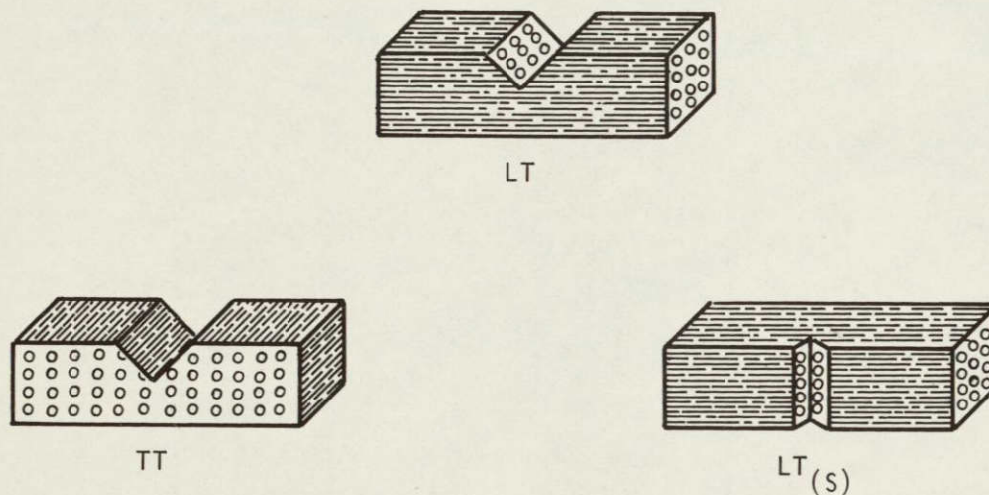
b. FILAMENT ORIENTATIONS AND SPECIMEN DESIGNATIONS

Figure 2. Charpy V-Notch Test Specimen Design.

3.1.2 Results and Discussion

The effect of bonding temperature on monotape tensile strength in 50v/o, 0.02 cm (8.0 mil) B-Al is shown in Table I. Tensile data for 400°C (750°F) and 428°C (800°F) bonding temperature in B-5052Al are missing due to incomplete monotape bond. In the B-1100Al system, the 428°C (800°F) bonding temperature results are questionable because of monotape debonding during testing. The highest average strength levels with both 1100Al and 5052Al were obtained on monotapes bonded at 455°C (850°F). The drop-off in tensile strength in specimens bonded at 482°C (900°F) is possibly the result of fiber degradation. It is also of interest to note that at both temperatures the average tensile strengths are higher in the B-5052Al. Typical microstructures of monotapes of 50v/o, 0.02 cm (8.0 mil) B-1100Al and 5052Al are illustrated in Figures 3 and 4 respectively. The monotapes show uniform fiber spacing, full consolidation and a sound matrix-matrix bond.

The effect of bonding temperature on tensile strength of five-ply B-1100Al and B-5052Al specimens fabricated by the monotape method is shown in Table II. In the B-1100Al system the longitudinal tensile strength is highest in specimens fabricated at 455°C (850°F). In the B-5052Al system the maximum strength corresponds to the 468°C (875°F) bonding temperature. In agreement with previous test data (Table I), tensile strength is consistently higher in the B-5052Al system. A slight reduction in tensile strength is observed in both systems in specimens fabricated at 482°C (900°F) bonding temperature.

Transverse tensile properties are consistently higher in the B-5052Al system. Contrary to the trend observed in the longitudinal specimens, the transverse tensile strength in both systems is higher at the 482°C (900°F) bonding temperature; this temperature effect is most pronounced in the B-5052Al system. The higher strength levels obtained with the B-5052Al system in specimens of both longitudinal and transverse filament orientation are attributed in part to the relatively higher strength of the 5052Al matrix. The improvement in the transverse tensile strength with increasing bonding temperatures in both B-5052Al and B-1100Al systems is largely attributed to a corresponding increase in filament-matrix bond strength. Transverse tensile strength of specimens fabricated at 455°C (850°F) is not available due to specimen damage (partial debonding) during machining.

The effect of bonding temperature on room temperature impact resistance is shown in Table III. In the B-1100Al system, impact data were obtained from the 482°C (900°F) panel only; other panels debonded during machining. The average impact energy levels obtained in these specimens are relatively low. In the longitudinal (LT) orientation, highest impact energy is found in the B-1100Al specimens fabricated at 482°C (900°F). In the B-5052Al system, longitudinal impact energy decreases with increasing bonding temperature.

TABLE I

EFFECT OF BONDING TEMPERATURE ON MONOTAPE

TENSILE STRENGTH IN 50 v/o, 0.02 cm (8.0 mil) B-Al

Matrix	Bonding Temp. °C (°F)	UTS, M N/m^2 (KSI)
1100	400 (750)	Incompletely bonded.
	428 (800)	1090.1 (158.2), 898.4 (130.3), 906.7 (131.5) (Debonded during test)
	455 (850)	1241.1 (180.3), 1415.5 (205.3), 1214.9 (176.2)
	482 (900)	1270.7 (184.3), 1301.1 (188.7), 1241.1 (180.0)
5052	400 (750)	Not bonded.
	428 (800)	Incompletely bonded.
	455 (850)	1661.7 (241.0), 1690.6 (245.2), 1603.8 (232.6)
	482 (900)	1277.0 (185.2), 1698.2 (246.3), 1432.1 (207.7)
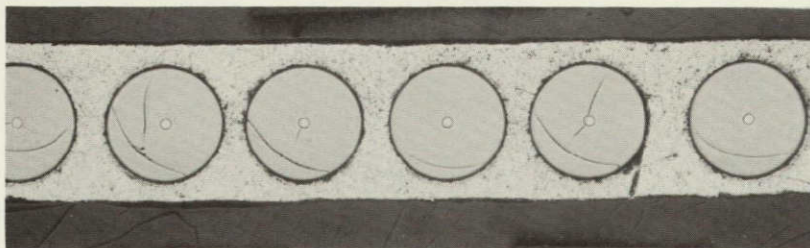
75X unetched
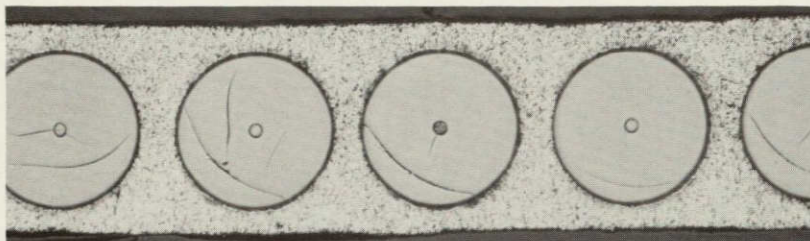
100X etched
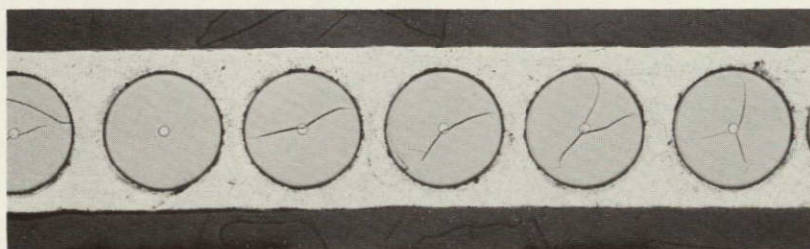
a. 455°C (850°F)
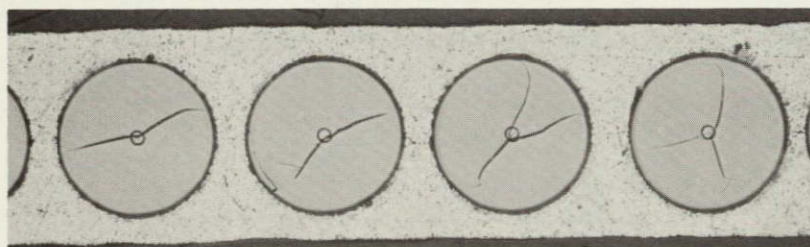
75X unetched

100X etched

b. 482°C (900°F)

Figure 3. Photomicrographs Showing the Effect of Bonding Temperature on the Quality of Matrix-Matrix Bond in 50 v/o, 0.02 cm (8.0 mil) B-1100Al Monotapes.
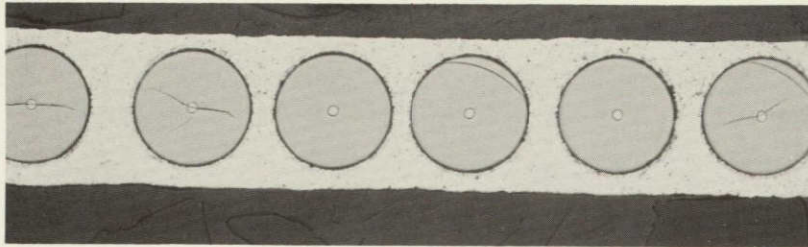
75X unetched
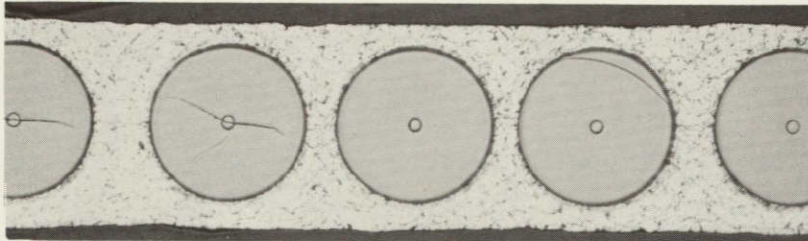
100X etched

a. 455°C (850°F)
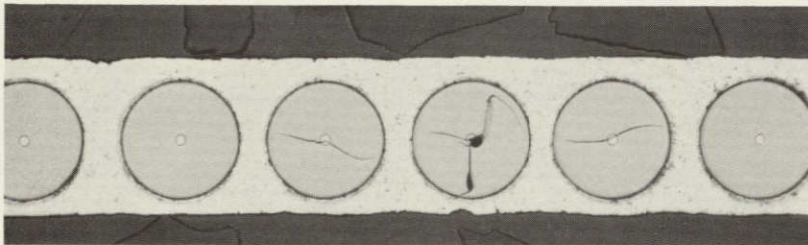
75X unetched
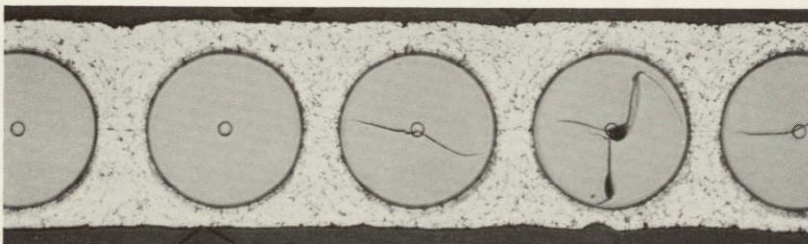
100X etched

b. 482°C (900°F)

Figure 4. Photomicrographs Showing the Effects of Bonding Temperatures on the Quality of Matrix-Matrix Bond in 50 v/o, 0.02 cm (8.0 mil) B-5052Al Monotapes.

TABLE II

EFFECT OF BONDING TEMPERATURE ON TENSILE STRENGTH
50 v/o, 0.02 cm (8.0 mil) B-Al PANELS

Panel No.	Matrix	Bonding Temp. °C.(°F)	Orien- tation	UTS NM/m^2 (ksi)	Modulus 10^6 MN/m^2 (10^6 psi)	Strain to Failure μ-cm/cm (μ-in/in)
14A	1100	455 (850)	Long	1272.0 (184.5)	231.0 (33.5)	5900
"	"	"	"	1244.0 (179.9)	290.0 (42.1)+	5600
18A	1100	468 (875)	Long	>695.7 (100.9)*	227.5 (33.0)	-
"	"	"	"	1181.1 (171.3)	-	1800
"	"	"	Trans	71.7 (10.4)	-	200
"	"	"	"	70.3 (10.2)	177.2 (25.7)	400
15A	1100	482 (900)	Long	1048.0 (152.0)	293.7 (42.6)+	3200
"	"	"	"	1140.4 (165.4)	307.5 (44.6)+	5800
"	"	"	Trans	93.8 (13.5)	163.4 (23.7)	15600
"	"	"	"	91.7 (13.3)	179.3 (26.0)	13400
14B	5052	455 (850)	Long	1338.3 (194.1)	199.3 (28.0)	12400
"	"	"	"	1447.3 (209.9)	188.2 (27.3)	17200
18B	5052	468 (875)	Long	1705.8 (247.4)	225.5 (32.7)	4200
"	"	"	"	1570.7 (227.8)	223.4 (32.4)	8200
"	"	"	Trans	97.9 (14.2)	191.0 (27.7)	400
"	"	"	"	119.3 (17.3)	197.2 (28.6)	800
15B	5052	482 (900)	Long	1576.4 (228.7)	188.3 (28.9)	7800
"	"	"	"	1624.5 (235.6)	212.3 (32.1)	7400
"	"	"	Trans.	195.8 (28.4)	159.3 (23.1)	4400
"	"	"	"	192.4 (27.9)	165.5 (24.0)	3800

* Tab Slippage.

+ Extensometer Slippage.

TABLE III

EFFECT OF BONDING TEMPERATURE ON CHARPY
IMPACT RESISTANCE IN 50 v/o, 0.02 cm (8.0 mil) B-Al

Initial Monotape Consolidation

Panel No.	Matrix	Bonding Temp. °C (°F)	Impact Orientation	Impact Energy N-m (ft-lb)
21	1100	455 (850)	LT	Not available.
			TT	" "
25	1100	468 (875)	LT	Not available.
			TT	" "
11	1100	482 (900)	LT	16.3 (12.0)
	"	"	"	28.5 (21.0)
	"	"	TT	5.4 (4.0)
	"	"	"	4.7 (3.5)
10	5052	455 (850)	LT	19.0 (14.0)
	"	"	"	23.0 (17.0)
	"	"	TT	2.3 (1.5)
	"	"	"	2.3 (1.5)
22	5052	468 (875)	LT	16.5 (11.0)
	"	"	"	13.6 (10.0)
	"	"	"	1.4 (1.0)
	"	"	"	1.4 (1.0)
12	5052	482 (900)	LT	11.5 (8.5)
	"	"	"	12.2 (9.0)
	"	"	TT	2.3 (1.5)
	"	"	"	1.4 (1.0)
38	1100	455 (850)	LT	63.7 (47.0)
	"	"	"	46.8 (34.5)
	"	"	TT	2.3 (1.5)
	"	"	"	2.3 (1.5)

14

The debonding problems encountered in the conversion of B-1100Al monotapes into panels in the 455°C (850°F) - 468°C (875°F) temperature range were attributed both to the relatively high tenacity of the oxide film compared to 5052Al and the negligible amount of plastic flow at the matrix-matrix interface during pressing. To better asses the potential of this matrix matrial with regard to impact resistance, a Charpy panel (No. 38) of 50v/o, 0.014 cm (5.6 mil) B-1100Al, was fabricated by the foil-filament array method at 455°C (850°F) bonding temperature. Charpy impact test results obtained from this panel (No. 38) are included in Table III.

In view of the high impact values obtained on test specimens of B-1100Al fabricated by the foil-filament method, all subsequent panel fabrication in the B-1100Al system was done by the foil-filament array method until the problem of monotape bonding was successfully resolved. The mono-tape method was continued with the 5052Al and matrix enhancement systems. Based on the mechanical and analytical test results, bonding parameters of 455°C (850°F), 57.0 MN/m^2 (8 ksi), 30 minutes were selected for the fabrication of uniaxial test panels in Task I Reiteration.

3.2 TASK I - Reiteration

The objective of this task was to fabricate and characterize boron-aluminum composite panels with reinforcement of uniaxial orientation. The scope of this task was expanded to include two filament diameters, two matrix compositions, two volume reinforcements, and matrix enhancement. The monotape method was used in the fabrication of B-5052Al and B-1100Al + Ti panels. Foil-filament array method was used in B-1100Al. Selected test panels of B-5052Al and B-1100Al + Ti were also fabricated by the foil-filament method to compare and evaluate the effect of the two fabrication methods on mechanical properties.

3.2.1 Experimental Procedures

The procedures employed in the fabrication of test panels by the monotape method have been described in previous sections. In the foil-filament array method, the panels were produced in a single pressing cycle. Filament mats and matrix foils were prepared as before. The thickness of the matrix foil was adjusted by acid etching to provide the desired volume reinforcement. Alternate layers of foils and filament mats were assembled to the desired thickness and vacuum encapsulated. Again, tensile panels were pressed in open dies but a channel-type die was used for the Charpy panels to provide lateral constraint.

The size of the test panels was the same as in Task I, Preliminary Study. Tensile panels consisted of five plies. Panel size was 15.24 cm (6.0 in) x 10.16 cm (4.0 in) x 1.02 cm (0.052 in) to provide

material for duplicate longitudinal and transverse specimens. Charpy panels were about 5.85 cm (2.3 in) x 8.9 cm (3.5 in) x 1.02 cm (0.4 in) to provide duplicate specimens in LT and TT orientations.

The procedure employed in the preparation and testing of tensile and Charpy impact specimens were described in detail earlier. To determine the effect of directionality on impact energy in longitudinal Charpy specimens, selected specimens were also impact tested in the alternate LT orientation. In the standard LT orientation, the notch is placed in the pressing surface of the panel and the specimen is impacted in the direction normal to the plane of the matrix foil in the composite layup. In the alternate LT orientation, which is labeled in this report as LTs, the notch is placed in the cut surface of the panel and the specimen is impacted in the direction normal to the cut edge of the matrix foil.

3.2.2   Results and Discussion

The influence of bonding temperature on tensile and impact properties in 0.02 cm (8.0 mil) B-1100Al and 0.02 cm (8.0 mil) B-5052Al composites with uniaxial reinforcement was discussed earlier. Based on the mechanical and analytical test results, bonding parameters of 455°C (850°F), 57.0 MN/m^2 (8 ksi), 30 minutes were selected for the fabrication and evaluation of tensile and Charpy panels with uniaxial filament reinforcement in Task I Reiteration. Typical microstructures of B-5052Al, B-1100Al and B-1100 Al + Ti illustrating the quality of bond and fiber distribution are shown in Figure 5. As part of the overall materials screening study, the tensile and impact test results are analyzed below in terms of matrix material, fiber diameter, volume reinforcement, matrix enhancement, fabrication method and directionality.

Effect of Matrix Materials

Of all the material variables studied in this task, the composite properties were found to be most strongly affected by the matrix material. In general, the effects of 1100Al and 5052Al matrix materials on tensile and impact properties are opposite. Tensile strength is higher in B-5052Al than in B-1100Al. In pendulum impact the matrix effect is reversed and a very significant improvement in impact resistance is obtained with the 1100Al matrix material.

Tensile properties of uniaxial composites fabricated at a constant temperature of 455°C (850°F) are summarized in Table IV. Tensile strength in B-5052Al is higher than in B-1100Al in both longitudinal and transverse orientations. The relatively higher tensile strength in B-5052Al is attributed in part to the moderately higher strength of the 5052Al matrix. Another important factor is chemical composition and the attendant surface conditions of the two matrix materials which influence
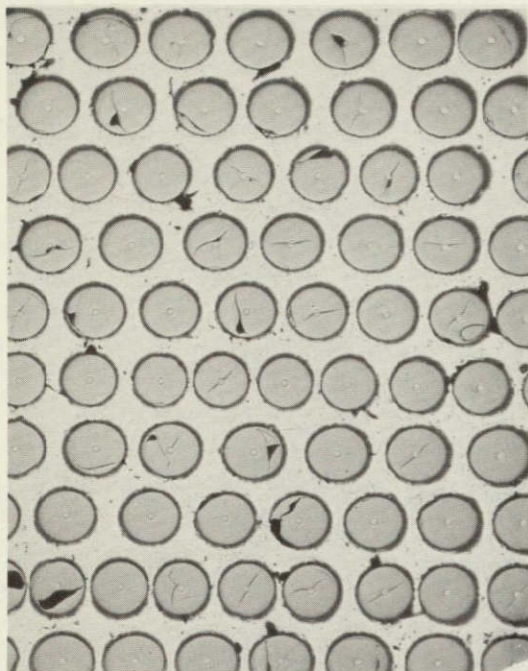
0.014 cm (5.6 mil) B-5052Al
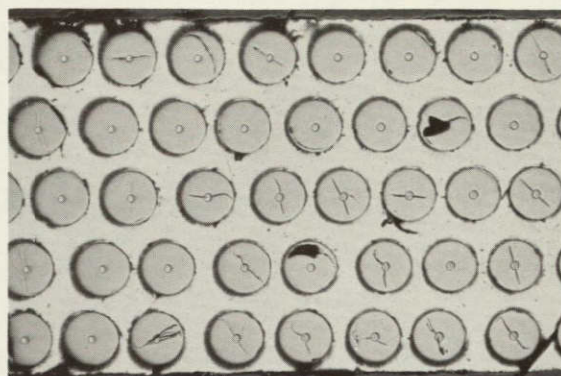
0.014 cm (5.6 mil) B-1100Al
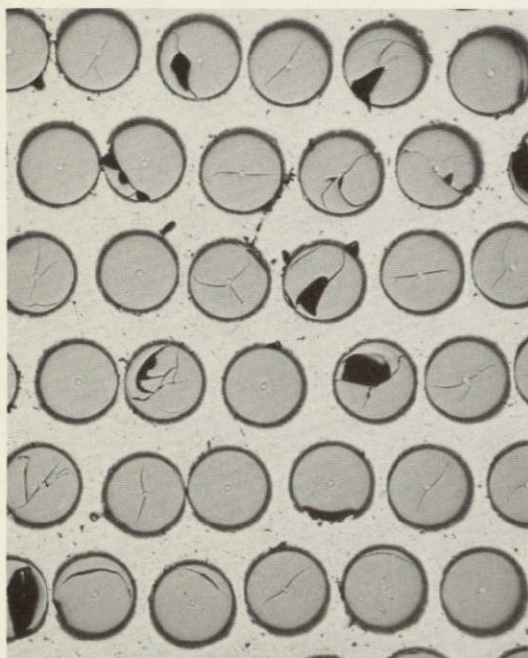
0.02 cm (8.0 mil) B-1100Al
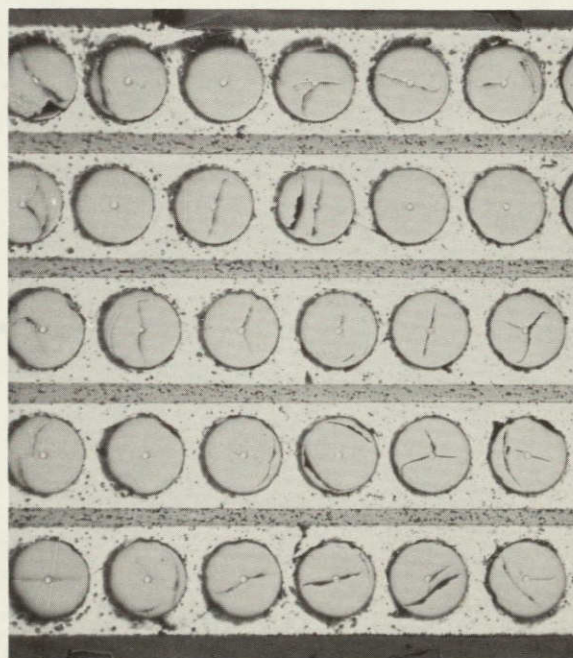
0.02 cm (8.0 mil) B-1100 Al + Ti.

Figure 5.   Typical Microstructures of 50 v/o B-5052Al, B-1100Al and B-1100Al
            + Ti Showing the Uniformity of Fiber Distribution and the Quality
            of Matrix-Matrix Bond.

50 X

17

TABLE IV

TENSILE PROPERTIES OF UNIAXIAL COMPOSITES

Panel No.	Matrix	Fiber Dia. cm (mils)	V/O	Fabrication Method	Orientation	UTS M N/m² (KSI)		Modulus 10⁶ MN/m² (10⁶ PSI)		Strain to Failure μ-cm/cm (μ-in/in)
33A	5052Al	0.014 (5.6)	50	Mono.	Long.	1892.7	(274.5)	226.8	(32.9)	8,600
"	"	"	"	"	"	1783.0	(258.6)	227.5	(33.0)	8,000
"	"	"	"	"	Trans.	58.6	(8.5)	125.5	(18.2)	400
"	"	"	"	"	"	119.3	(17.3)	158.6	(23.0)	600
33B	5052Al	0.014 (5.6)	30	Mono.	Long.	1141.8	(165.6)	161.3	(23.4)	8,400
"	"	"	"	"	"	1281.8	(185.9)	172.4	(25.0)	9,000
"	"	"	"	"	Trans.	85.5	(12.4)	81.4	(11.8)	4,000
"	"	"	"	"	"	97.2	(14.1)	103.4	(14.7)	3,600
48-1	1100Al	0.014 (5.6)	50	Foil-Fil.	Long.	1400.4	(203.1)	240.0	(34.8)	6,800
"	"	"	"	"	"	1321.8	(191.7)	215.1	(31.2)	6,800
"	"	"	"	"	Trans.	56.5	(8.2)	157.9	(22.9)	8,000
"	"	"	"	"	"	52.4	(7.6)	131.0	(19.0)	4,000
70-2	1100Al	0.02 (8.0)	50	Foil-Fil.	Long.	1213.5	(176.0)	200.0	(29.0)	6,400
"	"	"	"	"	"	1265.9	(183.6)	220.6	(32.0)	7,000
"	"	"	"	"	Trans.	63.4	(9.2)			
"	"	"	"	"	"	67.6	(9.8)	158.6	(23.0)	3,600
125-B	1100Al	0.02 (8.0)	50	Mono.	Long.	1540.3	(223.4)	219.3	(31.8)	7,400
"	"	"	"	"	"	1483.1	(215.1)			7,400
42-A	1100Al + Ti	0.014 (5.6)	44	Mono.	Long.	1647.9	(239.0)	215.8	(31.3)	9,400
"	"	"	"	"	"	1737.5	(252.0)	219.3	(31.8)	10,400
"	"	"	"	"	Trans.	242.7	(35.2)	120.0	(17.4)	15,200
"	"	"	"	"	"	225.5	(32.7)	115.8	(16.8)	15,200
14-B	5052Al	0.02 (8.0)	50	Mono.	Long.	1338.3	(194.1)	199.3	(28.9)	12,400
"	"	"	"	"	"	1447.3	(209.9)	188.2	(27.3)	17,200

(contd)

TABLE IV (continued)

TENSILE PROPERTIES OF UNIAXIAL COMPOSITES

Panel No.	Matrix	Fiber Dia. cm (mils)	V/O	Fabrication Method	Orientation	UTS M N/m^2 (KSI)		Modulus 10^6 M N/m^2 (10^6 PSI)		Strain to Failure, μ-cm/cm (μ-in/in)
42-B	1100Al	0.02 (8.0)	44	Mono.	Long.	1439.7	(208.8)	183.4	(26.6)	9,000
"	+Ti	"	"	"	"	1407.3	(204.1)	199.3	(28.9)	10,000
"	"	"	"	"	Trans.	243.4	(35.3)	88.9	(12.9)	13,000
"	"	"	"	"	"	232.4	(33.7)	97.9	(14.2)	11,800
70-1	1100Al	0.02 (8.0)	50	Foil-Fil.	Long	1226.0	(177.8)			5,000
"	+Ti	"	"	"	"	1102.5	(159.9)	273.0	(39.6)	6,200
"	"	"	"	"	Trans.	259.3	(37.6)	86.3	(12.5)	13,800
"	"	"	"	"	"	273.0	(39.6)	95.2	(13.8)	11,800

the relative strengths of matrix-matrix and matrix-fiber bond at otherwise identical processing conditions. Such bond is stronger in the alloyed 5052Al than in (commercially pure) 1100Al. The weaker bond in the latter is attributed to the tenacious oxide film which acts as a diffusion barrier.

Charpy impact data for uniaxial composites are summarized in Table V. The test data for B-5052Al are incomplete because the 5052Al matrix was eliminated from further study on account of low impact resistance. Impact resistance in transverse (TT) specimens is low and equivalent in both 0.014 cm (5.6 mil) B-1100Al and 0.014 cm (5.6 mil) B-5052Al panels fabricated by the foil-filament method.

Impact resistance of B-1100Al in notched Charpy specimens in the longitudinal (LT) impact orientation is several times higher than that of B-5052Al with both fibers. The overall appearance of the tested notched Charpy specimens of B-1100Al and B-5052Al are illustrated in Figure 6. The specimens of B-5052Al have a planar type of crack with a low level of filament pullout and no observable distortion of the remainder of the specimen. The specimens of B-1100Al, on the other hand, show a very irregular crack and a severe specimen deformation in the form of bending and shear as evidenced by the displacement at specimen ends. The higher impact resistance in B-1100Al as compared to B-5052Al is the combined effect of several factors. Of these, the high strain capability of the 1100Al matrix and the strength of fiber-matrix bond are the most influential. The high strain capability of the matrix permits a considerable deformation to occur in the specimens as a result of shear stresses generated in the matrix parallel to the fibers. It was pointed out earlier that, using identical foil preparation and bonding procedures, the fiber-matrix bond is invariably stronger in the B-5052Al than in the B-1100Al system. The difference in the fiber-matrix bond strength in B-5052 and B-1100Al, as evidenced by the varying degrees of aluminum coating on the pulled out fibers is illustrated in Figure 7. The effects of the two types of fiber-matrix bond strength on the overall appearance of the fractured surfaces in B-5052Al and B-1100Al are illustrated in Figure 8. The specimen of B-5052Al shows a planar type of fracture with no matrix delamination and a low level of fiber pullout (top). The high level of delamination and fiber pullout in B-1100Al as compared to B-5052Al is illustrated in Figure 9. The difference in the overall crack pattern and specimen deformation in the immediate vicinity of the crack is further illustrated in Figure 10. In addition to a ragged crack surface, B-1100Al specimen also shows a secondary crack some distance in from the primary crack. The combined effect of the fiber matrix disbonding and the attendant high level of fiber pullout in B-1100Al is to provide a crack blunting mechanism resulting in the absorption of additional impact energy. As will be shown later, the fiber-matrix disbonding also accounds for most of the shear displacement at specimen ends.

TABLE V

CHARPY IMPACT PROPERTIES OF UNIAXIAL B-Al COMPOSITES

Panel No.	Matrix	Fiber Dia. cm (mils)	V/O	Fabrication Method	Impact Orientation	Impact Energy N-m (ft-lb)
10	5052Al	0.02 (8.0)	50	Mono.	LT	19.0 (14.0)
"	"	"	"	"	"	23.0 (17.0)
"	"	"		"	TT	2.0 (1.5)
"	"	"		"	"	2.0 (1.5)
37	5052Al	0.014 (5.6)	30	Mono.	LT	13.6 (10.0)
"	"	"	"	"	"	12.9 (9.5)
"	"	"	"	"	TT	2.7 (2.0)
"	"	"	"	"	"	2.7 (2.0)
39	5052Al	0.014 (5.6)	50	Mono.	LT	16.3 (12.0)
"	"	"	"	"	"	17.6 (13.0)
"	"	"	"	"	TT	0.7 (0.5)
"	"	"	"	"	"	0.7 (0.5)
51	5052Al	0.014 (5.6)	50	Foil-Fil.	LT	12.2 (9.0)
"	"	"	"	"	"	11.5 (8.5)
"	"	"	"	"	TT	4.0 (3.0)
"	"	"	"	"	"	3.4 (2.5)
103	5052Al	0.014 (5.6)	50	Foil-Fil.	LT	17.6 (13.0)
"	"	"	"	"	"	24.4 (18.0)
"	"	"	"	"	LT	35.3 (26.0)*
"	"	"	"	"	"	34.6 (25.5)*
"	"	"	"	"	TT	0.7 (0.5)
"	"	"	"	"	"	1.4 (1.0)
38	1100Al	0.014 (5.6)	50	Foil-Fil.	LT	63.7 (47.0)
"	"	"	"	"	"	46.8 (34.5)
"	"	"	"	"	LT_s	28.5 (21.0)
"	"	"	"	"	TT	0.7 (0.5)
"	"	"	"	"	"	0.7 (0.5)

* Unnotched

(contd)

TABLE V (continued)

CHARPY IMPACT PROPERTIES OF UNIAXIAL B-Al COMPOSITES

Panel No.	Matrix	Fiber Dia. cm (mils)	V/O	Fabrication Method	Impact Orientation	Impact Energy N-m (ft-lb)
50	1100Al	0.02 (8.0)	50	Foil-fil.	LT	96.3 (71.0)
"	"	"	"	"	"	91.6 (67.5)
"	"	"	"	"	LT$_s$	47.5 (35.0)
"	"	"	"	"	TT	1.4 (1.0)
"	"	"	"	"	"	1.4 (1.0)
34	1100Al	0.014 (5.6)	44	Mono.	LT	29.8 (22.0)
"	+Ti	"	"	"	"	27.1 (20.0)
"	"	"	"	"	TT	3.4 (2.5)
"	"	"	"	"	"	3.4 (2.5)
36	110Al	0.02 (8.0)	44	Mono.	LT	41.4 (30.5)
"	+Ti	"	"	"	"	40.7 (30.0)
"	"	"	"	"	LT$_s$	11.5 (8.5)
"	"	"	"	"	TT	4.1 (3.0
"	"	"	"	"	"	4.1 (3.0)
126A	1100Al	0.02 (8.0)	50	Mono.	LT	27.1 (20.0)
"	"	"	"	"	"	28.5 (21.0)

LT = 63.7 N-m
(47.0 ft-lb)

TT = 2.0 N-m
(1.5 ft-lb)

0.014 cm (5.6 mil) B-1100Al

LT = 17.6 N-m
(13.0 ft-lb)

TT = 0.68 N-m
(0.5 ft-lb)
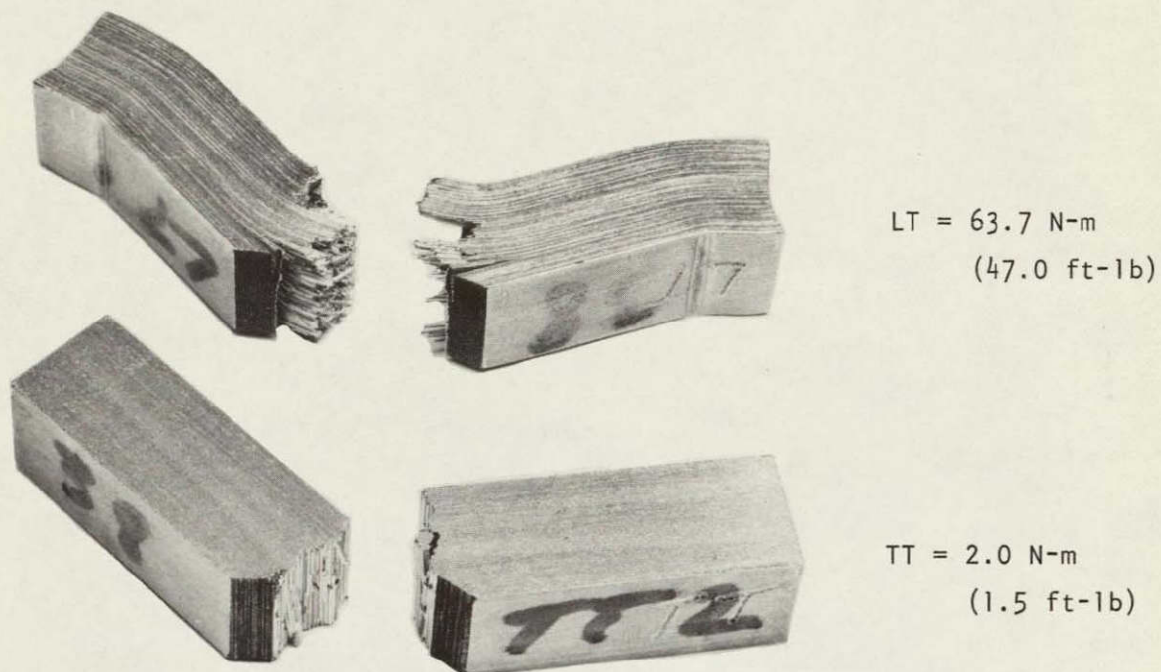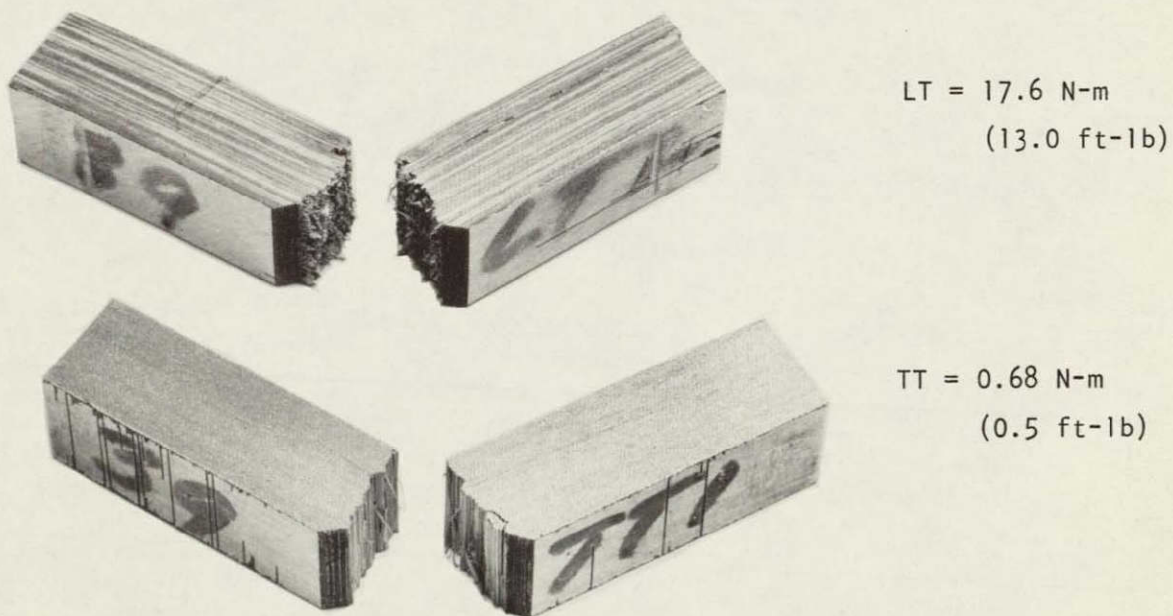
0.014 cm (5.6 mil) B-5052Al

Figure 6.   Fracture and Shear Deformation in Notched Charpy Specimens of
0.014 cm (5.6 mil) B-1100Al and 0.014 cm (5.6 mil) B-5052Al.
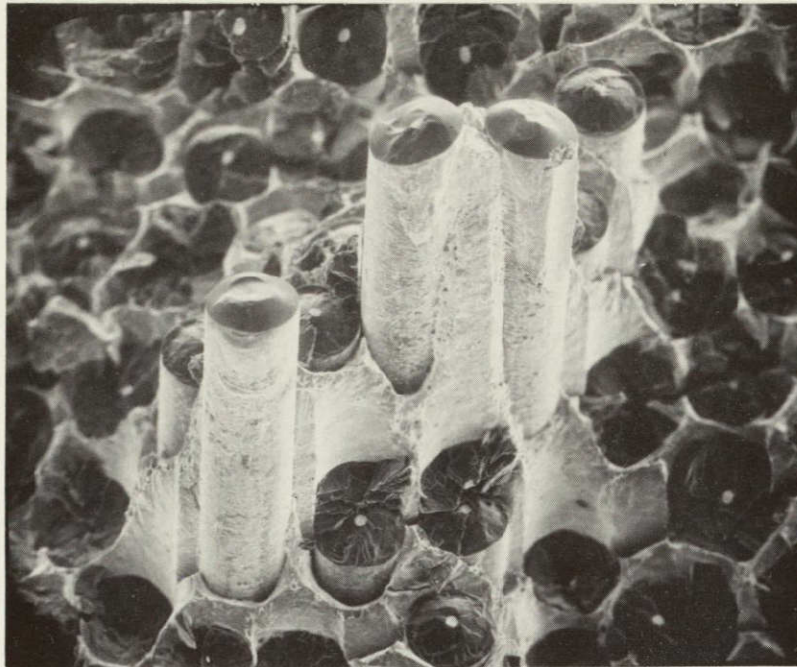
0.014 cm (5.6 mil) B-5052Al   100 X
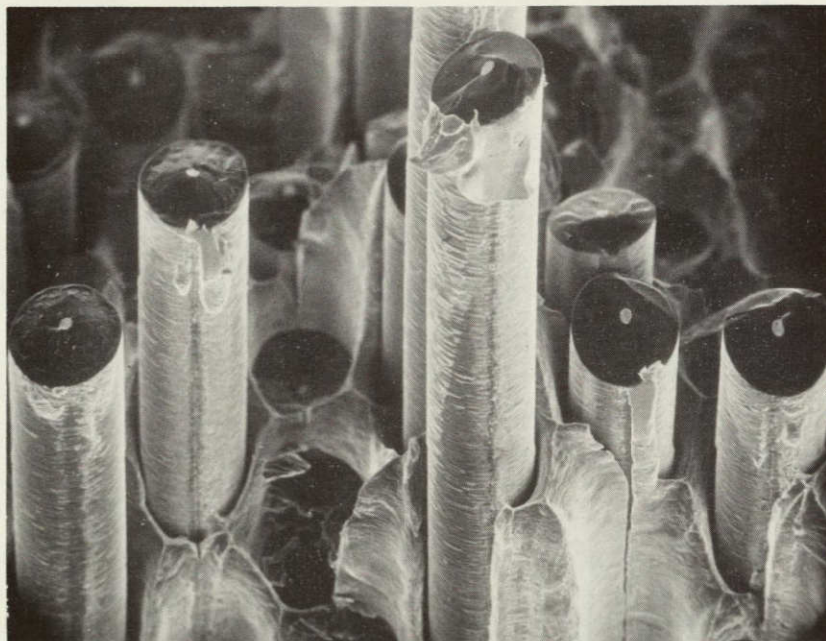
0.014 cm (5.6 mil) B-1100Al   100 X

Figure 7. SEM Fractorgraphs of Charpy Specimens Illustrating Completely
           Aluminized Filaments in the B-5052Al System (Top) and Partially
           Aluminized Filaments in the B-1100Al System (Bottom).
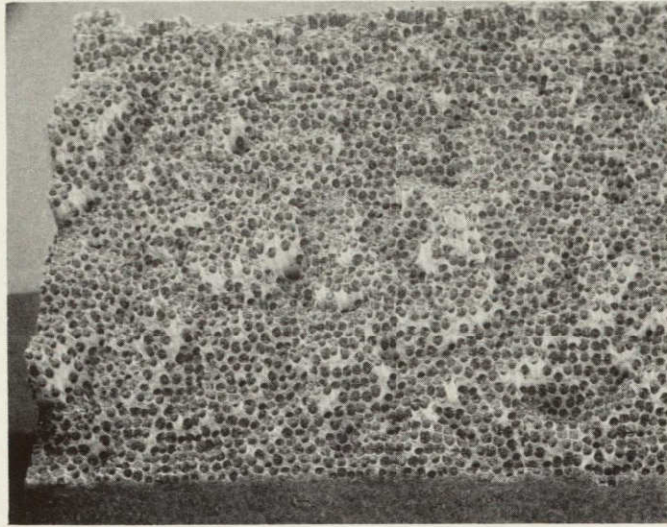
0.014 cm (5.6 mil) B-5052Al   10 X
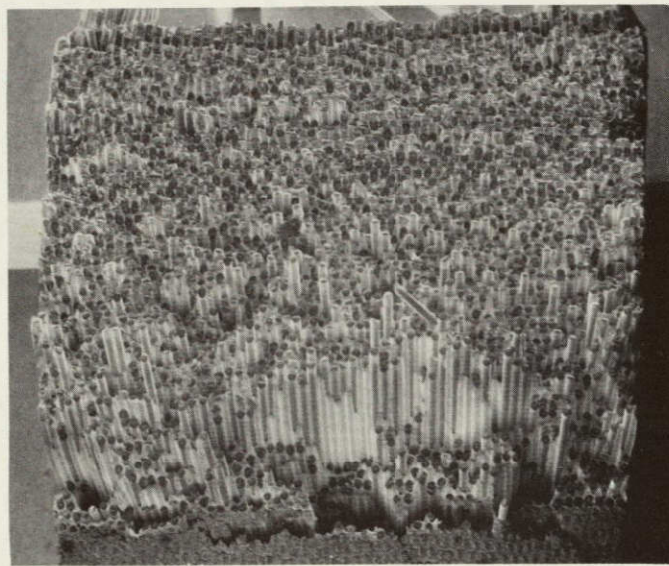
0.014 cm (5.6 mil) B-1100Al   10 X

Figure 8.   SEM Fractographs of Charpy Specimens of B-1100Al and
            B-5052Al Illustrating Two Types of Surface Fractures
            Associated with Varying Degrees of Fiber-Matrix Bond.
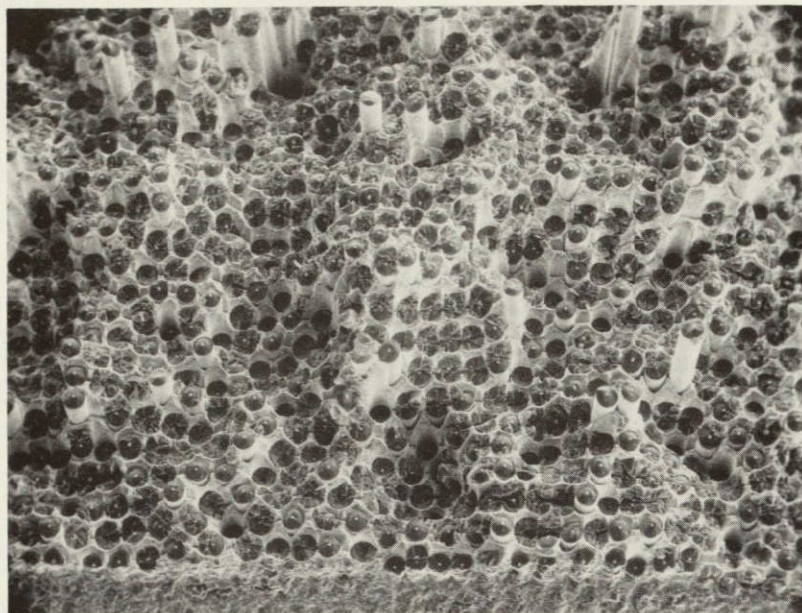
0.014 cm (5.6 mil) B-5052Al   20 X
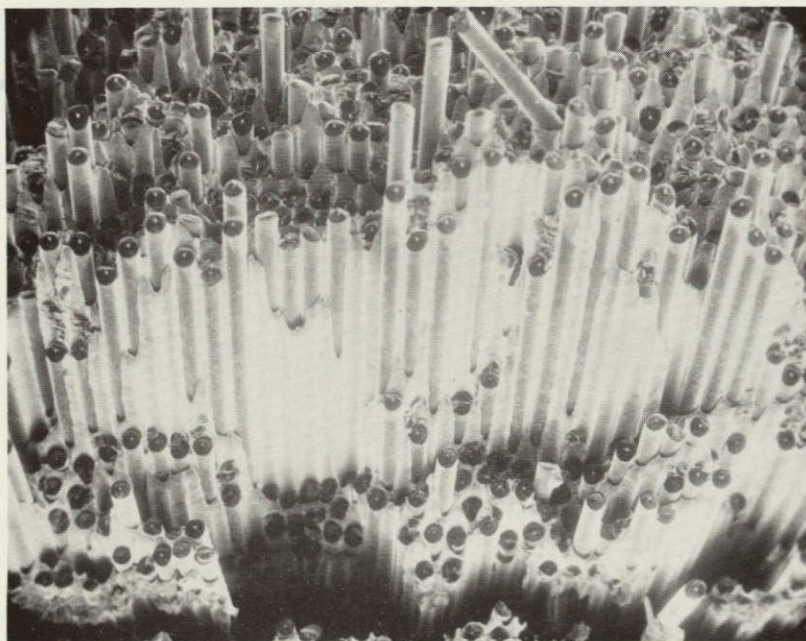
0.014 cm (5.6 mil) B-1100Al   20 X

Figure 9.   SEM Fractorgraphs of B-5052Al and B-1100Al Charpy Specimens
             Illustrating the Effect of Fiber-Matrix Bond Strength on
             Debonding and Fiber Pullout.
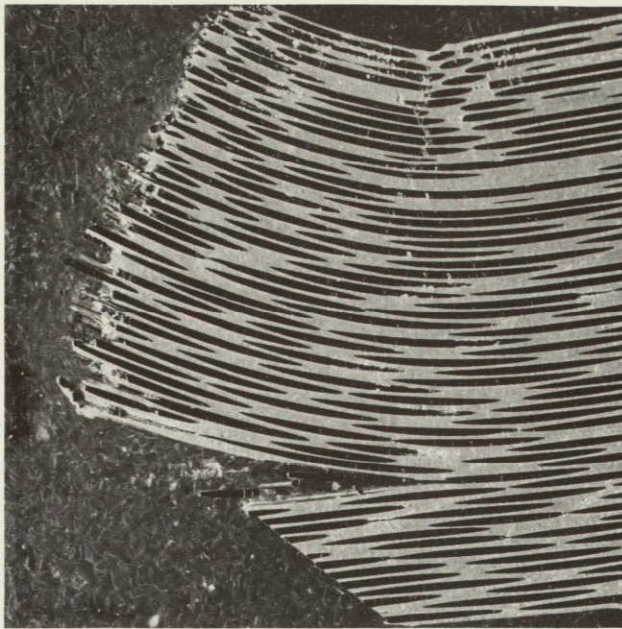
0.014 cm (5.6 mil) B-1100Al   10 X
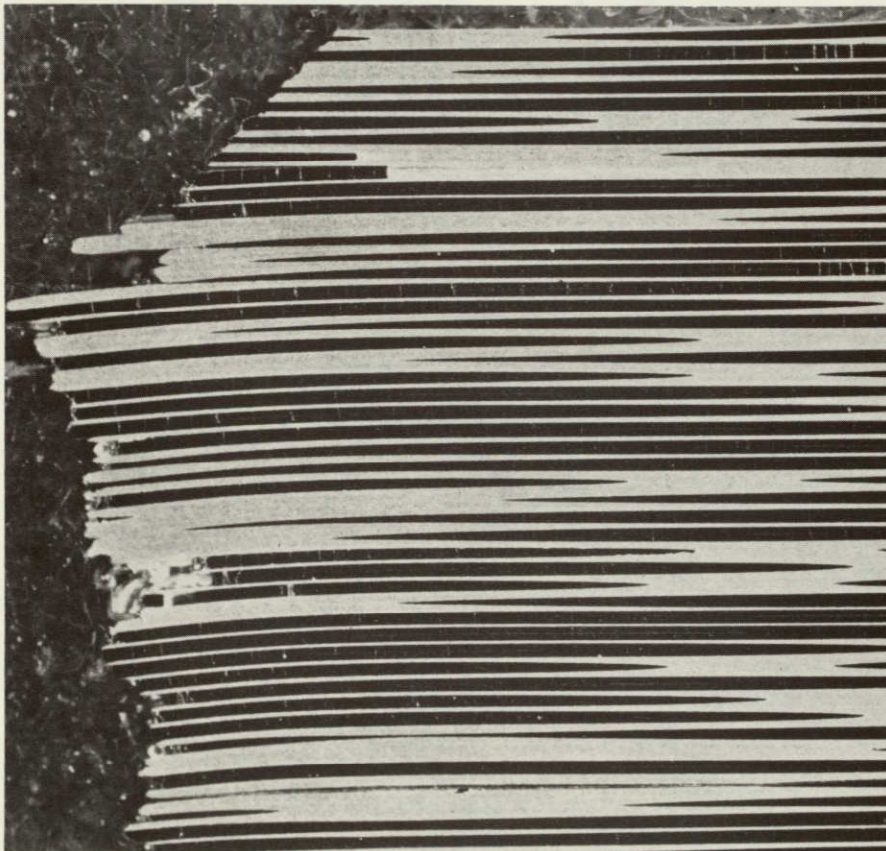
0.014 cm (5.6 mil) B-5052Al   10 X

Figure 10.   Metallography of Fractured Charpy Specimens Showing: 1) Severe
             Deformation and Secondary Crack in B-1100Al (Top) and 2) Planar
             Type of Fracture in B-5052Al (Bottom).

27

Effect of Fiber Diameter

The selection of the larger fiber sizes for this program was based on both theoretical considerations and experimental evidence indicating improved composite pendulum impact resistance with increasing fiber diameter. This trend of increasing impact resistance with increasing fiber diameter is supported by the test results obtained with the longitudinal (LT) Charpy impact specimens of B-1100Al.

In the uniaxial composites, Table IV, the longitudinal tensile strength is higher with 0.014 cm (5.6 mil) boron in panels of both B-5052Al and B-1100Al fabricated by the foil-filament method. In the transverse tensile specimens some strength improvement is observed with the 0.02 cm (8.0 mil) boron fiber in the 1100Al matrix system. It should be pointed out that this comparison is based on specimens of B-1100Al and B-5052Al obtained using a particular set of processing conditions. Tensile strength will be affected by changes in processing procedures other than bonding temperature. This is exemplified in the panels of 0.02 cm (8.0 mil) B-1100Al (70-2 and 125-B, Table IV); the higher tensile strength in Panel 125-B is mostly the result of changes in the procedure employed in the preparation of matrix foil.

Charpy impact data for uniaxial composites, Table V, indicate an increase in impact resistance with increasing fiber diameter in B-1100Al and B-5052Al systems in both longitudinal and transverse impact orientations. However, the effect of fiber diameter is more pronounced in the 1100Al matrix. The overall appearance of the 0.14 cm (5.6 mil) B-1100Al and 0.02 cm (8.0 mil) B-1100Al notched Charpy specimens tested in the LT orientation is shown in Figure 11. Although basically similar in appearance, the crack in the 0.02 cm (8.0 mil) boron specimen is more ragged and the shear displacement at specimen ends is more pronounced. The latter can be attributed to the larger packets of matrix which permit additional deformation to occur in the specimen as a result of the shear stresses generated in the matrix parallel to the fibers. It is also of interest to observe that the greater shear displacement in 0.02 cm (8.0 mil) B-1100Al is accompanied by a more severe bending of the specimen as exemplified by the contour of the specimen surface opposite the notch.

Effect of Volume Reinforcement

To determine the effect of lower than 50v/o fiber reinforcement on tensile but particularly impact strength, tensile and Charpy specimens with 30v/o fiber reinforcement in B-5052Al were fabricated and tested. Tensile test results are included in Table IV. The lower level of fiber content is reflected in a corresponding reduction in tensile strength in longitudinal specimens. However, no significant change in tensile strength with decreasing fiber content is observed in the transverse testing orientation. Impact test results for 30v/o and 50v/o are summarized for B-5052Al in Table V. Here again, the lower level of fiber reinforcement resulted in a corresponding decrease in impact energy in the specimens of the LT orientation. However, impact resistance in the TT orientation was slightly improved.

28

0.014 cm (5.6 mil) B-1100A1   0.02 cm (8.0 mil) B-1100A1
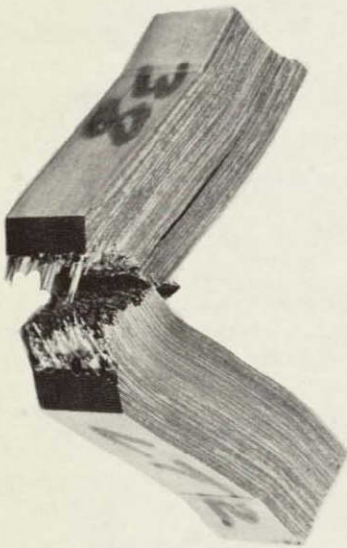
63.7 N-m (47.0 ft-lb)   96.3 N-m (71.0 ft-lb)

Figure 11. Comparison of the Effects of Filament Diameter on Crack Pattern
and Shear Deformation in Notched Charpy Specimens of B-1100A1.

It is of interest to note that in the longitudinal (LT) specimens of both 30v/o and 50v/o fiber reinforcement the cracks are of a similar brittle type and no shear deformation is found in the B-5052Al specimens with the higher matrix content. It is assumed that the B-1100Al data would be similar.

Because of the general reduction in both tensile and impact strength, the work with 30v/o fiber reinforcement was discontinued.

Effect of Matrix Enhancement

Matrix enhancement was incorporated in materials study because it provides a means of improving the transverse properties of B-Al system, particularly in the case of uniaxial fiber reinforcement. It has also been considered as a method to improve resistance to pullout in the blade root. Root pullout presents a potential problem with B-Al fan blades in the operating temperature range of 204°C (400°F) - 317°C (600°F) due to a drastic reduction in shear strength of aluminum.

Tensile test results for the B-1100Al + Ti system of uni-axial fiber reinforcement are presented in Table IV. Typical microstructure of the system is illustrated in Figure 5. It is of interest to note that in both B-1100Al and B-1100Al + Ti systems the longitudinal tensile strengths are consistently higher with the 0.014 cm (5.6 mil) boron fibers. In the uniaxial composites the effect of 12v/o Ti is reflected in about 25% increase in longitudinal and about fourfold increase in transverse tensile strength with both fibers. Significant improvement is also noticed in the strain to failure in the specimens of longitudinal but particularly transverse orientations. The elastic moduli are slightly lower in B-1100Al + Ti in both longitudinal and transverse orientations; the reduction is more pronounced, however, with the larger fibers.

The incorporation of titanium matrix enhancement foils into B-1100Al system produced a substantial reduction in impact resistance in the longitudinal (LT) and only a moderate improvement in the transverse (TT) impact orientations. Impact test data for the B-1100Al + Ti system with uniaxial fiber reinforcement are presented in Table V. In the longitudinal (LT) impact orientation the impact resistance is reduced (relative to B-1100Al) by about 50% in specimens with both 0.014 (5.6 mil) and 0.020 cm (8.0 mil) fibers. Impact resistance in the transverse (TT) orientation is slightly higher than in B-1100Al.

The reduction in impact resistance in the B-1100Al + Ti system can be attributed to the reduction of the overall matrix ductility as the result of incorporation of the stronger and less ductile Ti matrix into the B-1100Al system. This change in the overall matrix ductility is reflected in both the crack pattern and specimen deformation by shear. The appearance of the tested specimens of 0.0203 cm (8.0 mil) B-1100Al + Ti is illustrated in Figure 12. Compared to B-1100Al (Figure 11), the crack shows less distortion as well as a lower level of debonding and fiber pull-out. The shear displacement at specimens ends is also reduced. The crack

path in the longitudinal (LT) specimens of B-1100Al + Ti, illustrated in Figure 13, is significantly different from that observed in B-1100Al. It propagates in a steplike manner along the titanium foil planes and is accompanied by a moderate amount of debonding and fiber pullout.

Effect of Fabrication Method

The initial plan was to fabricate all test panels by the monotape method. Because of the debonding problems encountered early in the program in converting B-1100 monotapes into multi-ply test panels, the fabrication of test panels in this system was carried out by the foil-filament array method until the problem of low temperature bonding was resolved. However, selected panels were fabricated by both methods to compare mechanical properties. Longitudinal tensile strength values in the B-1100Al system were found to be nearly equivalent in panels fabricated at 455°C (850°F) by the monotape and foil-filament methods (Panel 14-A, Table II and Panel 70-2, Table IV).

Charpy impact properties of uniaxial B-5052Al, B-1100Al B-1100Al + Ti fabricated the monotape and foil-filament methods are presented in Table V. In B-5052Al, impact resistance is moderately higher in specimens fabricated at 455°C (850°F) by the monotape method (Panel #39 vs #51). Panel #103 was fabricated on an internal program by the monotape method at a lower 428°C (800°F) bonding temperature. The higher impact resistance in this panel is attributed to partial delamination between monotapes during testing. No direct comparison exists for Charpy impact resistance in B-1100Al system at 455°C (850°F) bonding temperature because the panel fabricated by the monotape method was damaged (partially delaminated) during machining. Using the available impact data obtained on specimens fabricated by the monotape method at 482°C (900°F) and the impact data for specimens fabricated at 455°C (850°F) by foil-filament method as a basis of comparison, a significant (about threefold) improvement in notched Charpy impact resistance is found in longitudinal (LT) specimens fabricated by the foil-filament method. Impact resistance with foil-filament B-1100Al was also higher than with foil-filament B-1100Al + Ti.

Due to economic considerations it was attempted to change the initial monotape method to get comparable results to foil-filament technique. The problem of low temperature bonding in B-1100Al was, therefore, investigated concurrently on a TRW internal program. As a result of this effort, a chemical surface treatment was developed for the 1100Al matrix which improved the matrix-matrix bond without change in bonding temperature. The effect of this improved monotape fabrication approach on impact resistance will be further discussed in Task IV.
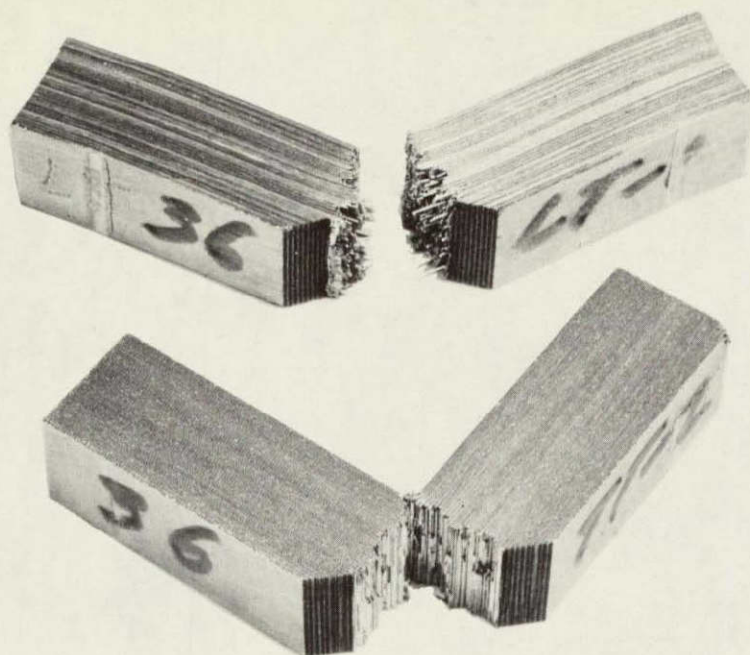
LT= 41.5 N-m (30.5 ft-lb)

TT = 4.1 N-m (3.0 ft-lb)
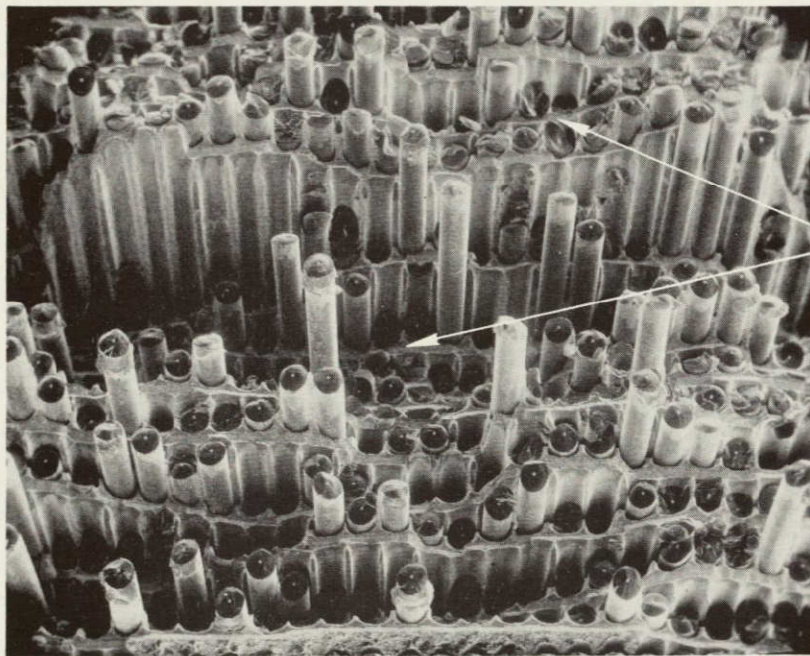
Figure 12. Fracture Mode and Shear Deformation in Notched Charpy Specimens
of B-1100Al + Ti.
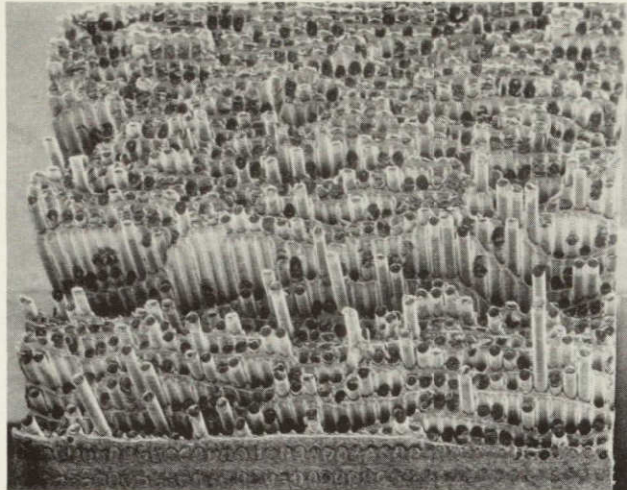
LT = 41.5 N-m (30.5 ft-lb)   10 X

Ti Foil

0.02 cm (8.0 mil) B-1100Al + Ti.   20 X

Figure 13.   Fractographs of 0.02 cm (8.0 mil) B-1100Al + Ti Charpy Specimens
Illustrating a Moderate Amount of Filament Pullout and a Step
Type of Crack Propagation Along Titanium Foil Planes.

Directionality Effect

To determine the effect of directionality on impact resistance, notched Charpy specimens of B-1100Al and B-1100Al + Ti were tested in the alternate longitudinal (LTs) impact orientation. Test results for these specimens are included in Table V. Impact energy in the LTs orientation is lower in all specimens. In the B-1100Al system impact energy is reduced by nearly 50%. In B-1100Al + Ti the reduction in impact energy is even greater. A comparison of the deformation pattern in specimens of B-1100Al tested in the standard LT and alternate LTs impact orientations is provided in Figure 14. The overall specimen deformation by bending and shear as evidenced by the material displacement of specimen ends is significantly greater in the standard LT than in the alternate LTs orientation. SEM fractographs in Figure 15 show a direct relationship between crack pattern and the extent of specimen deformation by bending and shear. The ragged appearance of the crack in the standard specimen is the result of entensive fiber - matrix delamination and the attendant fiber pullout. The orientation of the specimen also favors considerable deformation by shear to occur in the plane of the fibers as evidenced by the displacement at specimen ends. The orientation of the alternate specimen is less favorable in this respect. The result is a lower level of fiber-matrix debonding and fiber pullout as well as a smaller amount of specimen deformation by shear. However, the specimen shows significant spreading on the side of the striker.

STANDARD LT
Pressing Surface

LT = 96.5 N-m
(71.0 ft-lb)

ALTERNATE LT

Pressing Surface
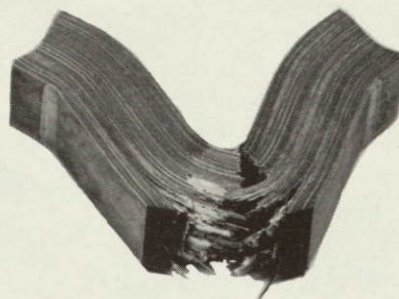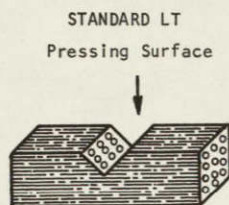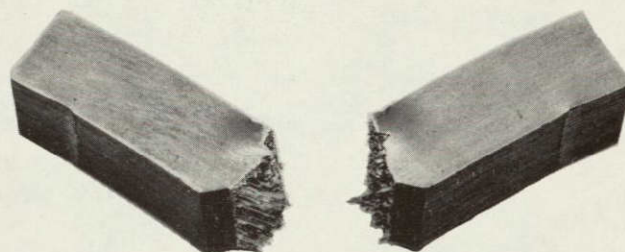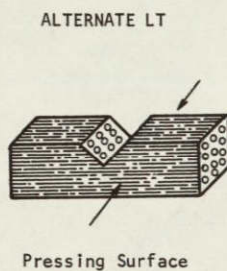
LTs = 47.5 N-m
(35.0 ft-lb)

0.02 cm (8.0 mil) B-1100Al

Figure 14.   Comparison of Crack Pattern and Shear Deformation in Charpy
              Specimens of 0.02 cm (8.0 mil) B-1100Al Tested in the
              Standard and the Alternate LT Impact Orientations.

35
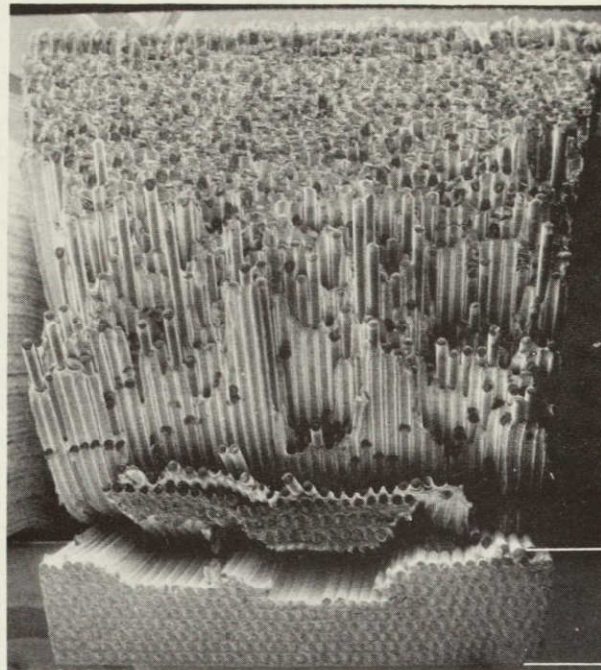
notch

6X
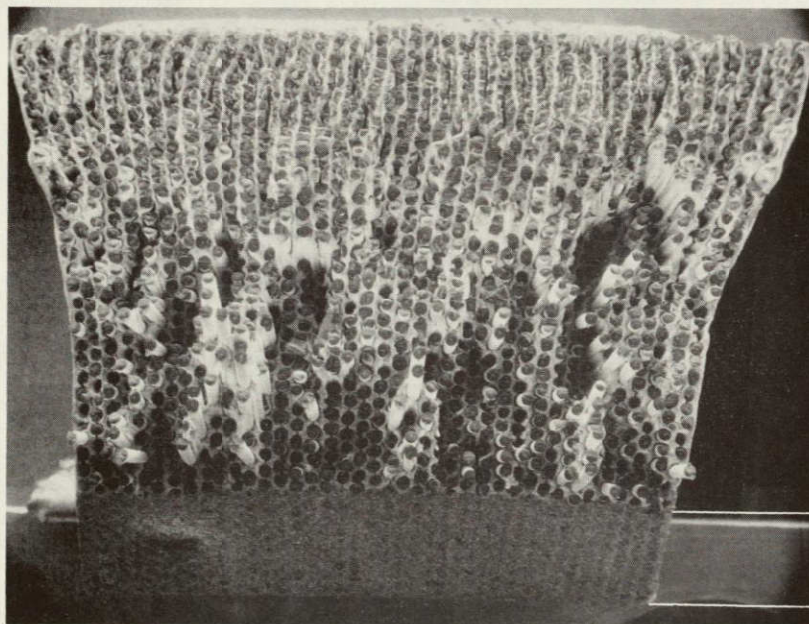
Spread Area

notch

0.02 cm (8.0 mil) B-1100Al.   6X

Figure 15. SEM Fractographs of Uniaxial B-1100Al Charpy Impact Specimens in
LT and LTs Orientations Illustrating: (a) Massive Interlaminar
Shear and Fiber Pullout (Top-LT) and, (b) Composite Cracks
Associated with the Compressive Deformation of the Specimen on
the Side Opposite the Notch (Bottom-LTs).

4.0 TASK II - FABRICATION AND CHARACTERIZATION
OF ANGLE-PLY REINFORCED COMPOSITE PANELS

The relatively low shear strength of aluminum results in a rapid reduction of tensile strength of uniaxially reinforced B-Al in orientations much over 5° from the filament axis. This characteristic renders uniaxial B-Al unsuitable for fan blade applications where complex stress conditions prevail. To combat this low off-axis strength and improve torsional rigidity, various angle-ply orientations and combinations of uniaxial and angle-plying have been proposed and evaluated. The selection of the angle-ply combination was usually based on particular blade design and performance requirement.

This task was designed to fabricate and characterize angle-ply reinforced composite panels. The best combination of materials and lay-up design selected in this task would be used in the evaluation of root attachments and the fabrication of a process demonstration fan blade.

Three angle-ply designs were investigated in this task. The first is commonly designated $(\pm 45/0_2)_s$. It consists of 50% of unidirectionally reinforced plies ·in the central core with 25% of the alternating $\pm 45°$ plies on each side of the core. The second is designated $(0/\pm 22)nT$ and ·consists of repetitive units of 0, +22, -22 plies up to the desired thickness. The third design is dispersed $\pm 15°$ and consists of alternate layers of +15, -15 plies up to the desired thickness. As part of the overall materials screening study, the above designs were evaluated in conjunction with two fiber diameters, two matrices, and matrix enhancement. Mechanical properties were evaluated both at room and elevated temperatures.

4.1   Experimental Procedures

The procedures employed in the fabrication of test panels by both the foil-filament array and the improved monotape methods have been described in detail in Task I. Tensile panels were pressed in open dies; the Charpy panels were pressed in a channel-type die to provide lateral constraint.

The number of plies in the tensile panels was based on symmetry considerations. Six plies were used in the $\pm 22°$, 0° construction. Eight plies were used in both the 0° core, $\pm 45°$ shell, and the $\pm 15°$ constructions. Panel size was 15.24 (6.0 in) x 10.16 cm (4.0 in) to provide duplicate tensile specimens of longitudinal and transverse orientations. Charpy panels were 12.7 cm (5.0 in) x 5.85 cm (2.3 in) to provide duplicate Charpy specimens of LT and TT orientations for room and elevated temperature testing. Bonding parameters of 455°C (850°F), 57.0 MN/m^2 (8 ksi), 30 min. were employed in the fabrication of B-5052Al panels by the monotape method. Bonding pressure of 70.0 MN/m^2 (10 ksi) was used for the fabrication of angle-plied composites by the foil-filament method. The procedures employed in the preparation and room temperature testing were described in Task I. Heating of specimens for elevated temperature impact testing was accomplished in a tube furnace.

4.2   Results and Discussion

In Task I, the influence of material and processing variables on mechanical properties in uniaxially reinforced composites were investigated. It was shown that composite property was strongly affected by the matrix material. Of the two matrices studies, 1100Al and 5052Al, the 1100Al matrix showed significantly higher impact resistance in notched Charpy specimens of the longitudinal (LT) orientation. Tensile strength, on the other hand, was higher in B-5052Al. Impact resistance increased with larger filaments but decreased with matrix enhancement. The composites also showed a strong directionality effect.

A similar pattern was also observed in the angle-plied composites studies in this task. In the following paragraphs the test results in Task II are analyzed in terms of matrix material, matrix enhancement, fabrication method, directionality, notch effect, processing variables and angle-plying.

Effect of Matrix Material

In Task I, tensile strength of uniaxial B-5052Al composite was found to be higher than that of B-1100Al. Impact resistance of B-5052Al, on the other hand, was rather poor in longitudinal (LT) specimens fabricated by both the monotape and the foil-filament methods. In Task II, selected Charpy panels of B-5052Al were fabricated and impact tested at room temperature to determine the potential of the 5052Al matrix in angle-plied constructions. Charpy impact test data for these panels are presented in Table VI. Impact resistance of the longitudinal (LT) specimens of 0°, $\pm 22°$ B-5052Al is quite low and represents only about 20% of the strength obtained in B-1100Al specimens of the same fiber size and angle-ply layup. Impact energy is also lower in the transverse (TT) orientation. About equally low strength levels are also observed in B-5052Al specimens with the dispersed (0/$\pm 45°$)nT layup. All specimens show a planar type of fracture and a low level of fiber pullout. Because of low impact resistance in both uniaxial and angle-plied constructions, further work with the 5052Al matrix was discontinued. With the exception of a limited number of matrix enhancement panels, all subsequent work in this program was limited to B-1100Al system.

Effect of Matrix Enhancement

The influence of matrix enhancement on tensile and impact properties of angle-plied composites were determined on specimens of $\pm 22°$, 0°, angle-plied B-1100Al. Tensile test results are summarized in Table VII. The longitudinal tensile strength in both B-1100Al and B-1100Al + Ti is about equivalent. The positive effect of matrix

38

TABLE VI

CHARPY IMPACT PROPERTIES OF ANGLE-PLIED COMPOSITES

Panel No.	Matrix	Fiber Dia. cm (mils)	Layup	Fabrication Method	Impact Orientation	Impact Energy N-m (ft-lb)
45	5052Al	0.014 (5.6)	±22°,0°	Mono.	LT	10.2 (7.5)
"	"	"	"	"	"	10.9 (8.0)
"	"	"	"	"	TT	4.0 (3.0)
"	"	"	"	"	"	2.7 (2.0)
44	5052Al	0.014 (5.6)	±45°,0°	Mono.	LT	8.1 (6.0)
"	"	"	Dispersed	"	"	7.5 (5.5)
"	"	"	"	"	TT	4.7 (3.5)
"	"	"	"	"	"	5.4 (4.0)
56	1100Al	0.014 (5.6)	±15°	Foil-Fil.	LT	49.5 (36.5)
"	"	"	"	"	"	54.9 (40.5)
"	"	"	"	"	LT	54.0 (40.0)*
"	"	"	"	"	"	54.9 (40.5)*
"	"	"	"	"	TT	6.1 (4.5)
"	"	"	"	"	"	6.1 (4.5)
93	1100Al	0.014 (5.6)	±15	Mono.	LT	38.0 (28.0)**
"	"	"	"	"	"	25.8 (19.0)
"	"	"	"	"	LT$_s$	14.9 (11.0)
"	"	"	"	"	"	13.6 (10.0)
49	1100Al	0.02 (8.0)	±15°	Foil-Fil.	LT	80.7 (59.5)
"	"	"	"	"	"	76.0 (56.0)
"	"	"	"	"	TT	8.8 (6.5)
"	"	"	"	"	"	8.1 (6.0)

* Unnotched, no failure.

** Unnotched.

(contd)

TABLE VI (continued)

CHARPY IMPACT PROPERTIES OF ANGLE-PLIED COMPOSITES

Panel No.	Matrix	Fiber Dia. cm (mils)	Layup	Fabrication Method	Impact Orientation	Impact Energy N-m (ft-lb)
99	1100Al	0.02 (8.0)	±15°	Mono.	LT	20.3 (15.0)**
"	"	"	"	"	"	5.4 (4.0)
"	"	"	"	"	LT$_s$	11.5 (8.5)
"	"	"	"	"	"	11.5 (8.5)
47	1100Al	0.014 (5.6)	±22°,0°	Foil-Fil.	LT	52.9 (39.0)
"	"	"	"	"	"	53.6 (39.4)
"	"	"	"	"	TT	17.0 (12.4)
"	"	"	"	"	"	14.2 (10.5)
69	1100Al	0.02 (8.0)	±22°,0°	Foil-Fil.	LT	55.6 (41.0)
"	"	"	"	"	"	48.8 (36.0)
"	"	"	"	"	"	66.5 (49.0) **
"	"	"	"	"	"	79.4 (58.5)
"	"	"	"	"	TT	12.9 (9.5)
"	"	"	"	"	"	19.5 (7.0)
94	1100Al	0.02 (8.0)	±22°,0°	Mono.	LT	74.6 (55.0) *
"	"	"	"	"	"	47.5 (35.0)
"	"	"	"	"	LT$_s$	15.6 (11.5)
"	"	"	"	"	"	14.9 (11.0)
67	1100Al +Ti	0.02 8.0)	±22°,0°	Foil-Fil.	LT	26.5 (19.5)
"	"	"	"	"	"	22.4 (16.5)
"	"	"	"	"	LT$_s$	8.1 (6.0)
"	"	"	"	"	"	13.6 (10.0)
"	"	"	"	"	TT	8.8) 6.5)
"	"	"	"	"	"	16.3 (12.0)

40

(contd)

TABLE VI (continued)

CHARPY IMPACT PROPERTIES OF ANGLE-PLIED COMPOSITES

Panel No.	Matrix	Fiber Dia. cm (mils)	Layup	Fabrication Method	Impact Orientation	Impact Energy N-m (ft-lb)
52	1100Al	0.014 (5.6)	±45,0°	Foil-Fil.	LT	127.5 (94.0) **
"	"	"	"	"	"	103.1 (76.0) **
"	"	"	"	"	LT$_s$	58.3 (43.0) **
"	"	"	"	"	"	50.9 (37.5) **
"	"	"	"	"	TT	59.0 (43.5) **
"	"	"	"	"	"	65.1 (48.0) **
53	1100Al	0.014 (5.6)	±45°,0°	Foil-Fil.	LT	42.0 (31.0)
"	"	"	"	"	"	32.6 (24.0)
"	"	"	"	"	TT	19.0 (14.0)
"	"	"	"	"	"	17.6 (13.0)
73	1100Al	0.02 (8.0)	±45°,0°	Mono.	LT	27.1 (20.0)
"	"	"	"	"	"	28.5 (21.0)
"	"	"	"	"	TT	9.5 (7.0)
96	1100Al	0.02 (8.0)	±45°,0°	Mono.	LT	46.1 (34.0)
"	"	"	"	"	"	46.1 (34.0)**
"	"	"	"	"	LT$_s$	27.1 (20.0)
"	"	"	"	"	"	27.8 (20.5)

TABLE VII

TENSILE PROPERTIES OF ANGLE-PLIED 50 V/O B-1100 Al COMPOSITES

Panel No.	Fiber Dia. cm (mils)	Layup	Orientation	UTS MN/m² (ft-lb)	Modulus 10⁶ M N/m² (10⁶ PSI)	Strain to Failure, μ-cm/cm μ-in/in
54-1	0.014 (5.6)	±15°	long.	1018.4 (147.7)	206.2 (29.9)	7,000
"	"	"	"	1000.5 (145.1)	235.1 (34.1)	7,200
"	"	"	trans.	7.0 (10.1)	141.3 (20.5)	3,000
"	"	"	"	6.1 (8.8)	158.6 (23.0)	-
48-3	0.02 (8.0)	±15°	long.	790.2 (114.6)	191.0 (27.7)	≥9,000
"	"	"	"	768.1 (111.4)	195.8 (28.4)	≥6,600
"	"	"	trans.	57.2 (8.3)	124.8 (18.1)	1,600
"	"	"	"	62.0 (9.0)	126.2 (18.3)	2,200
48-2	0.014 (5.6)	±22°, 0°	long.	856.4 (124.2)	215.8 (31.3)	6,200
"	"	"	"	930.1 (134.9)	205.5 (29.8)	8,000
"	"	"	trans.	54.0 (7.7)	137.9 (20.0)	≥2,400
"	"	"	"	65.5 (9.5)	110.3 (16.0)	3,800
68-2*	0.02 (8.0)	±22°, 0°	long.	730.2 (105.9)	188.9 (27.4)	7,000
"	"	"	"	597.0 (86.8)	203.4 (29.5)	5,000
"	"	"	trans.	53.8 (7.8)	117.9 (17.1)	2,600
"	"	"	"	50.3 (7.3)	137.2 (19.9)	-
68-1*	0.02 (8.0)	±22°, 0°	long.	714.3 (103.6)	162.7 (23.6)	7,000
"	+Ti	"	"	714.3 (103.6)	233.0 (33.8)	7,400
"	"	"	trans.	331.6 (48.1)	96.5 (14.0)	16,000
"	"	"	"	294.4 (42.7)	82.7 (12.0)	14,800
54-2	0.014 (5.6)	(±45°), 0°	long.	855.0 (124.0)	146.9 (21.3)	7,600
"	"	"	"	822.6 (119.3)	167.5 (24.3)	7,400
"	"	"	trans.	113.1 (16.4)	113.1 (16.4)	≥2,500
"	"	"	"	99.3 (14.4)	106.9 (15.5)	≥8,000

*Pressing run including panels 68-1 and 68-2 is suspect on account of lower than expected longitudinal tensile properties.

enhancement is observed in the transverse orientation showing about six-fold increase in tensile strength. The elastic moduli are lower with matrix enhancement in both longitudinal and transverse orientations. The effect of matrix enhancement on transverse strain is significant. Similar improvement in strain was also observed in uniaxial B-1100 Al + Ti in Task I.

Pendulum impact test results obtained on notched Charpy speci-mens of ±22°, 0°, B-1100Al are presented in Table VI. Consistent with the trend observed in Task I, the impact resistance in B-1100 + Ti is about 50% lower in specimens of the longitudinal (LT) and unchanged in the specimens of the transverse (TT) orientations. The reduction in the longitudinal (LT) impact resistance is also reflected in the lower level of specimen deformation by shear and a planar type of crack showing a moderate amount of fiber pullout. It is of interest to note that the relatively high strain capability of B-1100Al + Ti in tension is not in itself an indication of the material's performance under impact conditions.

Effect of Fiber Diameter

The effect of fiber diameter on tensile and Charpy impact properties in angle-ply reinforced composites is in agreement with the results obtained on uniaxial composites in Task I. Tensile properties of 50 v/o B-1100Al angle-plied composites are presented in Table VII. The ultimate tensile strength, strain to failure and elastic moduli, are generally higher with 5.6 boron fibers in the longitudinal and about equal in the transverse testing orientation for the same angle-ply con-structions. An exception to the above pattern is observed in the dis-persed ±15° construction where the strain to failure appears to be slightly higher in the longitudinal but lower in the transverse orienta-tions with the 0.02 cm (8.0 mil) fibers.

Charpy impact properties of angle-plied composites are summarized in Table VI. In the B-1100Al system, impact resistance is higher with 0.02 cm (8.0 mil) boron fibers in notched specimens of longitudinal (LT) orientation in all three types of angle-ply con-structions. In the transverse (TT) orientation, the ±22°, 0° construc-tion is an exception to the above pattern in that higher impact energy is found in specimens with 0.014 cm (5.6 mil) boron fibers. In general, the effect of fiber diameter on impact resistance in the transverse (TT) orientation is less pronounced.

Effect of Test Temperature

Duplicate sets of specimens of longitudinal (LT) and trans-verse (TT) orientations representing the three types of angle-ply con-structions were impact-tested at 205°C (400°F). The test results are presented in Table VIII. Included in the table are also room temperature tests for comparison. In the longitudinal (LT) orientation, a moderate

TABLE VIII

CHARPY IMPACT PROPERTIES OF ANGLE-PLIED COMPOSITES TESTED AT 205°C (400°F)

Panel No.	Matrix	Fiber Dia. cm (mils)	Layup	Fabrication Method	Impact Orientation	Impact Energy N-m (ft-lb)	
						RT	205°C (400°F)
49	1100Al	0.02 (8.0)	±15°	Foil-Fil.	LT	80.8 (59.5)	73.3 (54.0)
"	"	"	"	"	"	76.0 (56.0)	71.9 (53.0)
"	"	"	"	"	TT	8.8 (6.5)	10.9 (8.0)
"	"	"	"	"	"	8.1 (6.0)	10.9 (8.0)
47	1100Al	0.014 (5.6)	±22°,0°	Foil-Fil.	LT	52.9 (39.0)	67.8 (50.0)
"	"	"	"	"	"	53.6 (39.5)	69.2 (51.0)
"	"	"	"	"	TT	14.2 (10.5)	19.0 (14.0)
"	"	"	"	"	"	17.0 (12.5)	19.0 (14.0)
52	1100Al	0.014 (5.6)	±45°,0°°	Foil-Fil.	TT	59.0 (43.5)*	57.7 (42.5) *
"	"	"	"	"	"	65.1 (48.0)*	64.4 (47.5) *
53	1100Al	0.014 (5.6)	±45°,0°	Foil-Fil.	LT	42.0 (31.0)	41.4 (30.5)
"	"	"	"	"	"	32.6 (24.0)	44.1 (32.5)
"	"	"	"	"	TT	19.0 (14.0)	21.7 (16.0)
"	"	"	"	"	"	17.6 (13.0)	22.4 (16.5)

* Unnotched.

improvement in impact resistance with temperature is observed in the
+22°, 0° construction. No change is evident in the two other orienta-
tions. However, impact resistance is moderately higher at 204°C (400°F)
in all transverse (TT) specimens. .

Effect of Angle-Plying

Tensile properties for the three angle-ply constructions are
presented in Table VII.. In the B-1100A1 system, highest tensile strength
in the longitudinal testing orientation exists in the ±15° dispersed
angle-ply construction. Next in order of decreasing longitudinal tensile
strength are ±22°, 0° and ±45°, 0° constructions. Transverse properties
are generally low and are about-equivalent in the ±22°, 0° and ±15° con-
structions with both fibers. A moderate improvement in transverse
tensile strength is noticeable in the ±45°, 0° construction. Longitudinal
moduli are about equivalent in the ±22°, 0° and ±15°, but slightly lower
in the ±45°, 0° specimens. A similar pattern is also noticeable in the
transverse moduli.

Charpy impact properties of angle-plied composites are sum-
marized in Table VI. In the longitudinal (LT) orientation, impact
resistance is generally higher with the larger diameter fibers which is
consistent with the results obtained in Task I. Crack pattern and overall
specimen deformation by shear in the three types of angle-plied construc-
tions are illustrated in Figure 16. Of the three angle-ply orientations
studied, highest impact resistance in the longitudinal (LT) orientation
is found in the ±15° construction. Next in order of decreasing impact
resistance are ±22°, 0° and ±45°, 0° constructions. The sequence is the
same as in the tensile specimens tested in the longitudinal orientation.
In the transverse (TT) impact orientation, the order of impact resistance
is reversed. The highest impact resistance is found in the 0° core,
±45° shell construction; it is followed by ±22°, 0° and ±15° constructions.

The high impact resitance in the longitudinal (LT) Charpy
specimens of ±15° construction is basically the result of the low angle
of angle-plying relative to the direction of impact. Consequently, both
the strength of the material as well as the crack pattern and specimen
deformation by shear approximate that of the uniaxial material. In the
transverse (TT) impact orientation, the specimen fiber alignment is
closer to 90° orientation. Here the fracture mode typical of transverse
orientations predominates and the resultant impact resistance is low.
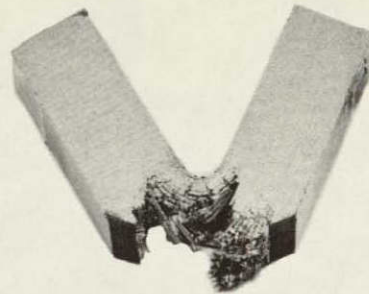
Notch Effect

To determine the effect of a notch on impact resistance of the
three types of angle-ply constructions, selected specimens were impacted
in both notched and unnotched conditions. Impact test results are pre-
sented in Table IX. The test data obtained with the ±15° construction are
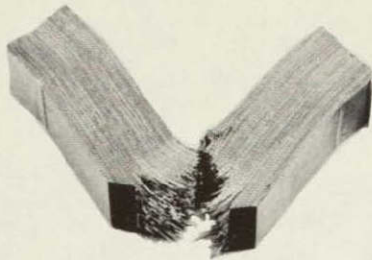
LT   /TT

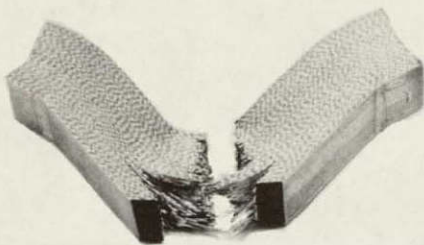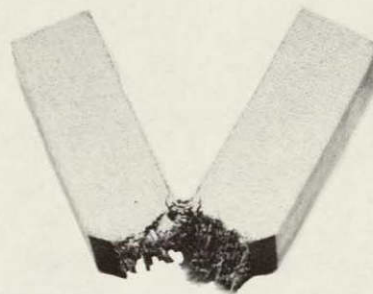(±22°, 0°), 0.014 cm (5.6 mil) B-1100Al.

LT   TT
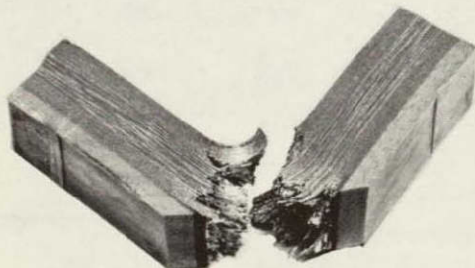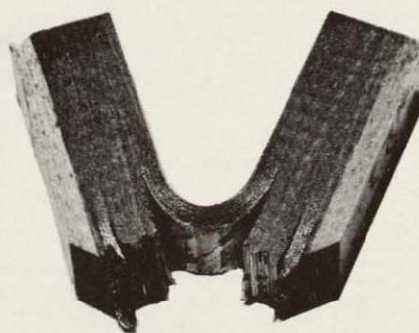

(±15°), 0.02 cm (8.0 mil) B-1100Al

LT   TT

(±45°, 0°)   0.014 cm (5.6 mil) B-1100Al.

Figure 16.   Fracture and Specimen Deformation in Angle-Plied B-1100Al.

46

TABLE IX

CHARPY IMPACT PROPERTIES OF UNNOTCHED ANGLE-PLIED COMPOSITES

| Panel No.	Matrix	Fiber Diameter cm (mils)	Layup	Fabrication Method	Impact Orientation	Impact Energy N-m (ft-lb) Unnotched	Notched
56	1100A1	0.014 (5.6)	±15°	Foil-Fil.	LT	54.2 (40.0)*	49.5 (36.5)
"	"	"	"	"	"	54.9 (40.5)*	54.9 (40.5)
69	1100A1	0.02 (8.0)	±22°,0°	Foil-Fil.	LT	66.4 (49.0)	48.8 (36.0)
"	"	"	"	"	"	79.3 (58.5)	55.6 (41.0)
52	1100A1	0.014 (5.6)	±45°,0°	Foil-Fil.	LT	127.5 (94.0)*	42.0 (31.0)
"	"	"	"	"	"	103.0 (76.0)	32.6 (24.0)
"	"	"	"	"	TT	59.0 (43.5)	19.0 (14.0)
"	"	"	"	"	"	65.0 (48.0)	17.6 (13.0)
"	"	"	"	"	LT$_s$	58.3 (43.0)	27.1 (20.0)
"	"	"	"	"	"	64.4 (47.5)	27.8 (20.5)

* No failure

47

meaningless because no fracture occurred and the specimens were deformed into a U-shape. In the ±22°, 0° construction, the absence of a notch resulted in a moderate increase in the longitudinal impact orientation. The significant increase in impact energy in the ±45°, 0° construction can be attributed to the presence of the ±45° angle-plied shell. The overall appearance of specimens is illustrated in Figure 17. In both longitudinal and transverse specimens, this shell has the same angle-ply orientation (±45°) with respect to the striker (impact direction). Because of its moderate strength and good ductility in bending, the shell provides a strong constraining force on the longitudinal oriented 0° core in the LT specimens. The effect of this constraint is to delay fracture by causing deformation to occur by specimen bending over a large radius. In the transverse (TT) specimens, the shell contributes to impact resistance in two ways. In the first place, the shell constrains the transversely (90°) oriented core and prevents it from breaking by a single crack of the type normally encountered in uniaxial specimens tested in the transverse (TT) orientation. Instead, the core fractures in several locations to varying depths, thus causing additional energy to be absorbed. Secondly, the shell located on the side opposite the striker does not fracture but deforms into a U-shape, absorbing energy in the process. A potential drawback of the core-shell construction as evidenced by the failure pattern found in these specimens is the relative weakness of the core-shell interface which becomes the plane of delamination.

Effect of Processing Variables

In Task I, it was found that composite property, but particularly impact resistance was most strongly affected by the matrix material. Notched Charpy impact resistance of B-5052Al was generally comparable to that of the more conventional composite systems such as B-6061Al and B-2024Al. The significant (about fivefold) improvement in notched Charpy impact resistance in B-1100Al over B-5052Al was attributed largely to matrix ductility. In the longitudinal (LT) specimens the relatively higher ductility of the 1100Al matrix permitted a considerable deformation to occur as a result of the shear stresses generated in the matrix parallel to the fibers.

Notched Charpy impact resistance in B-Al composites is also strongly influenced by the strength of the fiber-matrix bond. It was pointed out earlier that at the 455°C (850°F) bonding temperatrue the matrix-fiber bond was much stronger in B-5052Al than in B-1100Al. The weaker bond in B-1100Al was the result of tenacious oxide film on the matrix foil which acted as a diffusion barrier. This difference in the strength of fiber matrix bond was greatly responsible for the differences in the crack pattern and overall specimen deformation in B-5052Al and B-1100Al. The strong fiber-matrix bond in B-5052Al resulted in a planar type of crack showing an insignificant amount of fiber pullout and practically no fiber-matrix debonding. Also, no specimen deformation by shear was observed. In the B-1100Al specimens, on the other hand, the fiber-matrix debonding at the edge of the crack was rather pronounced and resulted in a significant fiber pullout. This condition is illustrated in Figure 9. The combined effect of debonding and fiber pullout
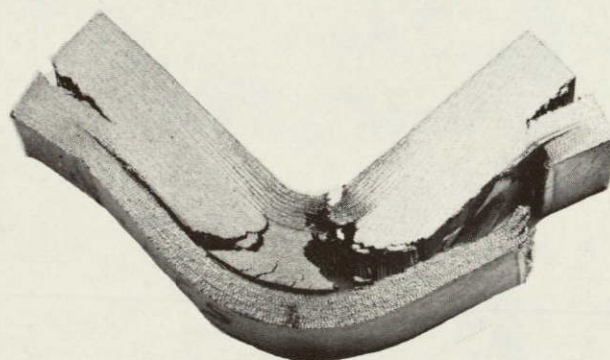
48
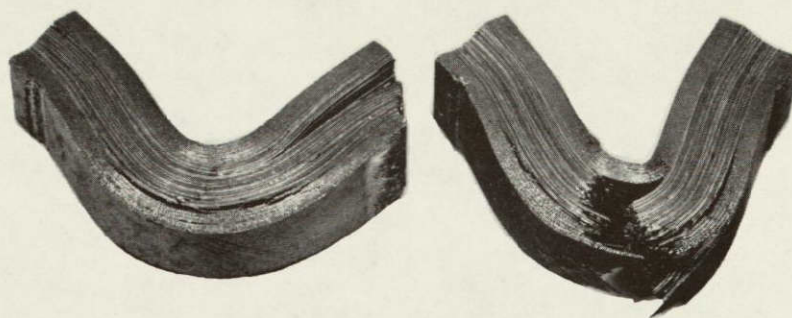
LT-1 = 127.5 N-m (94.0 ft-1b)   LT-2 = 103.0 N-m (76.0 ft-1b)
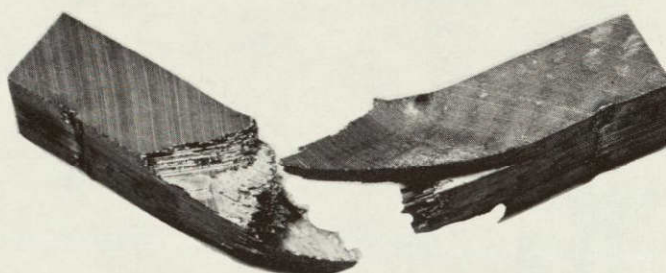
LT_S = 58.5 N-m (43.0 ft-1b)

TT = 59.0 N-m (43.5 ft-1b)

Figure 17.   Fracture Mode in Unnotched Charpy Specimens of $\pm45°$, 0° B-1100A1.

was both to blunt the crack edge and to form secondary cracks resulting in the absorption of additional energy. Furthermore, the stresses generated in the matrix also resulted in a significant amount of specimen deformation by shear as evidenced by the displacement at specimen ends, Figure 18 (bottom).

The strength of the fiber-matrix bond and impact resistance in B-1100Al is strongly affected by changes in processing variables such as bonding temperature and method of preparation of the matrix foil. The effect of matrix preparation on impact resistance as well as on the crack propagation and overall specimen deformation by shear is illustrated in Figure 18. Bonding temperature in both specimens was the same, but matrix foil preparation was different. Specimen #126A (Figure 18 - top) was fabricated on a TRW internal program as a part of the studies of the effects of various matrix foil surface treatments on low temperature bondability of 1100Al. The matrix foil used for this specimen was roughened to promote plastic deformation and breakup of the oxide film. Specimen #50 (Figure 18 - bottom) was fabricated using the conventional foil cleaning procedure which consists of etching in a nitric-hydrofluoric acid solution. The overall appearance of the crack in Specimen 126A is illustrated in Figure 19 (top). The crack is less irregular showing only a moderate amount of fiber pullout and practically no fiber-matrix debonding. The improvement in fiber-matrix bond as the result of foil-surface roughening is evidenced by the amount of aluminum coating adhering to the fiber surface, Figure 19 (bottom). As a consequence, specimen deformation by shear, as reflected by the displacement at specimen ends, has been substantially reduced.

The notched Charpy impact energy levels obtained on specimens of various material and angle-ply combinations were also found to be closely related to the extent of shear displacement at specimen ends. The relation between shear deformation and impact energy is illustrated in Figure 20. Test data for B-6061Al and B/SiC-(Ti(6,4) were obtained on TRW internal programs. Regardless of angle-ply and impact orientations, specimens with no observable shear displacement also show a low impact resistance, usually in the range of 10.8 N-m (8.0 ksi) - 20.3 N-m (15.0 ksi). Shear displacement increases with increasing impact energy and vice versa. Maximum shear displacement and impact energy is found in the uniaxial specimens of 0.02 cm (8.0 mil) B-1100Al tested in the standard LT orientation. The remaining data points for B-1100Al represent the effects of smaller fiber diameter, angle-ply orientations, changes in processing conditions, impact orientations and directionality.

The improvement in Charpy impact resistance of B-Al composites is illustrated in Figure 21. This was accomplished primarily by the use of larger diameter boron fibers, more ductile aluminum matrix material and optimization of the fiber-matrix bond strength.
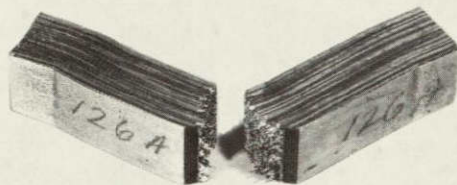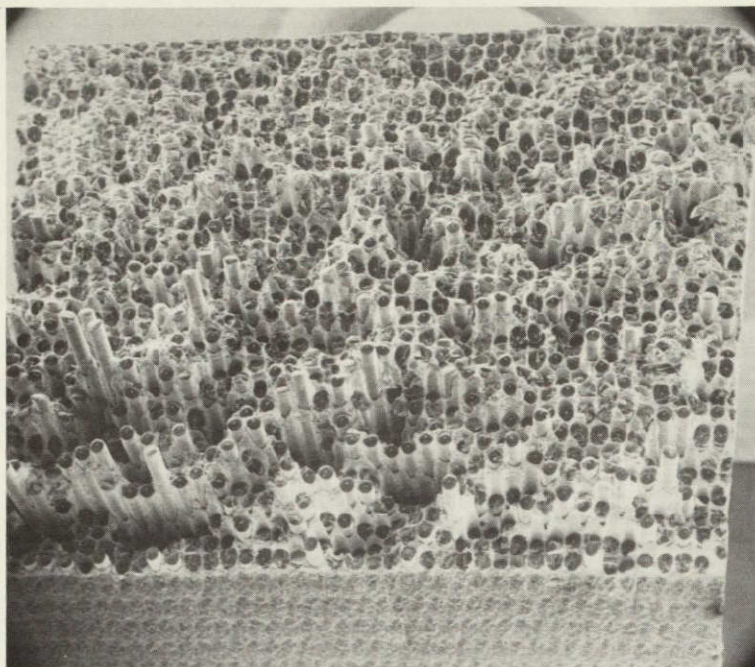
LT = 27.1 N-m (20.0 ft-1b)
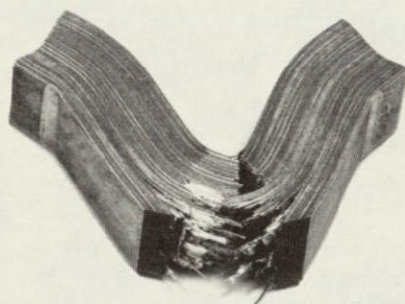
LT = 91.6 N-m(67.5 ft-1b)

0° U-D, 0.02 cm (8.0 mil)B-1100Al

Figure 18.   Effect of Processing Variables on Fracture Mode and Shear
Deformation in Uniaxial 0.02 cm (8.0) mil) B-1100Al.

LT = 27.1 N-m (20.0 ft-lb)   10 X
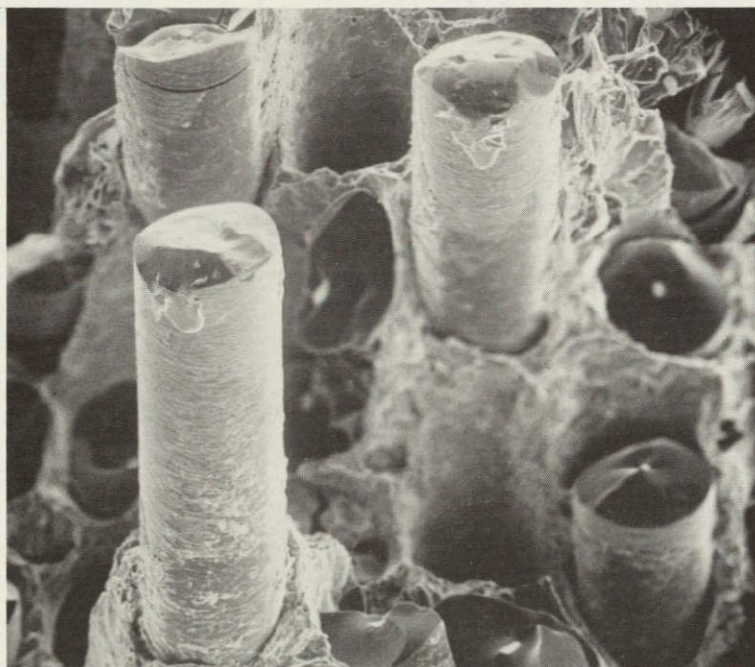
0° U-D, 0.02 cm (8.0 mil) B-1100A1   100 X

Figure 19.   SEM Fractographs of 0.02 cm (8.0 mil)B-1100A1 Charpy Specimens
              Illustrating the Effect of Processing Variables on Fiber-Matrix
              Bond and Fiber Pullout.

Figure 20.   Shear Deformation vs. Charpy Impact Resistance in
Metal Matrix Composites.

Figure 21.   Improvement in Charpy Impact Resistance in B-Al Composites.
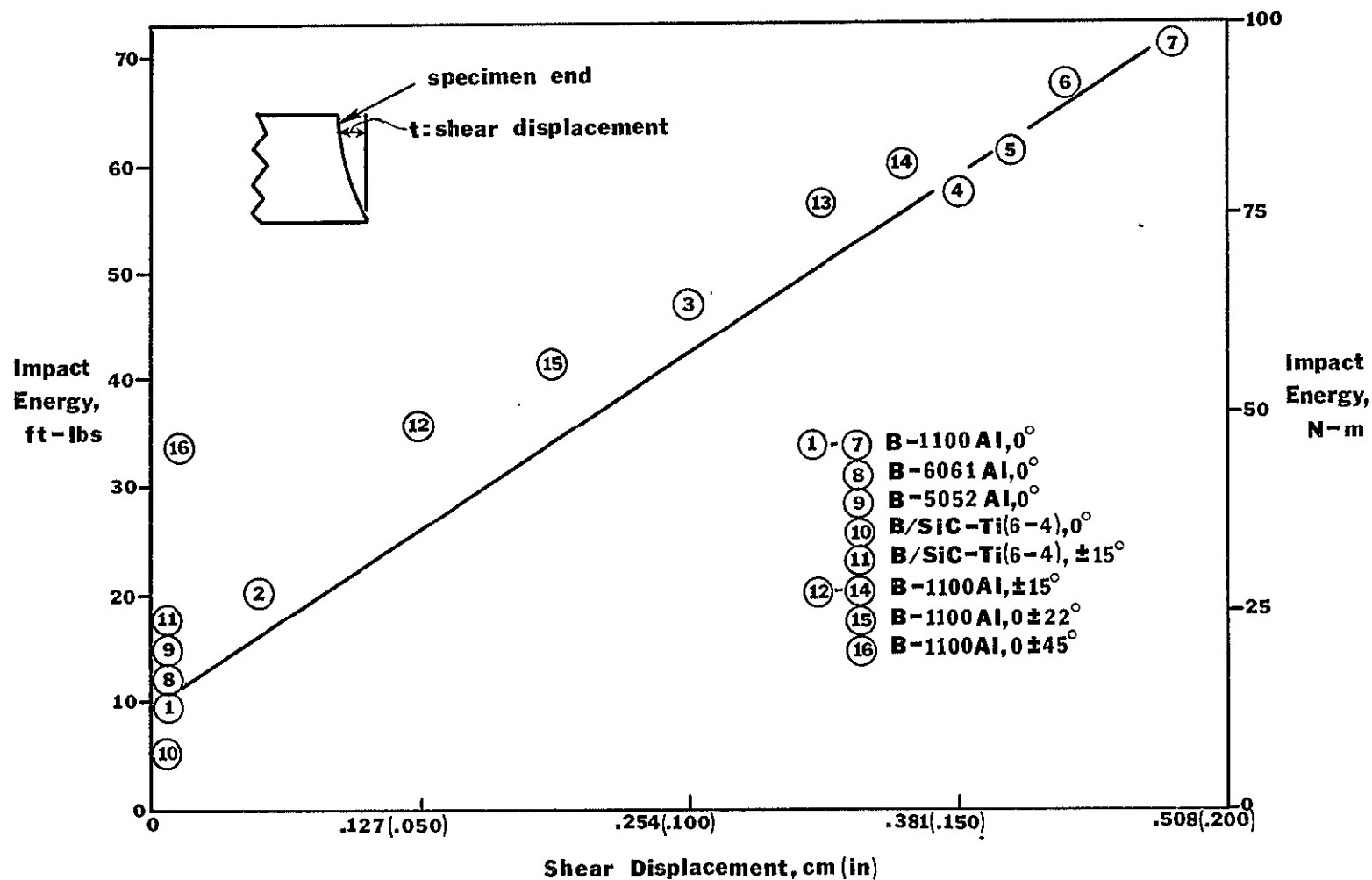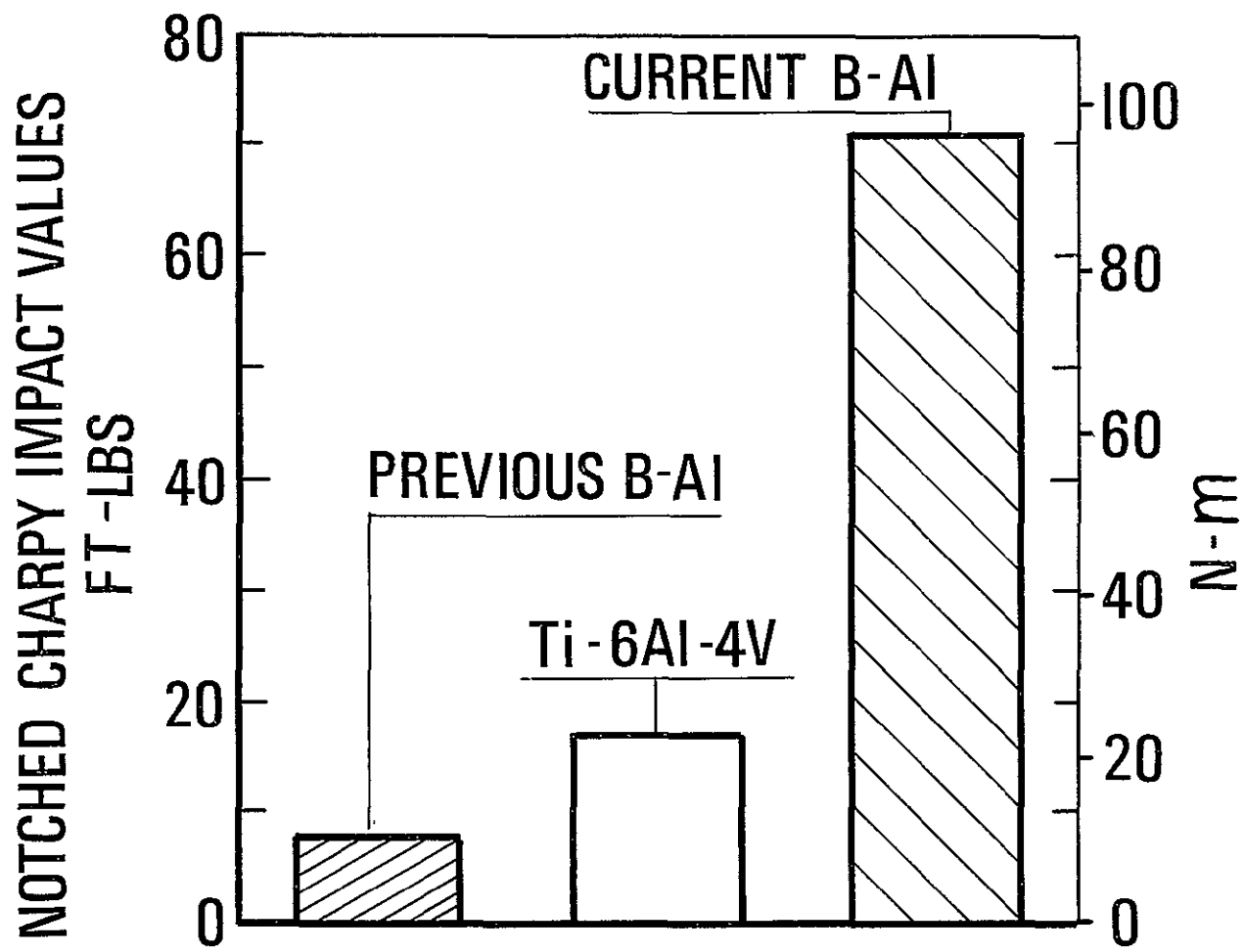
5.0 TASK III - DESIGN, FABRICATION AND CHARACTERIZATION
OF ROOT ATTACHMENT METHODS

Effective use of B-Al composite blades in gas turbines in the temperature range of 149°C (300°F) to 316°C (600°F) and full engine speeds requires root attachment schemes to prevent blade pullout in the root as a result of the combined forces imposed on the root under service conditions. Such root pullout occurs by interlaminar creep and is attributed to the inherently low shear strength of aluminum matrix materials. To minimize these problems, various types of root attachments have been employed depending on blade design and performance requirements. In general, these root attachment designs include titanium alloy root blocks with sufficient bearing strength to transfer loading to the disk and a splaying of reinforcing plies with internal wedges of materials such as titanium or aluminum. The objective of this task is to evaluate the various root designs and to select the most promising design to make the demonstration blades for Task IV.

The development work in Task III was carried out in two iterations. The details of root design and geometry employed in the first iteration are as follows:

1) Composite system: 50 v/o 0.02 cm (8.0 mil) B-1100Al.

2) Angle ply orientation: ±15°.

3) Root attachment design:

   a. Five-wedge consisting of 3 inner wedges and 2 outer wedges (root blocks).

   b. Three-wedge consisting of 1 inner wedge and 2 outer wedges (root blocks).

4) Wedge material:

   a. Outer wedges: Ti(6-4).

   b. Inner wedges: 6061Al in the five-wedge design; 6061Al and Ti(6;4) in the three-wedge design.

5) Cross section of specimen gauge: 1.9 cm (0.75 in) wide x 0.63 cm (0.26 in) thick.

6) Number of plies: 24.

7) Fabrication method: Monotape approach.

Four types of duplicate root specimens (or bladelike shapes) were fabricated:

Type A: 3 inner wedges of 6061Al.

Type B: 1 inner wedge of 6061Al.

Type C: 1 inner wedge of Ti(6,4).

Type D: All Ti(6,4) - machined from bar stock.

Within each type, one specimen was used for proof tensile testing and NDT; the other specimen was cut in half to provide two single root impact specimens.

The second iteration was to include one or more of the following:

a.   Foil filament approach.

b.   0.014 cm (5.6 mil) diameter boron.

c.   Another angleply orientation.

d.   Matrix enhancement in dovetail area.

Items a, b, c and d were to be performed with either 1 or 3 inner wedges, depending on the test results of the first iteration.

To complete this task, a root specimen of ±15°, 0.014 cm (5.6 mil) B-1100Al incorporating a single 6061Al inner wedge was fabricated by the monotape approach and tested in pendulum-Izod. Additional root specimens were fabricated as part of Task IV.

5.1   Experimental Procedures

Fabrication of Root Specimens (Bladelike Shapes)

All composite root specimens were fabricated by the monotape method. The monotapes were produced by vacuum hot pressure bonding, using pressing parameters of 455°C (850°F), 57.0 MN/m² (8 ksi), 15 min. The reduced (15 min) pressing cycle was used in the fabrication of monotapes to minimize 455°C (850°F) temperature exposure. Secondary fabrication was accomplished in a fully closed die cavity. The monotapes were first acid etched to size and chemical surface treated to enhance bondability. The individual ply and root attachment elements were then assembled in the pressing die cavity and vacuum encapsulated.

The inner and outer root wedges were precision machined from homogeneous Ti(6,4) and 6061Al. To facilitate specimen

assembly and eliminate possible shifting of elements, positive locators were incorporated into the root pieces which locked the assembly in the die cavity. The assembly is illustrated in Figure 22. Precautions were also taken to ensure that all root pieces were of the same volume. To accomplish this, the as-machined root pieces were standardized in weight by acid etching to remove excess stock.

Bonding parameters initially selected for the fabrication of root specimens were 455°C (850°F), 57.0 MN/m^2 (8 ksi), 15 min. Because of incomplete bond in the roots encountered in the first pressing, the specimen was subsequently repressed for 30 minutes in order to better determine the accuracy of the layup. Based on visual and radiography inspection results, bonding parameters of 455°C (850°F), 57.0 MN/m^2, (8 ksi), 30 min. were selected for the fabrication of·the remainder of the specimens.

The initial plan was to reduce specimen width from 2.54 cm (1 in) to 1.9 cm (0.75 in) by removing equal amounts of stock from each side of the specimen. The sole objective of this was to eliminate a possible detrimental edge effect (incomplete bond). But equally important was the high cost of original insert machining. The machining of the root specimens was therefore discontinued and the specimens were tested in both the as-pressed and trimmed conditions. This approach permitted fabrication of additional root specimens by reusing the original Ti(6,4) outserts and saving the cost of machining.

The above method was successfully employed for the fabrication of the balance of specimens in Task III and the additional specimens in Task IV. After pressing, testing and photography, the titanium root pieces were reclaimed by acid leaching without measurable stock loss.

After a minor ply adjustment (increase shank thickness) in the early stage, the fabrication of subsequent root specimens was carried out without change with good process reproducibility as evidenced by a uniformly sound bond in both the root and shank areas of the specimens.

Tensile Testing

Tensile testing of the root attachment specimens was accomplished in a Baldwin testing machine. A special set of grips was machined for this purpose to ensure a tight fit and uniform stress distribution on the outer wedge surfaces during testing. After loading in grips, backer plates were tightened against the flat root ends by means of threaded extension rods to prevent stress concentration and premature failure in any single root piece. During testing, cross-head deflection measurements were taken at 6.9 M N. (1000 lb) load increments to construct an approximate load-extension diagram.
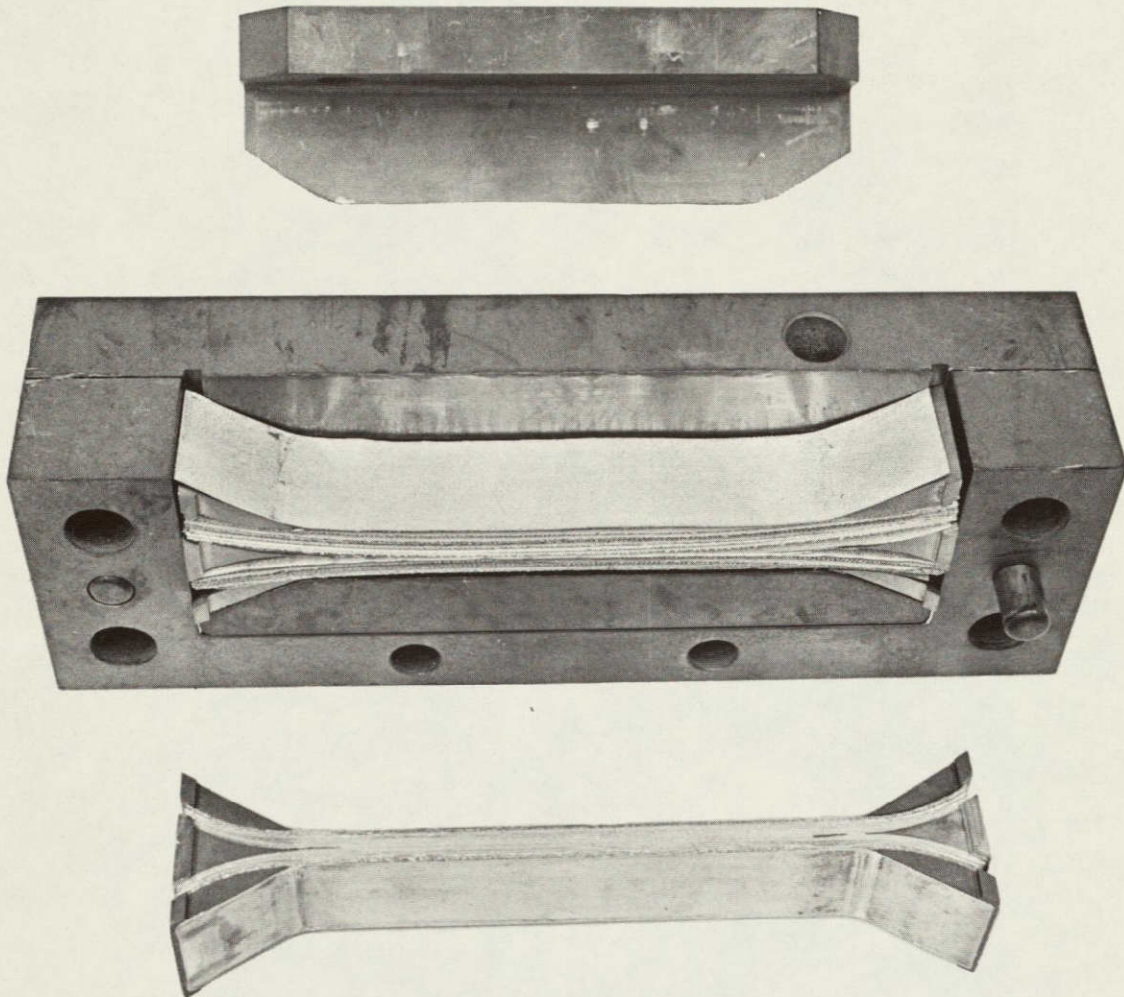
Figure 22.   Assembly of Monotape Plies and Root Wedges in the Bonding Die.

Pendulum Impact Testing

Pendulum impact testing was performed on a Sontag Universal testing machine. A specimen holder and an adaptation fixture were built to accommodate and secure this type of root configuration within the fixed clearances in the machine. The root specimens were impact-tested in the as-fabricated condition after they had been cut in half to provide two 7.62 cm (3.0 in) long test specimens. The point of impact was approximately two-thirds distance from the root radius, or about 1.8 cm (0.7 in) down from the specimen tip end. The overall testing setup is illustrated in Figure 23. Upon impact the absorbed energy was automatically recorded on the scale in ft-lbs. After testing the specimens were photographed and the titanium outserts reclaimed by acid leaching.

Analytical Tests

Analytical tests included visual and dimensional inspection, radiography, optical microscopy, and fiber extraction. Visual examination of the as-pressed specimens was primarily helpful in assessing the uniformity of stress distribution during pressing based on the appearance of flash pattern, particularly in the flat portion of the specimens. Ply delamination after impact testing also provided a quick visual assessment of any major inadequacy in the overall fabrication procedure. Radiography of the as-fabricated specimens in the side direction (normal to the pressing surface) was found very helpful during initial pressing experiments in that it revealed the lack of fill and/or bond in such critical areas as root blocks and root radius. Sequential leaching of plies was used to determine possible fiber breakage in the root and root transition radius.

5.2 Test Results and Discussion

Tensile Testing

Room temperature test results obtained on root attachment specimens are presented in Table X. The single and triple inner wedge root designs are illustrated in Figure 24. The white appearing strip in the single inner wedge specimen is homogeneous aluminum which was used to fill the void formed by the blunt edge of the titanium insert. Within the composite root specimens, maximum UTS value of 700.0 M N/m^2 (101.7 ksi) was obtained in the specimen of $\pm 15°$, 0.02 cm (8.0 mil) B-1100Al with a single 6061Al inner wedge. The failure occurred in the root radius with no readily observable delamination in the shank. The next highest UTS value of 685.0 M N/m^2 (99.5 ksi) was obtained in the specimen with the 0.014 cm (5.6 mil) boron fiber of the same layup and root design. The specimen also failed in root radius without delamination in the shank. The slightly lower UTS value obtained with this specimen is somewhat surprising in view of the consistently higher tensile values obtained with 0.014 cm (5.6 mil) fiber in Tasks I and II of the program. This may be attributed in part to the splayed radius in the root specimen which
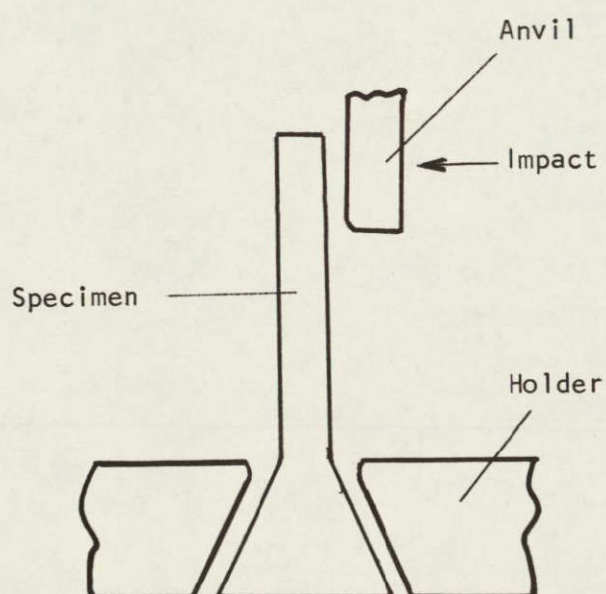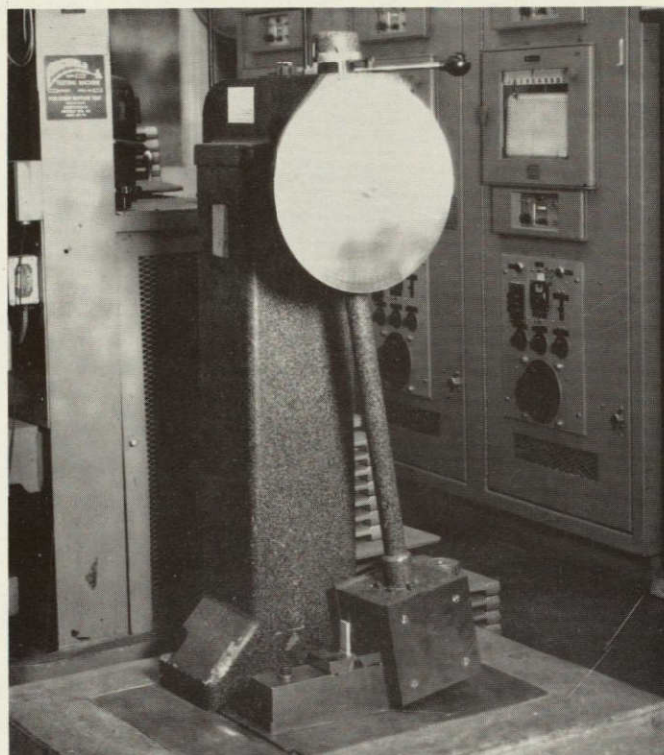
Figure 23.   Pendulum Impact Testing Setup for Bladelike Shape Specimens.

TABLE X

ROOT ATTACHMENT SPECIMEN TENSILE TEST RESULTS

| Specimen No.	System	Condition	Root Type	UTS M N/m^2 (KSI)	Remarks
1	0.02 cm (8.0 mil) B-1100Al	Trimmed	3 Inner Wedges 6061 Al	371.6 (53.9)	Failed in mid-shank by monotape delamination.
2	0.02 cm (8.0 mil) B-1100Al	Trimmed	3 Inner Wedges 6061Al	517.8 (75.1)	Failed in midshank by monotape delamination.
5	0.02 cm (8.0 mil) B-1100Al	As-Pressed	1 Inner Wedge 6061Al	701.2 (101.7)	Failed just above root radius.
7	0.02 cm (8.0 mil) B-1100Al	Trimmed	1 Inner Wedge Ti(6,4)	316.5 (45.9)	Failed in midshank by monotape delamination.
8	Ti(6,4)	Machined	Homogeneous Ti(6,4)	(1010.1 (146.5)	
10	0.014 cm (5.6 mil) B-1100Al	As-Pressed	1 Inner Wedge 6061Al	(686.0 (99.5)	Failed in root radius.

61
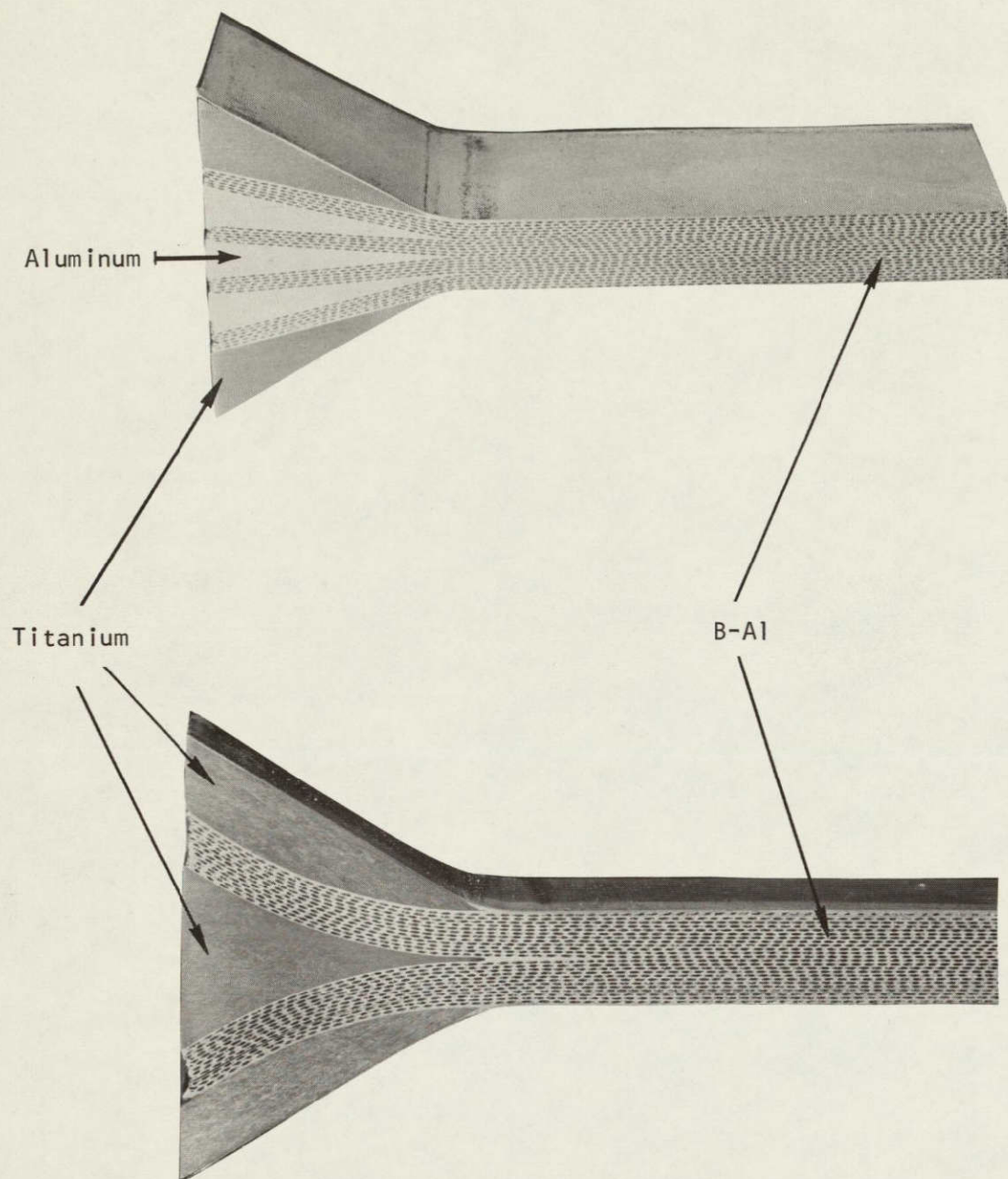
Figure 24. Macrophotographs of Bladelike Shape Test Specimens of Triple and Single Inner Wedge Designs.

would be expected to change failure mechanism and possibly reduce the effect of the differences in tensile strength of the two fibers. The presence of splayed fibers in the radius of the root specimen associated with a different fiber orientation to the head axis than in flat specimens can also account for the generally lower strength levels in the root specimens compared to standard tensile specimens of the same fiber diameter and ply orientation. The root specimen with the triple 6061Al inner wedge failed in the shank area at 518.0 M N/m^2 (75.1 ksi). Both the lower strength level and the location of failure in this specimen are attributed to monotape delamination. The above is also true of the root specimen with a single Ti(6,4) inner wedge which failed at 318.0 M N/m^2 (45.9 ksi).

Fiber integrity in the airfoil to root transition radius is very important because fiber breakage in that area would result in the reduction of load carrying capability in the critical portion of the blade. To determine the extent, if any, of fiber breakage, sequential leaching of plies was performed on root specimens and fiber integrity in individual layers was examined. No fiber breakage whatever was found in the root specimens of single and triple inner wedge design as illustrated in Figure 25.

Pendulum Impact Testing

Room temperature impact test results for the root attachment specimens are presented in Table XI. Failure modes in B-1100Al and homogeneous Ti(6,4) specimens are illustrated in Figure 26. No true failure occurred in the specimens RS-3, RS-4 and RS-6 due to debonding in the shank area. The resultant energy levels are low. The failure mode in these specimens is illustrated in Figure 26 (top). This lack of monotape bond in the initial set of specimens was caused by the excess material in the root area of the specimens which (in the absence of metal flow in a fully enclosed die cavity) resulted in the reduction of bonding pressure in the flat portion of the specimen. It may be of interest to point out that acid leaching of the tested specimens revealed no fiber breakage whatever in the root radius or the shank in spite of the fact that these specimens had undergone a double deformation: the initial impact and the reverse impact on the return of the pendulum to its starting position.

In the well consolidated specimens of ±15° construction with a single 6061Al inner wedge, higher impact energy was obtained with the 0.020 cm (8.0 mil) fibers. The test results are therefore consistent with those of Charpy specimens. However, the differences in the relative energy levels are more pronounced in the root specimens.

Table XI also includes energy data for two specimens which after initial testing were utilized for lay-up modifications in the shank area. Of these, specimen 5A was initially tested in tension and specimen 6-2A in pendulum impact. After repressing, both specimens were tested in impact. Specimen 6-2A is of interest in that it produced the highest
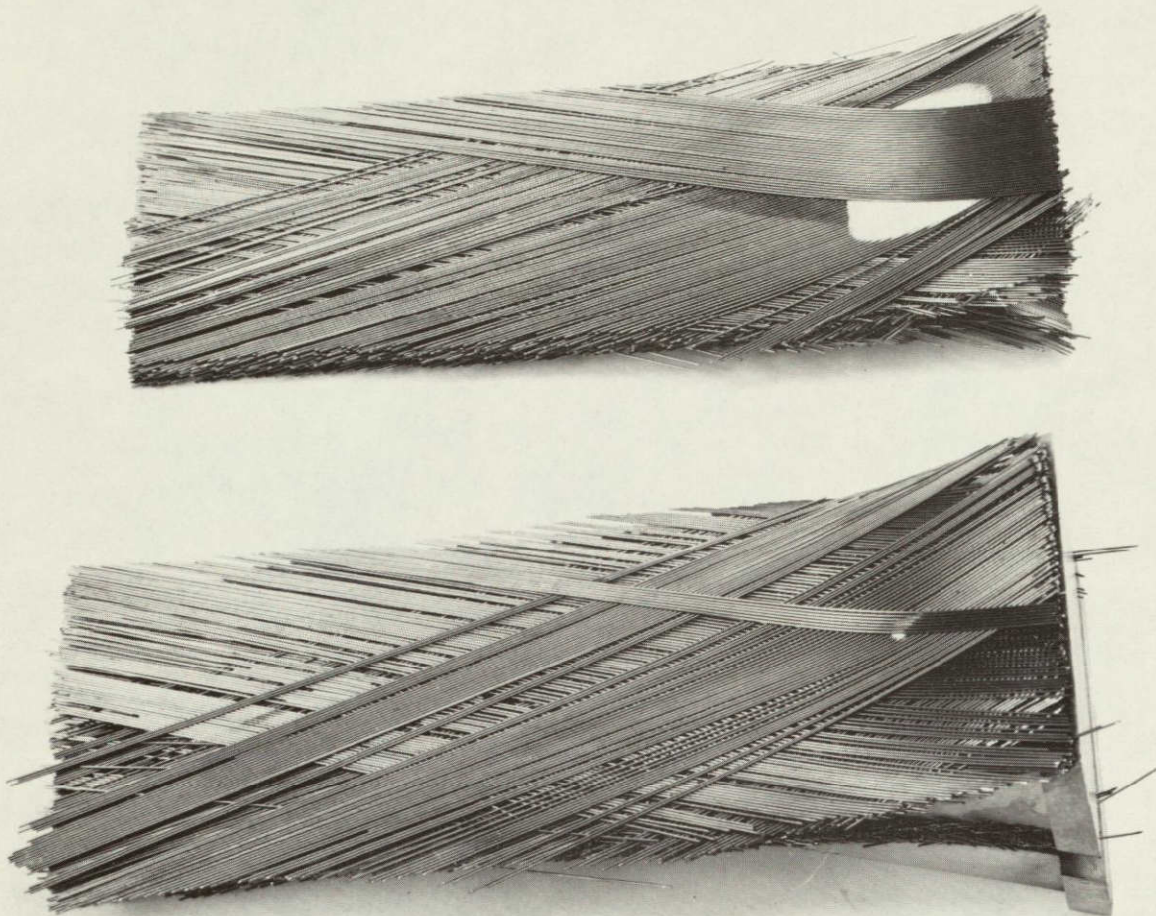
Figure 25. Sequential Leaching of Plies Showing the Absence of Fiber Breakage in the Root Transition Radii in Specimens of Triple (Top) and Single (Bottom) Inner Wedge Designs.

TABLE XI

ROOT ATTACHMENT SPECIMEN IZOD IMPACT TEST RESULTS

| Spec-imen No.	Material & Layup	Condition	Root Type	Impact Energy N-m (ft-lb)	Remarks
3-1	±15°, 0.02 cm (8.0 mil) B-1100Al	Trimmed	3 Inner Wedges 6061Al	54.9 (40.5)	No failure; monotapes delaminated in the shank area.
3-2	"	"	"	46.1 (34.0)	
4-1	±15°, 0.02 cm (8.0 mil) B-1100Al	As-Pressed	1 Inner Wedge 6061Al	19.7 (14.5)	No failure; monotapes delaminated in the shank area.
4-2	"	"	"	18.3 (13.5)	
6-1	±15°, 0.02 cm (8.0 mil) B-1100Al	As-Pressed	1 Inner Wedge Ti(6,4)	35.9 (26.5)	No failure; monotapes delaminated in the shank area.
6-2	"	"	"	34.6 (25.5)	
6-2A	"	Repressed	1 Inner Wedge Ti(6,4)	101.7 (75.0)	Failed in mid-shank; partially delaminated.
8-1	Ti(6,4)	Machined	Homogeneous Ti(6,4)	139.0 (102.5)	Failed in root radius.
8-2	"	"	"	119.3 (88.0)	Failed in root radius.
5-A	±15°, 0.014 cm (5.6 mil) B-1100Al	Repressed after tensile testing.	1 Inner Wedge 6061Al	79.3 (58.5)	Failed in mid-shank; partially delaminated.
9-1	±15°, 0.02 cm (8.0 mil)	As-Pressed	1 Inner Wedge 6061Al	78.6 (58.0)	Failed in root radius, no delamination.
9-2	"	"	"	77.3 (57.0)	Failed in root radius, no delamination.
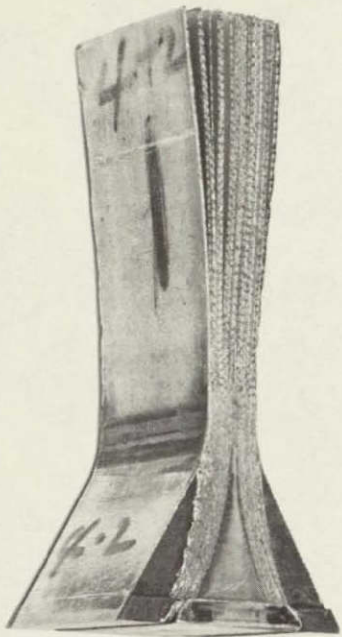
19.7 N-m (13.5 ft-lb)
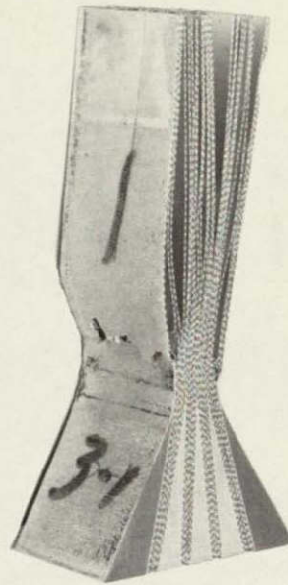
46.0 N-m (34.0 ft-lb)
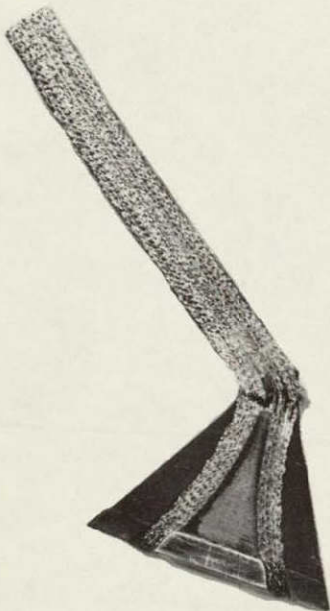
79.0 N-m (58.0 ft-lb)
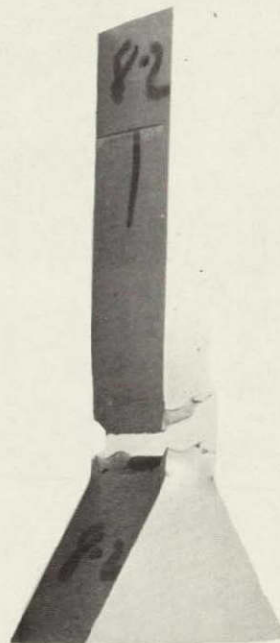
119.0 N-m (88.0 ft-lb)

Figure 26. Fracture Modes in ±15°, 0.02 cm (8.0 mil) B-1100Al
and Homogeneous Ti (6-4) Root Specimens.

strength value of all the specimens studied in this task. The high impact value in this specimen is attributed to a partial debonding between monotapes adjacent to the crack which acted as a crack blunting and energy absorbing mechanism. An analogy can be drawn between this and the Charpy test results in Tasks I and II in specimens characterized by a moderately strong fiber matrix bond. The relatively high impact energy obtained in specimen 5A indicates that little, if any, fiber breakage or other damage occurred in this specimen under tensile stress of 700.0 M N/m^2 (101.7 ksi). The effects of processing on pendulum impact resistance of root specimens of $\pm 15°$ B-1100Al with a single Al inner wedge is illustrated in Figure 27.

In summary, three types of failure were encountered in the pendulum tested root specimens, depending on the strength of monotape bond. Specimens with a relatively weak bond failed by extensive monotape delamination at low impact energy levels. Specimens characterized by a strong monotape bond failed in the transition radius without ply delamination at intermediate energy levels. The specimen with a moderately strong monotape bond failed slightly above the transition radius without ply delamination in the shank, but some ply separation in the vicinity of the crack. The resultant impact energy was higher than in the two previous cases.

CONDITION: A-INCOMPLETE BONDING
B-COMPLETE BONDING
C-RE-PROCESSING OF A
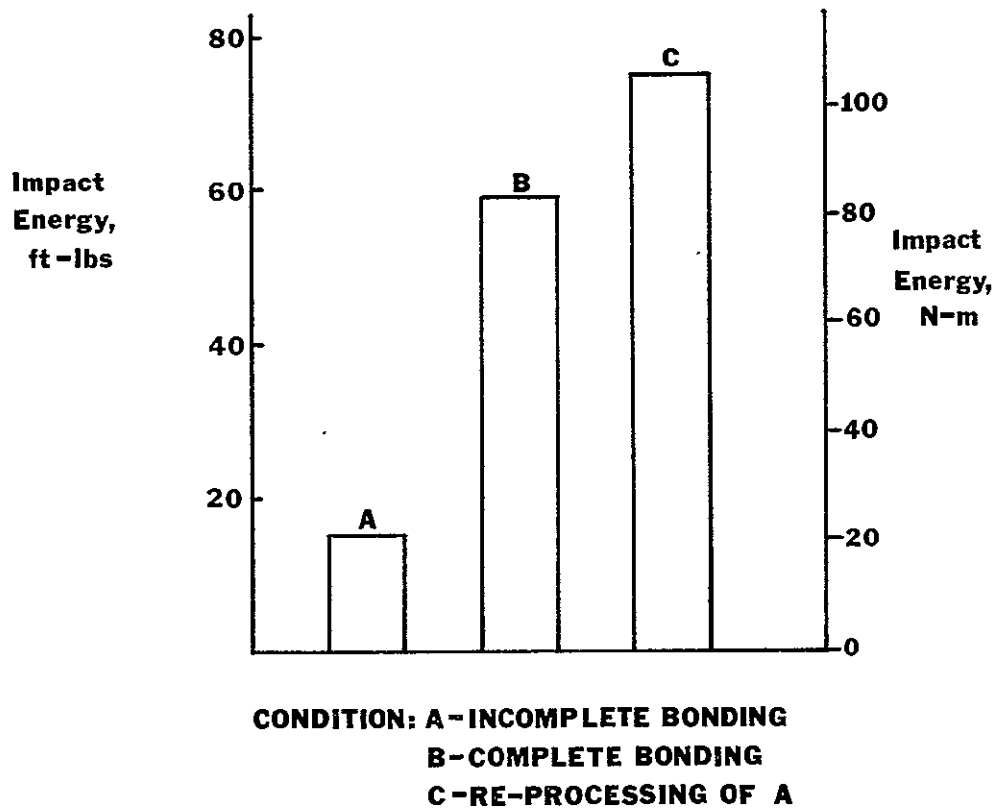
PROCESSING EFFECTS

±15, 0.02 cm (8.0 mil)B-1100Al, Single Al Wedge
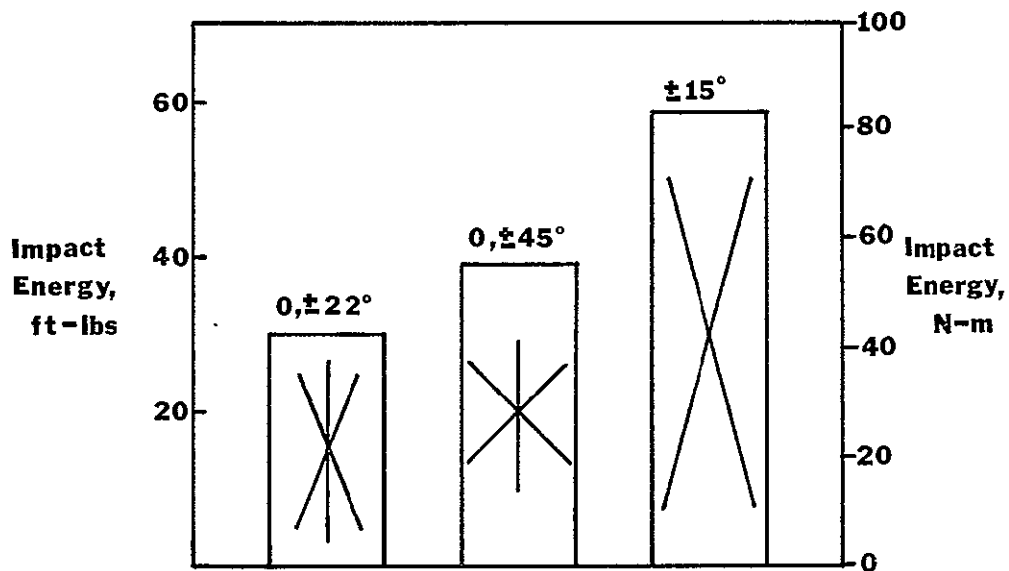
FILAMENT ORIENTATION EFFECT

0.02 cm (8.0 mil)B-1100Al, Single Al Wedge

Figure 27. Effect of Processing Variables and Filament Orientation on
Pendulum-Izod Impact Resistance of 0.02 cm (8.0 mil)B-1100Al.

6.0 TASK IV - FABRICATION AND CHARACTERIZATION
OF DEMONSTRATION FAN BLADES

According to the initial plan, Task IV was to be devoted to the ballistic impact testing of composite plates and bladelike shapes, and to the fabrication and testing of process demonstration fan blades. However, after completion of Task III, a major modification in Task IV development effort and program completion requirements were introduced. In essence, this modification entailed the fabrication and testing of additional bladelike shapes and the fabrication of only one process demonstration fan blade, giving highest priority to pendulum and ballistic impact testing. During the performance of Task IV activities it was decided to spend more time in the area of ballistic impact studies than was initially anticipated and hence it was recognized that not enough funding was available to fabricate a sound process demonstration fan blade. A summary of the blade fabrication work status is given at the end of this section.

6.1. Experimental Procedures

... Experimental procedures employed in the fabrication and testing of Charpy impact test panels, ballistic impact test plates and root attachments (bladelike shapes) are described below.

Fabrication

Four types of Charpy panels were fabricated in B-1100A1.

Panel	Fil. Dia.	Angle Ply
1	0.02 cm (8.0 mil)	0, ±22
2	0.02 cm (8.0 mil)	±15
3	0.014 cm (5.6 mil)	±15
4	0.02 cm (8.0 mil)	0, ±45

Panel size was 5.85 cm (2.3 in) x 8.9 cm (3.5 in) x 1.02 cm (0.4 in) to provide duplicate specimens in the standard and modified LT orientations. The panels were fabricated by the monotape method. Bonding parameters employed in the fabrication of monotapes and conversion of monotapes into panels were 455°C (850°F), 57.0 M N/m^2 (8.0 ksi), 15 min. The reduced pressing time of 15 min. was used to minimize total elevated temperature exposure. The procedures employed in the preparation of monotapes were the same as in Task I. After pressing the monotapes were cleaned and surface treated to enhance low temperature bondability. Charpy specimens were machined by a combination of abrasive and EDM cutting techniques as described earlier.

Three types of test plates were fabricated for evaluation in ballistic impact:

1. +15°, 0.014 cm (5.6 mil) 1100Al, 12 ply, 0.216 cm (0.085 in) thick.

2. +15°, 0.02 cm (8.0 mil) B-1100Al, 8 ply, 0.216 cm (0.085 in) thick.

3. Homogeneous Ti(6,4), 0.2 cm (0.085 in) thick.

The procedures employed in the fabrication of the composite plates were the same used for the fabrication of Charpy panels above. Four panels 21.6 cm (8.5 in) x 15.2 cm (6.0 in) with each fiber were fabricated to provide a total of 32 - 15.2 cm (6.0 in) x 5.0 cm (2.0 in), 0.216 cm (0.085 in) thick ballistic impact test specimens. The control specimens were cut from 0.2 cm (0.085 in) thick Ti(6,4) sheet.

A total of eight (8) root specimens (bladelike shapes) were fabricated as follows:

			Number of Tests	
Wedge Mat'l	Fil. Dia.	Angle-Ply	Tensile	Impact
Al	0.014 cm (5.6 mil)	±15		1
Al	0.02 cm (8.0 mil)	0, ±45	1	1
Al	0.02 cm (8.0 mil)	0, ±22		1
Al	0.02 cm (8.0 mil)	±15	1	1
Ti	0.02 cm (8.0 mil)	±15	1	

All root specimens were fabricated by the monotape method using layup procedures and bonding parameters optimized in Task III. Aluminum inner wedges for these specimens were machined from 6061Al bar stock. Ti(6,4) inner and outer wedges were re-used from Task III by chemical leaching of the wedges after specimen testing.

6.1.1   Testing

Pendulum-Charpy

Charpy specimens were tested at room temperature on a Sontag Universal Testing machine. Duplicate specimens in each type of angle-ply layup were tested in the alternate LT impact orientation. Specimens in the standard LT orientation were included for control purposes.

Tensile

Root attachment tensile specimens were tested at 232°C (450°F). Testing was performed in a Baldwin testing machine using a cross-head speed of 0.05 cm (0.020 in)/min. Heating of the specimens was accomplished in a

70

tube-furnace mounted inside the machine. Temperature was measured and controlled by thermocouples attached to the specimen roots. In three specimens tensile testing was terminated at about 0.76 cm (0.3 in) specimen elongation.

Pendulum-Izod

Pendulum impact testing of the root attachment specimens was performed on a Sontag Universal testing machine using the adaptation fixture described in Task III. A standard Izod striker was used.

Ballistic

Ballistic impact testing was performed on a facility designed and constructed by TRW. The system consisted of a launch tube operated by helium gas pressure, the projectile which was carried by a styrofoam sabot, and the timing circuit employing photodiode sensors. The launch tube contained an accumulator which was charged to a given helium pressure and a rapid acting solenoid valve which triggered the launch. The projectile was carried in a styrofoam sabot. Projectile materials were steel, gelatin or RTV silicone rubber and the projectile shape was either a sphere or a cylinder. The mass of the projectiles ranged from 1/2 to 6 grams. The projectile velocity was determined between two points with photodiode sensors and an electronic timer. Velocities of 152.4 m/sec (500 ft/sec) - 365.76 m/sec (1200 ft/sec) were employed. By knowing the mass and velocity of the projectile, the kinetic energy could be calculated. It was assumed that all of this energy was transferred to the specimen. A schematic of the appratus is shown in Figure 28. The plate specimens were 5.08 cm (2.0 in) x 15.24 cm (6.0 in) and gripped 2.54 cm (1.0 in) from the bottom. The impingement angle ranged from 90°, that is the specimen normal to the projectile line of flight, to 15°. The specimen was impacted to the center of the width and approximately 6.35 cm (2.5 in) from the top. A photo of the test apparatus is shown in Figure 29.

6.2   Results and Discussion

Pendulum-Charpy

Charpy impact test results are summarized in Table XII. The main objective was to determine the Charpy impact resistance of the three angleply layups in the alternate LTs impact orientation. In the notched condition, highest impact energy was obtained in the 0°, $\pm45°$ construction. Next in order of decreasing impact resistance were 0°, $\pm22°$ and $\pm15°$ constructions. However, the difference in the average impact energy in the latter two types was very small. The impact energy levels obtained in the notched, standard LT specimens (control specimens) of 0°, $\pm22°$ and 0°, $\pm45°$ construction are generally in agreement with those obtained in Task II, which indicates that comparable impact values are obtainable by both (foil-filament and monotape) fabrication methods.
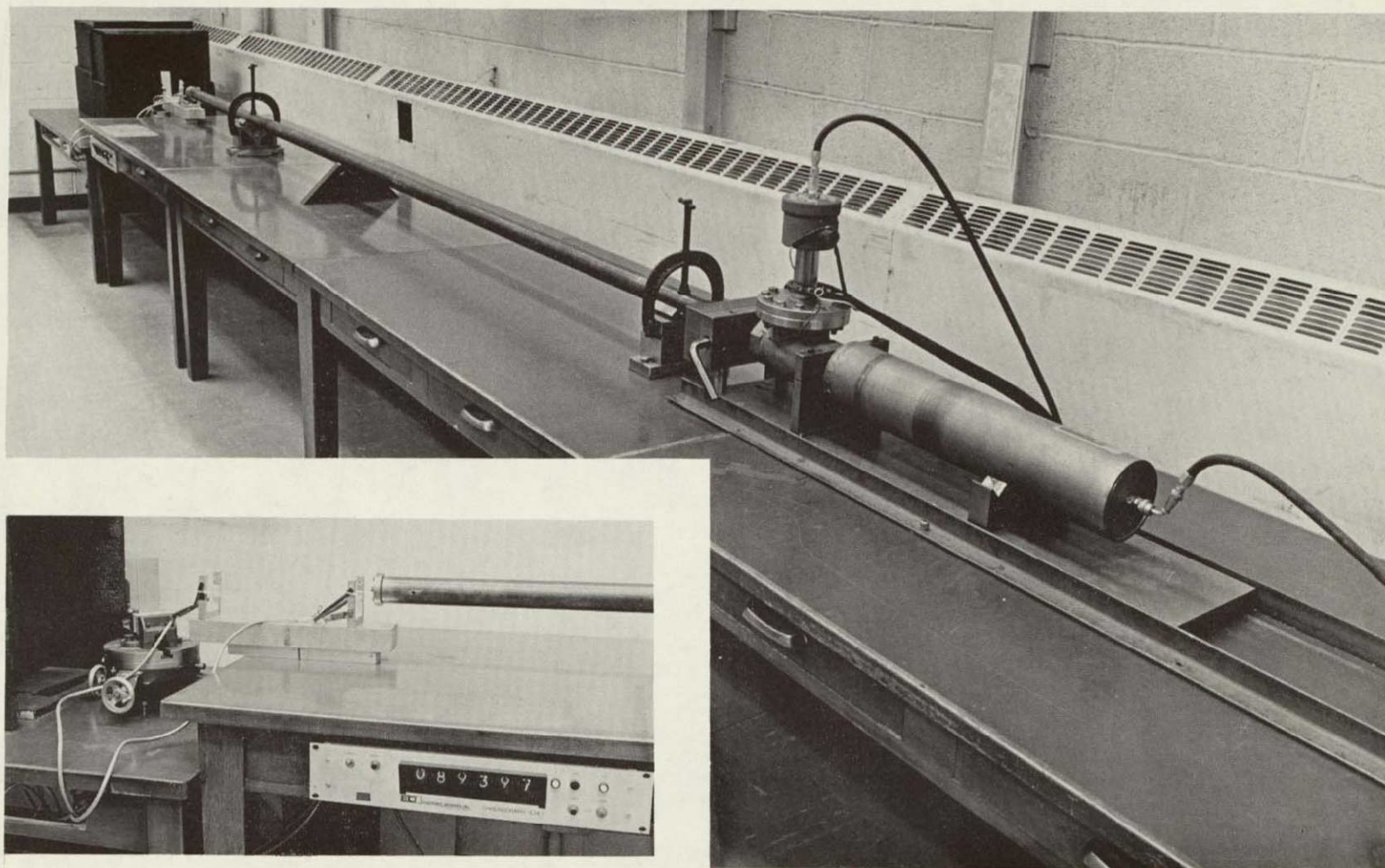
71

Figure 29.   TRW BAllistic Impact Facility.

TABLE XII

CHARPY IMPACT PROPERTIES OF ANGLE-PLIED
50 V/O B-1100A1 COMPOSITES *

Panel No.	Fiber Dia. cm (mils)	Layup	Condition	Impact Orientation	Impact Energy N-m (ft-lb)
93	0.014 (5.6)	±15°	Unnotched	LT	38.0 (28.0)
"	"	"	Notched	LT	25.8 (18.0
"	"	"	Notched	LT_s1	14.9 (11.0)
"	"	"	Notched	LT_s2	13.6 (10.0)
94	0.02 (8.0)	0°,±22°	Unnotched	LT	74.6 (55.0)**
"	"	"	Notched	LT	47.5 (35.0)
"	"	"	Notched	LT_s1	15.6 (11.5)
"	"	"	Notched	LT_s2	14.9 (11.0)
96	0.02 (8.0)	0°,±45°	Unnotched	LT	46.1 (34.0)
"	"	"	Notched	LT	46.1 (34.0)
"	"	"	Notched	LT_s1	27.1 (20.0)
"	"	"	Notched	LT_s2	27.8 (20.5)
99+	0.02 (8.0)	±15°	Unnotched	LT	20.3 (15.0)
"	"	"	Notched	LT	30.5 (22.5)
"	"	"	Notched	LT_r	25.3 (18.5)
"	"	"	Notched	LT_s	19.7 (14.5)

* Impact values in the unnotched specimens are not corrected for
the larger cross-section area.

** No fracture.

\+ Temperature overshot during processing.

The lower than expected Charpy values obtained with the ±15° angle-plied specimens in the standard LT orientation are attributed to unsatisfactory · matrix-matrix bond in Panel #93 and excessively strong fiber-matrix bond in Panel #99. The dependence of fiber-matrix interface condition on impact resistance in B-1100Al has been described earlier. The test results obtained on the ±15° angle-plied panels suggest that further refinement of bonding parameters on the monotape method are needed to ensure a better product reproducibility.

Tensile.

Elevated temperature tensile properties of B-1100Al blade-like shapes are summarized in Table XIII. The various failure modes are illustrated in Figure 30. In all four specimens failure occurred in the specimen roots in the upper specimen grip where the temperature was approximately 10°C (50°F) higher than in the bottom specimen root. No composite damage occurred in the specimen of ±15°, 0.02 cm (8.0 mil) B-1100Al with the 6061Al inner wedge. The specimen failed by a combination of shear at the composite - Ti outer wedge interfaces and deformation of the inner 6061Al wedge. In specimens RS-15 and RS-16 failure was initiated by the shearing of one composite splay at the airfoil to root transition radius. Specimen RS-17 fractured slightly above the transition radius after a moderate amount of root pullout. The lack of extensive root pullout in this specimen may be attributed in part to the slightly lower temperature of the upper root during testing.

Pendulum - Izod

Pendulum-Izod test results obtained on root attachment specimens (bladelike shapes) representing three angle-ply orientations and two fiber sizes are summarized in Table XIV. The appearance of the specimens after testing is illustrated in Figure 31. It should be noted that all specimens failed in the transition radius and only specimen sheared at the centerline. The impact energies are also rather consistent in each set.

The effect of fiber diameter on impact energy in the ± 15° layup specimens is in agreement with the results obtained with Charpy specimens in Task II; higher impact energy is associated with the larger fiber. However, the difference in the relative energy levels is more pronounced in the root specimens.

With regard to ply orientation, highest impact resistance is found in specimens with the alternate ±15° layup. The results are therefore consistent with those obtained on Charpy specimens tested in the notched condition. It should be noted that no true failure (therefore no true Charpy impact value) was obtained with the same type of Charpy specimens tested in the unnotched condition. Next in order of decreasing impact resistance are ±45°, 0° and ±22°, 0° constructions. Here again the results are consistent with those of Charpy specimens tested in the unnotched condition. The effect of filament orientation on impact energy in 0.02 cm (8.0 mil) B-1100Al root specimens with a single Al wedge is shown in Figure 27.

75

TABLE XIII

ELEVATED TEMPERATURE TENSILE PROPERTIES OF B-1100A1 BLADELIKE SHAPES

| Specimen No.	Fiber Dia. & Layup	Root Inner Wedge	Temp. °C (°F)		M N/m² (KSI)	Test Terminated
			Top	Bottom		
RS-14	0.02 cm (8.0 mil) ±45, 0°	6061A1	238 (460)	400 (205)	417.8 (60.6)	0.762 cm (0.3 in) elongation, 206.6 M N/m² (30.0 ksi).
RS-15	0.02 cm (8.0 mil) ±15°	Ti (6·;4)	238 (460)	193 (380)	426.1 (61.8)	0.762 cm (0.3 in) elongation, 179.3 M N/m² (26.0 ksi).
RS-16	0.02 cm (8.0 mil)	6061A1	238 (460)	210 (410)	409.5 (59.4)	1.14 cm (0.45 in) elongation, 213.7 M N/m² (31.0 ksi).
RS-17	0.014 cm (5.6 mil) ±15°	6061A1	229 (445)	207 (405)	385.4 (55.9)	Fractured at 0.47 cm (0.185 in) 353.7 M N/m² (51.3 ksi).
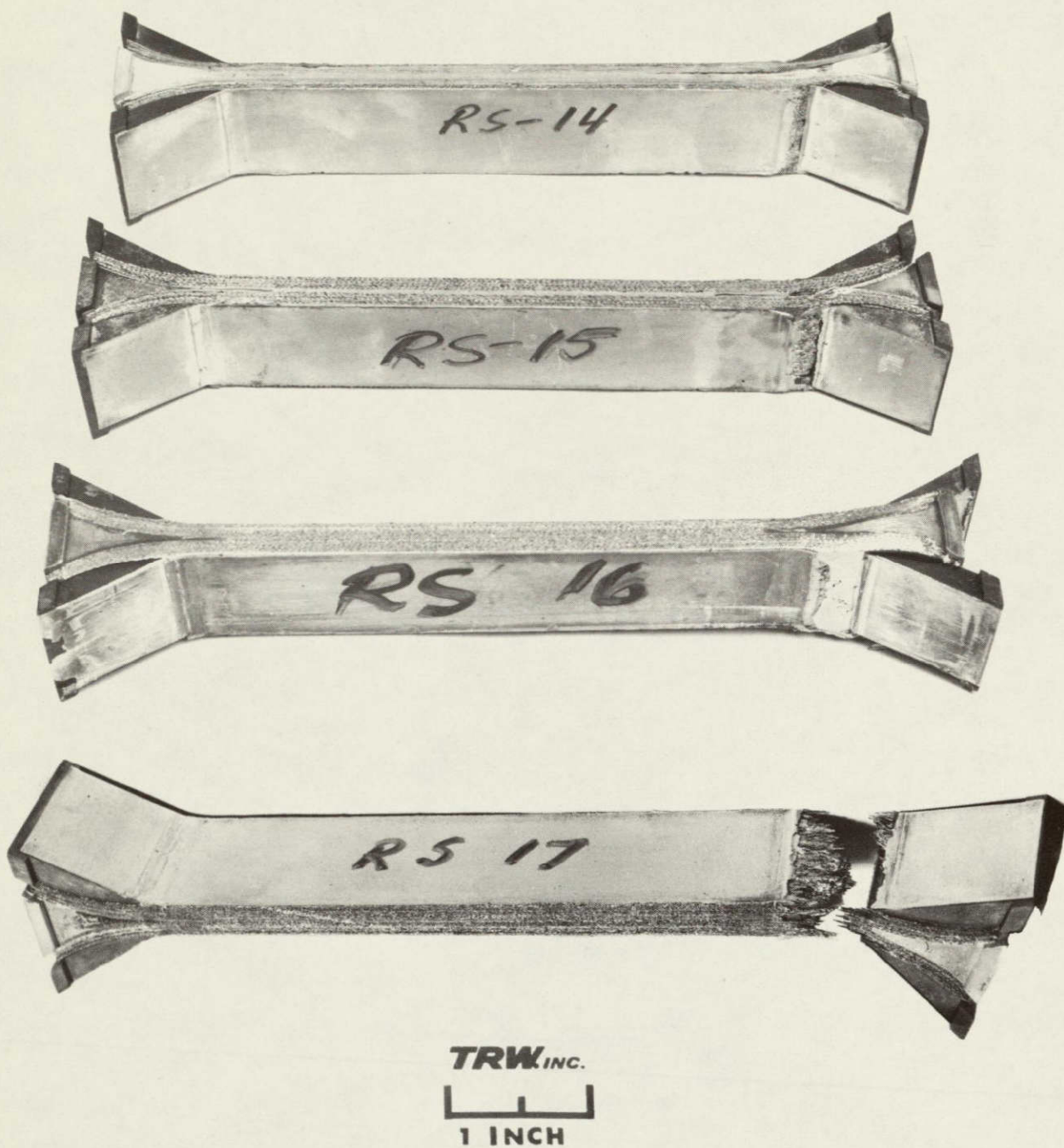
Figure 30. Failure Modes in B-1100Al Tensile Root Specimens (Bladelike Shapes) Tested at 232°C (450°F).

TABLE XIV

ROOT ATTACHMENT SPECIMEN IZOD IMPACT TEST RESULTS

Specimen No.	Material & Layup	Condition	Root Type	Impact Energy N-m*	(ft-lb)	Remarks
9-1	±15°, 0.02 cm (8.0 mil) B-1100Al	As Pressed	1 Inner Wedge 6061Al	78.6	(58.0)	Failed in root radius, no delamination.
9-2	''	''	''	77.3	(57.0)	''
11-1	±15°, 0.014 cm (5.6 mil) B-1100Al	As Pressed	1 Inner Wedge 6061Al	42.7	(31.5)	''
11-2	''	''	''	44.1	(32.5)	''
12-1	(±45° 0°)0.02 cm(8.0 mil) B-1100Al	As Pressed	1 Inner Wedge 6061Al	53.6	(39.5)	''
12-2	''	''	''	52.2	(38.5)	''
13-1	(±22°,0°)0.02 cm(8.0mil) B-1100Al	As Pressed	1 Inner Wedge 6061Al	42.7	(31.5)	''
13-2	''	''	''	46.1	(34.0)	''

*Not adjusted for cross-section area.
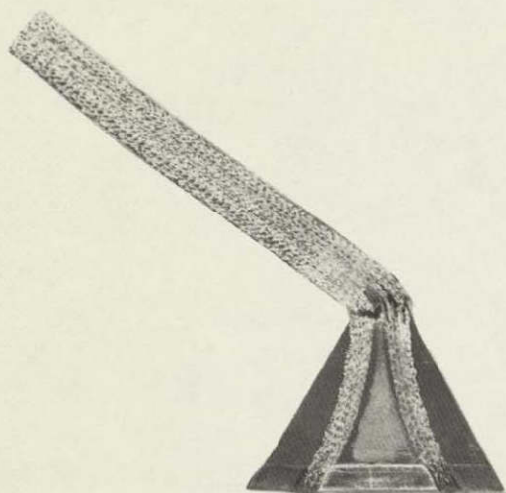
+15°, 0.02 cm (8.0 mil) B-1100A1
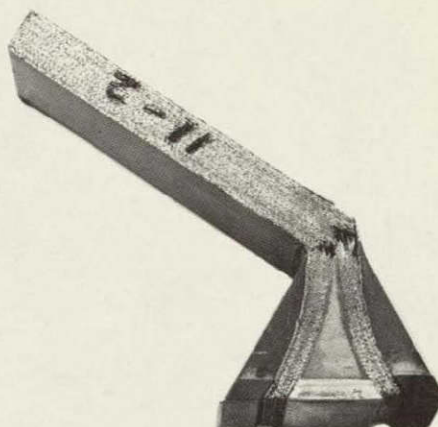
+15°, 0.014 cm (5.6 mil) B-1100A1
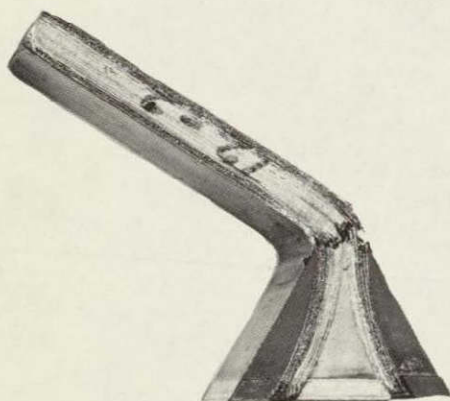
+45°C, 0° 0.02 cm (8.0 mil) B-1100A1
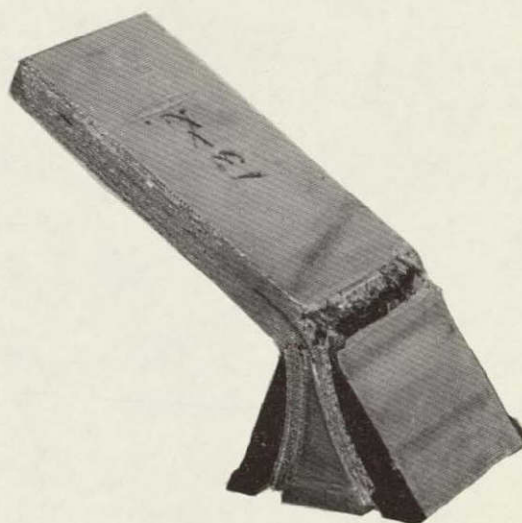
+22°, 0° 0.02 cm (8.0 mil) B-1100A1

Figure 31.   Fracture in Pendulum-Izod Impact Tested Root Specimens
(Bladelike Shapes) of B-1100A1.

Ballistic

Initial ballistic impact testing was performed using panels of 50 volume percent boron-1100 aluminum with 0.014 cm (5.6 mil) or 0.02 cm (8.0 mil) fiber diameter. The panels were either 12 or 8 layers thick to provide a final nominal thickness of .216 cm (0.085 in) and were 5.08 cm (2.0 in) x 15.24 cm (6.0 in) in size. Fiber orientation was ±15° relative to the 15.24 cm (6.0 in) dimension. The ballistic impact test is comparative in that keeping specimen geometry, projectile velocity, and projectile energy constant will produce a ranking of material resistance to damage. Typical results illustrating various degrees of damage obtained with 1.27 cm 0.5 in) diameter spherical gelatin projectiles are shown in Figure 32. Damage is indicated as light where some visible indentation occurred, moderate where appreciable indentation was found, and severe where appreciable indentation was accompanied by cracking. Cracking occurred first on the back side and, with a more severe impact, on the front side.

The degree of damage was also influenced by the projectile material used. In comparing gelatin, RTV rubber and steel at comparable impact energies, the gelatin produced slightly less damage than RTV rubber. The mass and kinetic energy are thus distributed over a wider area. It was also found that the gelatin projectile tended to separate during launching and hit over a wider area. For this reason, most of the testing was performed with RTV silicone rubber. The use of steel projectiles produced penetration at very low energy values. Typical examples are shown in Figure 33. The hole was relatively smooth in circumference and the projectile appeared to punch through the panel. Radiography and ultrasonic C-scan indicated no other damage caused by the projectile in the area around the hole. Penetration is due to the non-deforming nature of the projectile and the relatively high unit energy of the non-distributed impact. The use of steel projectile models the nut and bolt type of FOD damage but does not bear any relationship to soft impacts. Penetration was achieved for both 0.014 cm (5.6 mil) and 0.02 cm (8.0 mil) B-1100Al at energy levels of 5.43 N-m (4.0 ft-lb) - 8.1 N-m (6.0 ft-lb) using 0.41 cm (5/32 in) projectiles.
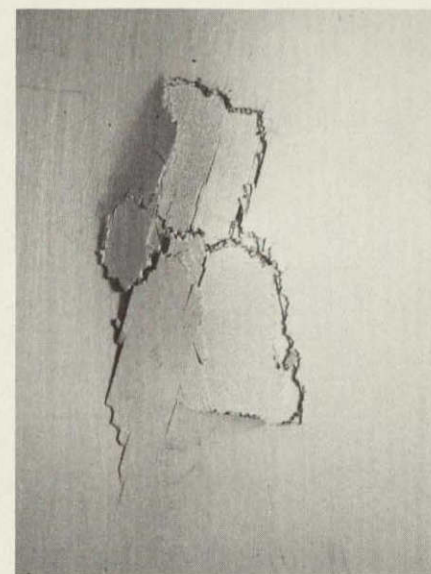
The ballistic impact resistance of 0.014 cm (5.6 mil) B-Al, 0.02 cm (8.0 mil) B-Al, and unreinforced Ti(6,4) were compared using RTV projectiles. Results of the degree of damage and ultrasonic C-scans of specimens after ballistic impact are shown in Figures 34 through 37. The results are summarized in Figure 38. In general, the degree of damage was similar for the two diameters of boron but slightly more extensive with the 0.02 cm (8.0 mil) fiber. The unreinforced Ti(6,4) survived the 52.3 N-m (40 ft-lb) impact without visible damage. A summary of ballistic impact runs is presented in Table XV.

Some runs were also performed at an impingement angle of 15° using RTV rubber projectiles. Because the area projected by a 5.08cm (2.0 in) wide specimen is only about 1.43 cm (9/16 in) compared to the 1.27cm (1/2 in) projectile diameter, accurate placement of the projectile was a problem. There is also the problem of knowing what fraction of the projectile kinetic energy

80

Front View

Back View

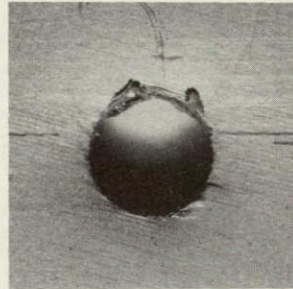| 150.9 m/sec (495 ft/sec) | 243.8 m/sec (800 ft/sec) | 342.6 m/sec (1124 ft/sec) |
| 10.9 N-m (8.0 ft-lb) | 28.5 N-m (21.0 ft-lb) | 55.6 N-m (41.0 ft-lb) |
| LIGHT DAMAGE | MEDIUM DAMAGE | SEVERE DAMAGE |

Figure 32. 0.02 cm (8.0 mil) B-1100A1 Ballistically Impacted with
1.27 cm (0.5 in) Gelatin

81

0.014 cm (5.6 mil) B-1100Al
170.0 m/sec (558 ft/sec)
0.41 cm (5/32 in) Steel
3.5 N-m (2.6 ft-lb)

0.02 cm (8.0 mil) B-1100Al
201.2 m/sec (660 ft/sec)
0.64 cm (1/4 in) Steel
21.0 N-m (15.5 ft-lb)

Figure 33.   Ballistic Impact with Steel Projectiles Illustrating
Penetration of Panels at Low Kinetic Energy.

Front
View

Back
View

152.4 m/sec (500 ft/sec)
14.9 N-m (11.0 ft-lb)

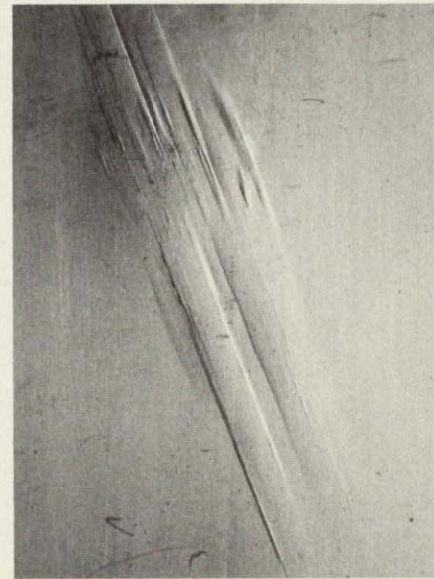246.0 m/sec (807 ft/sec)
38.0 N-m (28.0 ft-lb)

294.7 m/sec (967 ft/sec)
54.3 N-m (40.0 ft-lb)

Figure 34.   0.02 cm (8.0 mil) B-1100Al Ballistically Impacted
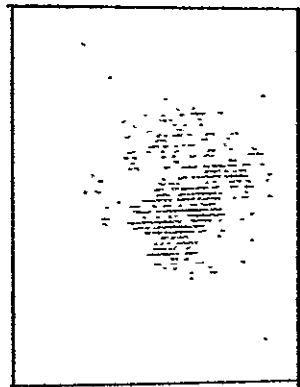with 1.27 cm (0.5 in) RTV Rubber.

Front View

Back View
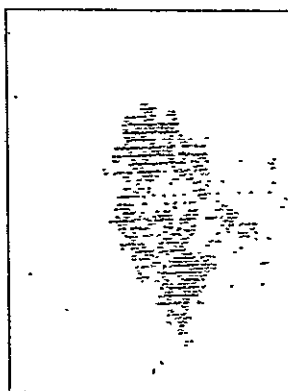
84

152.4 m/sec (500 ft/sec)
14.9 N-m (11.0 ft-lb)

246.0 m/sec (807 ft/sec)
38.0 N-m (28.0 ft-lb)

301.1 m/sec (988 ft/sec)
57.0 N-m (42.0 ft-lb)
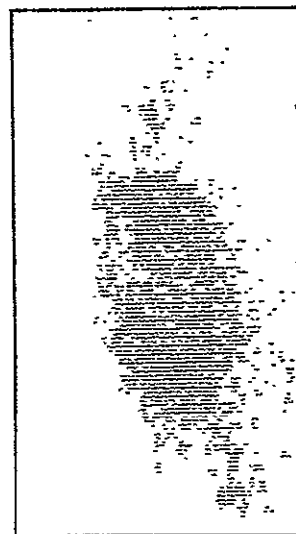
Figure 35. 0.14 cm (5.6 mil) B-1100A1 Ballistically Impacted with
1.27 cm (0.5 in) RTV Rubber.

52.4 m/sec (500 ft-sec)   246.0 m/sec (807 ft/sec)   294.7 m/sec (967 ft/sec)
14.9 N-m (11.0 ft-1b)   38.0 N-m (28.0 ft-1b)   54.3 N-m (40.0 ft-1b)

Figure 36.   Ultrasonic C-Scans of 0.02 cm (8.0 mil) B-1100Al
Ballistically Impacted with 1.27 cm (0.5) RTV Rubber.

52.4 m/sec (500 ft/sec)   246.0 m/sec (807 ft/sec)   301.1 m/sec (988 ft/sec)
14.9 N-M (11.0 ft-lb)   38.0 N-m (28.0 ft-lb)   57.0 N-m (42.0 ft-lb)

Figure 37.   Ultrasonic C-Scan of 0.014 cm (5.6 mil) B-1100Al Ballistically
Impacted with 1.27 cm (0.5 in) RTV Rubber.
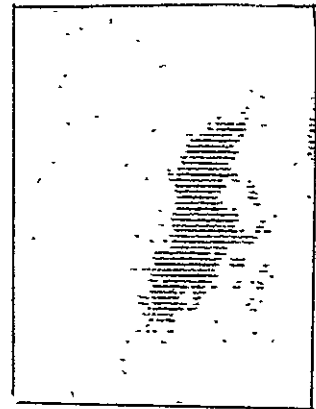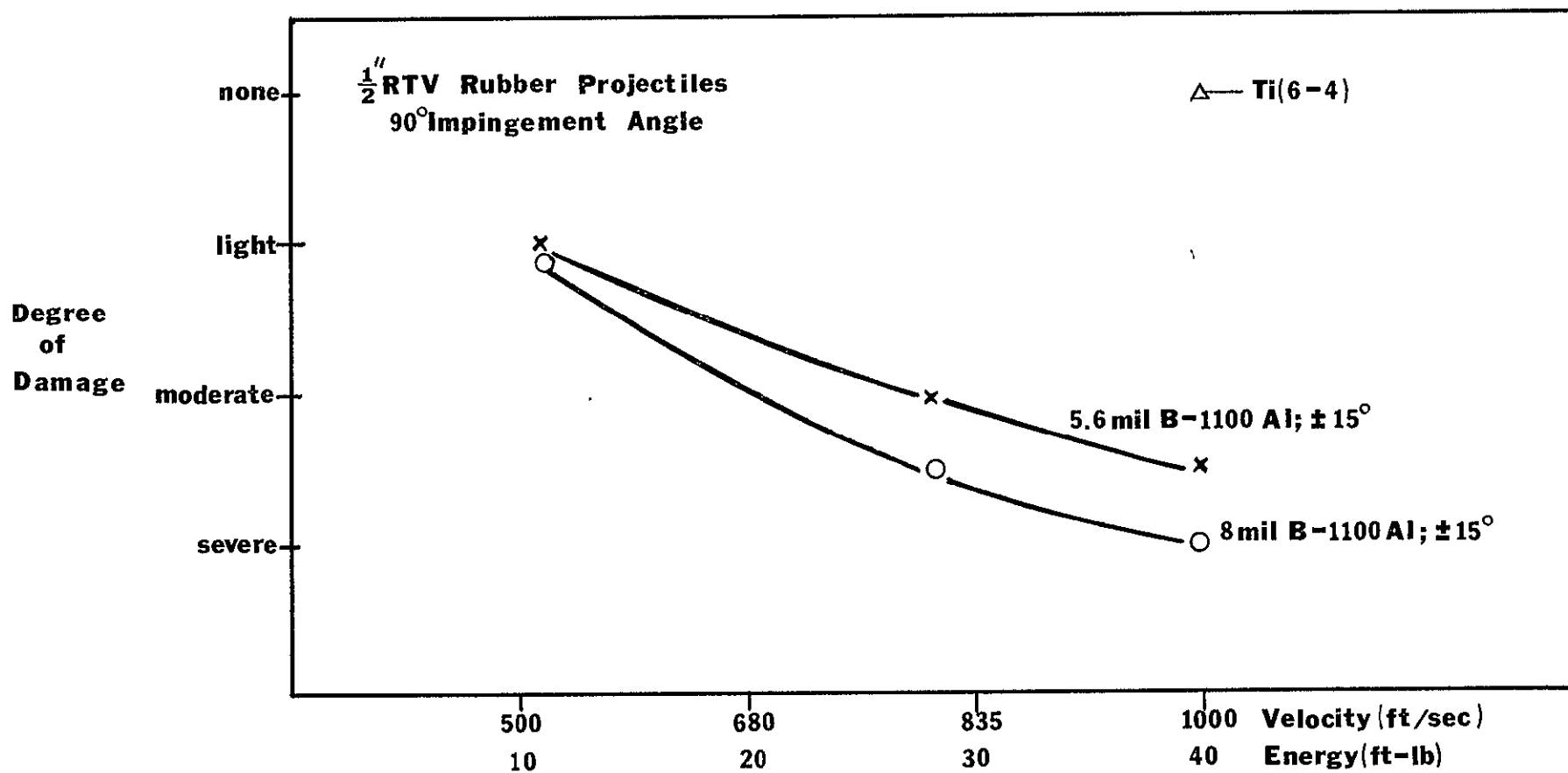
Figure 38. BALLISTIC IMPACT DAMAGE VERSUS PROJECTILE VELOCITY AND ENERGY.

TABLE XV

SUMMARY OF BALLISTIC IMPACT TESTING

Panel	Projectile	Velocity M/sec (ft/sec)		Energy N-m (ft/lb)		Impingement Angle(°)	Remarks
0.02 cm (8.0 mil)	1.27 cm (1/2 in)	150.9	(495)	10.8	(8)	90	Light damage
B-1100Al ±15°	gelatin	243.8	(800)	28.5	(21)	90	moderate damage
		342.6	(1124)	55.6	(41)	90	severe damage, cracks both sides
		243.8	(800)	27.1	(20)	15	no damage
		243.8	(800)	27.1	(20)	25	" "
		243.8	(800)	27.1	(20)	35	" "
		243.8	(800)	27.1	(20)	45	light damage
0.02 cm (8.0 mil)	RTV	152.4	(500)	14.9	(11)	90	light damage
B-1100Al ±15°		246.0	(807)	38.0	(28)	90	moderate severe damage, crack on back
		294.7	(967)	54.2	(40)	90	severe damage, cracks both sides
		304.8	(1000)	58.3	(43)	15	no damage
		156.7	(514)	66.4	(49)	15	no damage
0.014 cm (5.6 mil)	RTV	152.4	(500)	14.9	(11)	90	light damage
B-1100Al ±15°		246.0	(807)	38.0	(28)	90	moderate damage
		301.1	(988)	57.0	(42)	90	moderate-severe, crack on back
		297.5	(976)	55.6	(41)	15	no damage
Ti(6,4)	1.27 cm(1/2in) RTV	304.8	(1000)	58.3	(43)	90	no damage
0.02 cm (8.0 mil)	0.63 cm(1/4 in)	251.5	(825)	32.5	(24)	90	penetrated
B-1100Al ±15°	Steel	201.2	(660)	21.7	(16)	90	"
	0.41 cm(5/32)Stl.	257.3	(844)	8.3	(6.1)	90	"
0.014 cm(5.6 mil)	0.63 cm(1/4 in)"	190.5	(625)	19.0	(14)	90	penetrated
B-1100Al ±15°	"	137.2	(450)	9.5	(7)	90	"
	0.41cm(5/32 in)"	170.1	(558)	3.5	(2.6)	90	"
	"	210.6	(691)	5.6	(4.1)	90	"

is transferred to the specimen. No visible damage was noted at the 15°
impingement angle. If the energy absorbed by the specimen were a simple ·
trigometric relationship involving the sine of 15°, about 13.56 N-m (10.0
ft-lb) would have been absorbed which should have produced some specimen
deformation based upon the 90° results. Either a sine relationship is not
followed or the entire projectile did not hit the specimen. An impinge-
ment angle of 45° was required for visible deformation using gelatin projec-
tiles at 243.8 m/sec (800 ft/sec) velocity.

Ballistic impact testing was also performed on simulated root
attachment specimens. The root attachment specimen was designed to eval-
uate the effectiveness of different root wedge and splay geometries and
materials considered in various blade designs. The specimen also provided
a measure of composite material and angle-ply geometry in resisting gross
damage as compared to the localized modes of damage tested with panels.
The specimens were held at the root end and hit 1·.93 cm (0.75 in) from the
free end with RTV rubber projectiles. Specimens after testing are illus-
trated in Figure 39.

All of the specimens did undergo a gross or structural form of
damage. The degree of permanent deformation may be seen in Figure 39.
Deformation was confied primarily to the root area. The shank of the spec-
imen remained straight, indicating little bending strain and the rip of the
specimen remained square to the surface, indicating little shear strain.
Specimens from which the matrix was leached away at the root area showed
no evidence of filament breakage. The angle-ply construction apparently
permits sufficient matrix flow to accommodate the gross plastic deforma-
tion without fiber breakage. The specimens were ranked according to the
degree of deformation for impacts in the 94.9 N-m (70 ft-lb) - 108.5 N-m
(80 ft-lb) range. The +15°, 0.02 cm (8.0 mil) B-1100Al deformed least
while the +45°, 0°, 0.02 cm (8.0 mil) B-1100Al deformed most. One speci-
men withstood 240 N-m (184 ft-lt) without fracture. It was assumed that
all the kinetic energy of the projectile was transferred to the specimen.

The +45° specimen contained a delamination failure. The frac-
ture was in the matrix rather than in a filament-matrix plane. Unlike the
other three specimens, this sample displays a curved shank indicating con-
siderable bending strain. The plane of delamination is close to the center
of the section which is also the location of maximum shear stress. It is
concluded that the delamination was due to large shear strains set up during
impact, but whether a weak matrix-matrix bond existed in this location after
secondary bonding could not be determined.

The bladelike shapes correlated well with the Charpy impact
results in regard to the relatively large plastic strain absorbed by the
specimen. The ability to absorb and distribute this strain is important
in providing impact resistance in fan blades.
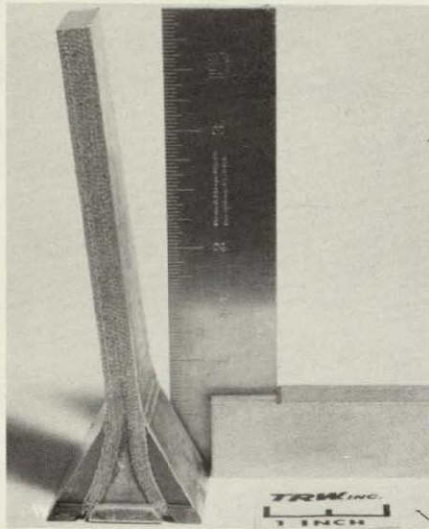
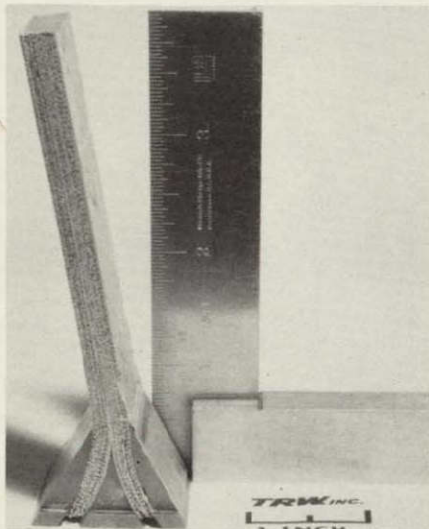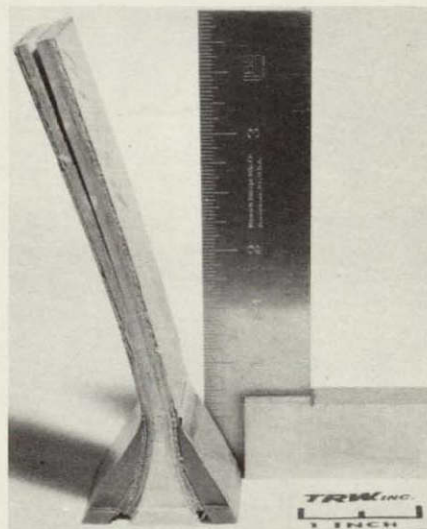+15°, 0.02 cm (8.0 mil)B
203.3 m/sec (667 ft/sec)
116.7 N-m (84.0 ft-lb)
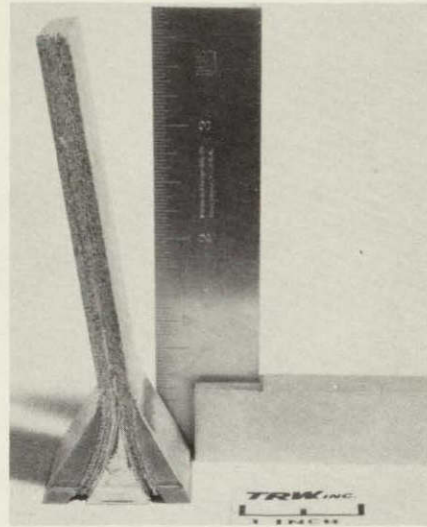
+15°, 0.014 cm (5.6 mil)B
189.3 m/sec (621 ft/sec)
100.4 N-m (74.0 ft-lb)

+15°, 0.02 cm (8.0 mil)B
Ti(6,4) Inner Wedge
291.4 m/sec (856 ft/sec)
249.6 N-m (184.0 ft-lb)

(+45°, 0°), 0.02 cm (8.0 mil)B
182.0 m/sec (597 ft/sec)
95.0 N-m (70.0 ft-lb)

Figure 39.   Ballistic Impact Tests of Root Attachment Specimens.

C.2

90

6.3   Fabrication of Process Demonstration Fan Blade

The best root design and the optimum materials and processing combinations determinated in the preceding tasks were utilized for the fabrication of the process demonstration fan blade in Task IV. The actual blade selected for this purpose was the third stage TF-30 fan blade. The composite system selected for the blade was 0.02 cm (8.0 mil) B-1100Al with a dispersed ±15° angle-ply layup. Root attachments consisted of a single 6061Al inner wedge and homogeneous Ti(6,4) outer root blocks. The blade was to be fabricated by the monotape method.

The government-owned TF-30. third stage B-Al bonding dies as well as blade drawings and charts were furnished to TRW by P&WA. Root attachments for the blade were made at P&WA. Two sets of TRW-owned F-100 monotape forming dies were modified for forming of monotapes for the demonstration blade. Blade ply charts were computerized at TRW. To gain lead time, computer ply design was started before all testing in Task III was completed. Blade ply charts were therefore computerized for both 0.014 cm (5.6 mil) and 0.02 cm (8.0 mil) boron plies.

Computer ply development involved the following steps. First, the computer blade chart data provided by P&WA was checked against blade drawings. This was accomplished by plotting selected blade sections from the computer blade chart data and checking these against the furnished blade drawings. The ply configuration was computerized using the so called ply "peeling" method. The method involved dividing each blade section into parallel strips starting on the outer surfaces of the blade. The intersection of these parallel lines with the section split line formed the boundaries of the particular plies in the respective blade sections. The original "F" and "G" coordinates that located ply end points at each section were not usable in that form. They were all referenced to different origins and did not relate the points to the blade XYZ coordinate syste. Section twist was not accounted for either. The templates were defined by using computer calculated coordinates as follows. The "F" and "G" coordinates were translated to the stacking axis as the origin and then rotated through two angles: the twist angle and the bonding pressure angle. The coordinates were now in usable form.

Unfortunately the contract ran out of funds and the blade design could not be finished and the blade could not be fabricated under this contract.

7.0   CONCLUSIONS AND RECOMMENDATIONS

The following conclusions are drawn from the work on this program:

1. The program resulted in a significant improvement in pendulum
    impact resistance in B-Al composites.

2. Composite properties were found to be strongly dependent on matrix
    material: Charpy impact resistance was significantly greater in
    B-1100Al than B-5052Al, but tensile strength was moderately higher
    in B-5052Al.

3. The high impact resistance in B-1100Al Charpy specimens is largely
    the result of high matrix ductility and moderately strong fiber
    matrix bond whose combined effect was to promote debonding and
    fiber pullout at the crack surface as well as specimen deformation
    by shear in the plane of the filaments. However, impact energy in
    B-1100Al is strongly affected by processing variables such as bond-
    temperature and matrix preparation, both of which can strongly
    affect the nature of the fiber-matrix interface.

4. The larger 0.02 cm (8.0 mil) diameter fibers resulted in a moderate
    improvement in pendulum impact resistance but no significant change
    in tensile strength, compared with 5.6 mil.

5. Matrix enhancement by titanium foil improved tensile strength,
    especially in the transverse direction, and elastic modulus but
    caused a significant reduction in Charpy impact resistance.

6. Angle-plying has reduced directionality for both tensile and Charpy
    properties. Of the three different types of angle-plied composites
    (namely 0±22°; 0+45° and ±15°) which were investigated, the highest
    longitudinal Charpy values and tensile strengths were obtained with
    the ±15° construction.

7. In root attachments (bladelike shapes) highest room temperature
    tensile strength was obtained in specimens of ±15°, 0.02 cm (8.0 mil)
    boron with a single 6061Al inner wedge. Nearly equivalent strength
    level was also obtained with the smaller fiber in the same angle-ply
    construction. Tensile strength of root attachments was reduced by
    about 40% at the test temperature of 233°C (450°F), where failure
    occurred by shearing process at the root wedge aluminum matrix
    interface.

8. Pendulum-Izod impact resistance of root specimens was found to be
    strongly dependent on processing conditions; highest impact resis-
    tance was obtained on specimens which produced a moderate amount of
    ply separation adjacent to the crack. In pendulum-Izod, highest
    impact energy was found in root attachment specimens of ±15°, 0.02 cm
    (8.0 mil) boron with a single 6061 Al inner wedge. The effect of

angle-ply orientation on pendulum-Izod impact resistance was consistent with the results obtained in Charpy specimens of the same fiber size and angle-ply construction.

9. Testing of root attachment shapes indicated that the energy withstood under ballistic impact is as great or greater than absorbed by Charpy testing. Hard projectiles, 0.41 (5/32 in) and 0.64 cm (1/4 in) steel balls, completely penetrated the test panels at very low energy levels while the soft projectiles, 1.27 cm (1/2 in) gelatin and RTV rubber, produced a more distributed form of damage. The 0.014 cm (5.6 mil) B-1100Al panels were better in soft projectile ballistic impact resistance than 0.02 cm (8.0 mil) B-1100Al, while unreinforced Ti(6,4) was undamaged at ballistic impact energy levels which produced severe damage in boron-aluminum.

The following are recommended follow-efforts to encourage the application of boron-aluminum as a fan blade material:

1. Improve pendulum impact resistance of boron-aluminum through additional material-process optimization. In B-1100Al, shear deformation is a major source of energy dissipation. To control the extent of this plastic shear deformation, process selected constructions combining a higher shear strength matrix with a lower shear strength matrix should be investigated. Titanium or higher shear strength aluminum matrix can be selectively used in the center plies (high shear stress area) to improve resistance to excessive shear deformation.

2. Matrix enhancement for improving resistance to local ballistic impact damage should be reinvestigated using it at/and near the surface on a selective rather than on a uniform distribution basis.

3. Lower manufacturing cost of boron-aluminum blade by changing from vacuum-bonding to air-bonding and reducing press diffusion bonding time.

4. Develop meaningful accept-reject criteria for quality control, including FOD tolerance, for boron-aluminum blades.

5. Establish low cost, FOD tolerant production material/process specification and qualitications.

DISTRIBUTION LIST

(All addressees will receive one copy unless otherwise specified.)

NASA Headquarters
600 Independence Avenue
Washington, D. C. 20546
Attn: G. C. Deutsch (RW)

NASA-Lewis Research Center
21000 Brookpark Road
Cleveland, Ohio 44135
Attn: Tech. Util. Office (3-19)
      Report Control (5-5)
      Library (60-3)   (2)
      Cont. Sect. B(500-313)
      R. H. Kemp (49-3)
      T. T. Serafini (49-3)
      C. C. Chamis (49-3)
      J. W. Weeton (49-3)
      R. G. Barrows (106-1)
      R. A. Signorelli (106-1)
      D. L. McDanels (106-1) (37)
      J. C. Freche

NASA-Langley Research Center
Langley Field
Hampton, Va. 23365
Attn: W. A. Brooks, Jr. (188M) (1)
      Library   (1)

NASA
Marshall Space Flight Center
Alabama 35812
Attn: Library, ASGIL   (1)
      F. Lalacona   (1)

NASA-Johnson Space Center
Houston, Texas 77058
Attn: Library - Code JM6   (1)
      Mat. Tech. Br.- Code ES5 (1)

Jet Propulsion Laboratory
4800 Oak Grove Drive
Pasadena, California 91102
Attn: Library

NASA Scientific & Tech.
   Information Facility
P.O. Box 33
College Park, Maryland 20740 (10)

Defense Documentation Center
Cameron Station
5010 Duke Street
Alexandria, Va. 22314   (2)

Department of the Air Force
Air Force Materials Lab.
Wright-Patterson AFB, Ohio 45433
Attn: J. H. Ross (MBC)
      V. DiBenedetto (LTN)
      S. R. Lyon (LLM)
      W. A. Schulz (LC)
      E. Joseph (LLC)

Department of the Air Force
AFAPL/TBP
Wright-Patterson AFB, Ohio 45433
Attn: T. Norbut

Department of the Air Force
Office of Scientific Research
Washington, D. C. 20525
Attn: Library

Department of the Army
Army Air Mobility R&D Lab.
Fort Eustis, Va. 23604
Attn: J. White (SAVDL-EU-TA)

Department of the Army
AMMRC
Watertown, Mass. 02172
Attn: A. P. Levitt

Department of the Army
MAAGS Research Center
Watervliet Arsenal
Watervliet, New York 12189
Attn: I. Ahmad

Department of the Navy
Bureau of Naval Weapons
Washington, D. C. 20525
Attn: T. F. Kearns (RRMA-2)

Department of the Navy
NASC Air-52031B
Washington, D. C.   20361
Attn: I. Machlin

Department of the Navy
ONR - Code 429
Washington, D. C.   20525
Attn: R. Roberts

U. S. Atomic Energy Commission
Washington, D. C.   20525
Attn: J. Simmons

National Bureau of Standards
Inst. for Applied Technology
Bldg. 225, Room B-105
Washington, D. C.   20234
Attn: K. G. Kreider

Oak Ridge National Laboratory
P.O. Box X
Oak Ridge, Tenn.   37830
Attn: Tech. Library-Ref. Sect.

MCIC
Battelle Memorial Institute
505 King Avenue
Columbus, Ohio   43201

Aerospace Corporation
P.O. Bx. 92957
Los Angeles, California   90009
Attn: E. G. Kendall

Amercom, Inc.
9060 Winnetka Ave.
Northridge, California   91324
Attn: G. W. Burt

Astro Research Corp.
1330 Cacique Street
Santa Barbara, Calif. 93103
Attn: H. Muir

AVCO Corporation
Lycoming Division
550 South Main Street
Stratford, Conn.   06497
Attn: B. Goldblatt

AVCO Corporation
Lowell Industrial Park
Lowell, Mass. 01850
Attn: V. Krukonis

Battelle Memorial Institute
Columbus Laboratories
505 King Avenue
Columbus, Ohio   43201
Attn: K. R. Handby   (1)
       Library   (1)

Battelle Memorial Institute
Battelle-Northwest Laboratories
3000 Stevens Drive
Richland, WA   99352
Attn: K. Robinson

Bell Aerosystems Company
P.O. Box 1
Buffalo, New York   14205
Attn: Engineering Lab.

Boeing Company
P.O. Bx 733
Renton, WA   98055
Attn: W. E. Binz

Commonwealth Scientific Co.
500 Pendleton Street
Alexandria, Va.   22314
Attn: A. P. Divecha

COMSAT Laboratories
Materials Technology Branch
Clarksburg, Maryland   20734
Attn: L. Sparrow   (1)
       Tech Library   (1)

Curtiss-Wright Corporation
Wright Aeronautical Division
Woodridge, N.J.   07075
Attn: A. Eisenlohr

Dow Chemical Company
Contract R&D-Bldg. 566
Midland, MI   48640
Attn: R. F. Helmreich

Dolowy-Webb Associates
22072 Rayen Street
Canoga Park, Calif 91304
Attn: J. F. Dolowy, Jr.

Drexel University
Department of Metallurgy
Philadelphia, Penna. 19104
Attn: A. Lawley

E. I. duPont de Nemours & Co.
Textile Fibers Department
Wilmington, Dela. 19898
Attn: C. Zweben (B-262/Rm-433)

Fiber Materials, Inc.
Biddeford Industrial park
Biddeford, Maine 04005
Attn: R. T. Pepper

General Dynamics/Convair
P.O. Box 748
Fort Worth, Texas 76101
Attn: Tech Library (6212)

General Dynamics/Convair
P.O. Box 1128
San Diego, Calif. 92112
Attn: N. R. Adsit

General Electric Co.
Mat. & Proc. Technology Labs
Cincinnati, Ohio 45215
Attn: R. W. Harrison   (1)
         Library   (1)

General Electric Company
Valley Forge Space Tech.Center
P.O. Box 8555
Philadelphia, Penna. 19101
Attn: L. R. McCreight

General Electric Company
Adv. Technology Lab.
Schenectady, New York 12305
Attn: Library

General Motors Corp.
Detroit Diesel-Allison Div.
Materials Laboratory
Indianapolis, Indiana 46206
Attn: M. Herman

Grumman Aircraft Eng. Corp.
Bethpage, New York 11714
Attn: W. Wolkowitz

Hough Laboratory
708 Rice Street
Springfield, Ohio 45505
Attn: R. L. Hough

IIT Research Institute
Technology Center
10 West 35th Street
Chicago, Ill. 60616
Attn:Tech. Library

Lehigh University
Department of Metallurgy
Bethlehem, Penna. 18015
Attn: R. W. Kraft

Lockheed-Georgia Company
Marietta, Georgia 30060
Attn: Tech. Library

Lockheed-Palo Alto Res. Lab.
Materials & Scientific Lab.
3251 Hanover Street
Palo Alto, Calif. 94303
Attn: W. Bradshaw

Lockheed Missiles & Space Co.
111 Lockheed Way
Sunnyvale, Calif 94088
Attn: M. I. Jacobson (B-150)

P. R. Mallory Company
Northwest Industrial Park
Burlington, Mass. 01803
Attn: R. H. Krock

Martin-Marietta Corp.
P.O. Box 5837, MP 129
Orlando, Florida 32805
Attn: R. A. Mayor

McDonnell-Douglas Astronautics Co.
M & P Development
Dept. 247, Bldg. 32
St. Louis, Missouri 63166
Attn: G. B. Billow

Midwest Research Institute
425 Volker Blvd.
Kansas City, Missouri 61110
Attn: J. R. Hancock

NETCO
Suite 906
110 Pine Avenue
Long Beach, Calif 90802
Attn: L. W. Davis

Northrup Corp.
Norarir Division
3901 W. Broadway
Hawthorne, Calif. 90250
Attn: E. Harmon

Philco-Ford Corporation
Aeronutronic Division
Ford Road
Newport Beach, Calif. 92663
Attn: W. M. Fassell

Rensselaer Polytechnic Inst.
Materials Engineering Dept.
Troy, New York 12181
Attn: R. J. Diefendorf

Rockwell International
Los Angeles Division
International Airport
Los Angeles, Calif. 90045
Attn: C. Hamilton (SB08)

Rockwell International
P.O. Box 1259
4300 East Fifth Ave.
Columbus, Ohio 43216
Attn: Tech. Inf. Cent.

Sandia Corporation
P.O. Bx. 5800
Albuquerque, New Mexico 87115
Attn: D. M. Schuster - 5840
       W. R. Hoover - 5844

Dr. E. Scala
Consulting Engineer
P.O. Box 1362
Cortland, New York 13045

Solar Div. - Int. Harvester Co.
2200 Pacific Highway
San Diego, Calif. 92138
Attn: A. G. Metcalfe

Technics, Inc.
80 N. Gordon Street
Alexandria, Va. 22304
Attn: D. F. Bazzarre

TRW Inc.
Equipment Laboratories
Materials Technology
23555 Euclid Avenue
Cleveland, Ohio 44117
Attn: Dr. I. J. Toth

TRW Inc.
TRW Systems Group
One Space Park
Redondo Beach, Calif. 90278
Attn: A. Toy (ol/2171)

Union Carbide Corp.
Parma Technical Center
P.O. Box 6116
Cleveland, Ohio 44101
Attn: Tech. Inform. Serv. (1)
       R. V. Sara   (1)

United Aircraft Corp.
Pratt & Whitney Div.
West Palm Beach, Florida 33402
Attn: Tech. Library

United Aircraft Corp.
Hamilton-Standard Div.
Windsor Locks, Conn. 06096
Attn: W. A. Percival

United Aircraft Corp.
Sikorsky Aircraft Div.
Stratford, Conn. 06497
Attn: M. J. Salkind

United Aircraft Corp.
Research Laboratories
East Hartford, Conn. 06108
Attn: F. S. Galasso
       M. A. DeCresente
       K. M. Prewo